

**THE TRANSPORT AND REMOTE OXIDATION OF  
COMPARTMENT FIRE EXHAUST GASES**

by

David S. Ewens

Thesis submitted to the Faculty of the  
Virginia Polytechnic Institute and State University  
in partial fulfillment of the requirements for the degree of

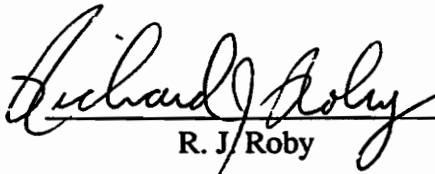
**MASTER OF SCIENCE**

in

**Mechanical Engineering**

**APPROVED:**

  
U. Vandsburger, Chairman

  
R. J. Roby

  
L. A. Roe

February, 1994  
Blacksburg, Virginia

C.2

LD

5655

V855

1994

E948

C.2

# **THE TRANSPORT AND REMOTE OXIDATION OF COMPARTMENT FIRE EXHAUST GASES**

by

David S. Ewens

Committee Chairman: Uri Vandsburger

Mechanical Engineering

**(ABSTRACT)**

The majority of deaths and injuries in compartment fires result from inhalation of the toxic gas, carbon monoxide (CO), especially in locations remote from the burning compartment. This causes the transport and oxidation of CO in burning buildings to become an important topic. Studies have been conducted to determine the toxic environments produced inside, and in locations remote from, a burning compartment; however, no studies have investigated the composition of the exhaust gases during transport to remote locations. The goal of this study was to investigate fire exhaust gas transport through a hallway to determine the important parameters affecting the efficiency of sustained external burning in oxidizing toxic gases, including the hydrodynamic effects of different hallway configurations.

Underventilated compartment fire experiments were performed with a compartment exhausting along the axis of a hallway. The design of the compartment allowed direct measurement of the global equivalence ratio which was used as a main correlating parameter. Characteristic global equivalence ratios and an ignition index concept were investigated to determine when sustained external burning would occur. Gas sampling was performed downstream of the hallway to determine the overall

efficiency of sustained external burning, and in the hallway to provide detailed data on the processes occurring in the hallway.

The oxidation of the exhaust gases traveling through the hallway was determined to vary among different species, and also to be very sensitive to the hydrodynamic mixing between the rich exhaust plume and the cooler ambient air in the hallway. In general, the overall oxidation of hydrocarbons was much more complete than for CO or soot. The gas temperatures in the hallway and fuel vaporization rate were also determined to affect oxidation in the hallway. Variations in the hallway inlet and exit soffits affected the hydrodynamic structure of the exhaust plume and oxidation efficiencies, with the inlet soffit exhibiting the strongest effect.

## **Dedication**

I dedicate this work to my family;  
my mother Pat, my brother Andy, and my wife Micki.

## Acknowledgments

First of all, I thank Dr. Uri Vandsburger, not only for adopting this project, but also for allowing me to work with him on this project. I thank him for his shared wisdom and guidance all along the way. I thank Dr. Rick Roby for initially introducing me into the field of combustion as an undergraduate. His thoughts, advice and insight have truly enhanced this project. I thank Dr. Larry Roe for serving on my committee.

I thank all of the undergraduate assistants that I have shared this project with; Wade Cole, Harrison Smith, Owen Wells, and Brad Bumgarner. Without their endless hours of effort, my research would have never been completed. I also thank my fellow graduate students, Ralf Ochel and Brian Lattimer, for their direct involvement and assistance on this project. Their thoughts and ideas always brought a fresh perspective to the project. I thank all of the graduate students of the reacting flows laboratory at Virginia Tech, past and present, not only for their assistance in times of need, but for sharing their own projects with me.

I thank Dr. Dan Gottuk for his initial guidance and continued assistance since he handed me the reins of this project. I thank the people at NIST/BFRL, especially Bill Pitts, for their support and funding for this project. I also thank the technical and administrative support at Virginia Tech, for their support and assistance during this project.

I especially thank my entire family who have always encouraged and supported me in my endeavors. I thank my mother, Pat, for her support through all of my years of life, and for influencing me to be who I am today. I thank my brother, Andy, for all of the good times we have shared growing up and will continue to share. I thank both my brother Andy, and my grandfather Chips Rehfeld, for our shared interest and curiosity in

the natural world, which has always encouraged and motivated my own pursuit of knowledge. I also thank my in-law's, Jack and Sharon Littley, for their continued support and encouragement.

Finally, I thank my wife Micki. Her support and understanding through all of the trying times allowed me to keep going. I can only repay her by giving her my eternal love.

## TABLE OF CONTENTS

	page
Abstract.....	ii
Dedication.....	iv
Acknowledgments .....	v
Table of Contents .....	vii
List of Figures .....	ix
List of Tables.....	xii
 CHAPTER 1 INTRODUCTION.....	 1
1.1 Motivation.....	1
1.2 Background .....	3
1.3 Previous Work.....	4
1.3.1 Introduction .....	4
1.3.2 In-Compartment and Open Jet Experiments.....	5
1.3.3 Corridor Flame Experiments.....	7
1.3.4 Remote Environment Experiments.....	10
1.4 Scope of Thesis.....	14
 CHAPTER 2 EXPERIMENTAL APPARATUS AND PROCEDURE .....	 16
2.1 Introduction.....	16
2.2 Experimental Apparatus.....	16
2.2.1 Compartment .....	16
2.2.2 Hallway.....	22
2.2.3 Exhaust System.....	24
2.2.4 Gas Sampling System.....	25
2.2.5 Gas Analysis System .....	27
2.2.6 Data Acquisition System .....	31



2.3 Experimental Procedure .....	33
2.4 Data Reduction .....	34
2.4.1 Data Reduction Program .....	34
2.4.1.1 Species Concentrations and Yields.....	34
2.4.1.2 Smoke Extinction Coefficient and Yield.....	37
2.4.1.3 Global Equivalence Ratio.....	39
2.4.1.4 Temperatures .....	40
2.4.1.5 Ignition Index .....	40
2.4.2 Video Data Reduction .....	42
2.4.3 Data Averaging .....	43
CHAPTER 3 RESULTS AND DISCUSSION.....	46
3.1 Introduction.....	46
3.2 Characteristic Equivalence Ratios.....	48
3.3 Ignition Index .....	60
3.4 Species-Sampled Results.....	64
3.4.1 Hallway Soffits: 0 cm inlet / 0 cm exit .....	64
3.4.2 Hallway Soffits: 0 cm inlet / 20 cm exit.....	73
3.4.3 Hallway Soffits: 20 cm inlet / 0 cm exit.....	77
3.4.4 Hallway Soffits: 20 cm inlet / 20 cm exit.....	83
CHAPTER 4 SUMMARY AND CONCLUSIONS .....	88
4.1 Summary .....	88
4.2 Conclusions .....	93
CHAPTER 5 RECOMMENDATIONS .....	97
REFERENCES .....	101
APPENDIX A: DATA REDUCTION PROGRAM .....	104
APPENDIX B: UNCERTAINTY ANALYSIS.....	121
VITA .....	133

## LIST OF FIGURES

Figure	page
1.1 HCN concentrations versus CO concentrations measured at the exit from the burn room to the hallway leading to the second floor and in the second floor room for all tests. (Reproduced from Reference [5]).....	12
1.2 Acrolein concentrations versus CO concentrations measured in the second floor room for all tests. (Reproduced from Reference [5]).....	12
2.1 Schematic of experimental apparatus. ....	17
2.2 Schematic of fire compartment structure.....	18
2.3 Schematic of air inlet duct housing .....	20
2.4 Schematic of gas sampling and analysis systems.....	26
2.5 Schematic of total hydrocarbon (THC) analyzer. ....	30
3.1 Characteristic equivalence ratios versus exhaust vent area. Experimental conditions: 0/0 soffit case, 23 cm diameter fuel pan. Each point represents the average of many tests, 95% confidence intervals shown except for single test data points.....	50
3.2 Characteristic equivalence ratios versus exhaust vent area. Experimental conditions: 0/0 soffit case, 20 cm diameter fuel pan. Each point represents the average of many tests, 95% confidence intervals shown except for single test data points.....	51
3.3 Characteristic equivalence ratios versus exhaust vent area. Experimental conditions: 0/20 soffit case, 20 cm diameter fuel pan. Each point represents the average of many tests, 95% confidence intervals shown except for single test data points.....	55
3.4 Characteristic equivalence ratios versus exhaust vent area. Experimental conditions: 20/0 soffit case, 20 cm diameter fuel pan. Each point represents the average of many tests, 95% confidence intervals shown except for single test data points.....	57
3.5 Characteristic equivalence ratios versus exhaust vent area. Experimental conditions: 20/20 soffit case, 20 cm diameter fuel pan. Each point represents the average of many tests, 95% confidence intervals shown except for single test data points.....	59

3.6	CO Yield versus "Quasi" steady state GER. Soffit case: 0/0, 0/20. The total heat release rate of the underventilated fires ranged from 254 - 562 KW for the 0/0 soffit case, and 360 - 554 KW for the 0/20 soffit case. Each point represents a single experiment. ....	65
3.7	THC Yield versus "Quasi" steady state GER. Soffit case: 0/0. The total heat release rate of the underventilated fires ranged from 254 - 562 KW. Each point represents a single experiment. ....	67
3.8	Normalized species concentrations and gas temperature versus hallway axial distance. Experimental conditions: 0/0 soffit case, 20 cm diameter fuel pan, 1200 cm <sup>2</sup> exhaust vent. Average GER: 2.0, average total heat release rate of fires: 413 KW. Sample location: 5.1 cm from ceiling, center width. Normalizing concentrations given in legend. ....	69
3.9	Normalized species concentrations and gas temperature versus hallway distance from ceiling. Experimental conditions: 0/0 soffit case, 20 cm diameter fuel pan, 1200 cm <sup>2</sup> exhaust vent. Average GER: 2.3, average total heat release rate of fires: 434 KW. Sample location: 1.83 m axially from compartment, center width. Normalizing concentrations given in legend. ....	72
3.10	THC Yield versus "Quasi" steady state GER. Soffit case: 0/20. The total heat release rate of fires ranged from 360 -554 KW. Each point represents a single experiment. ....	74
3.11	Normalized species concentrations and gas temperature versus hallway distance from ceiling. Experimental conditions: 0/20 soffit case, 20 cm diameter fuel pan, 1200 cm <sup>2</sup> exhaust vent. Average GER: 2.8, average total heat release rate of fires: 444 KW. Sample location: 1.83 m axially from compartment, center width. Normalizing concentrations given in legend. ....	76
3.12	CO Yield versus "Quasi" steady state GER. Soffit case: 20/0. The total heat release rate of fires ranged from 294 - 423 KW for low fuel rates, and 480 - 574 KW for high fuel rates. Each point represents a single experiment. ....	78
3.13	CO Yields versus fuel vaporization rate for all soffit combinations. GER range: 1.5 to 3.5 for all tests. Range of total heat release rate of fires: 254 to 574 KW for all tests. ....	79
3.14	Normalized species concentrations and gas temperature versus hallway axial distance. Experimental conditions: 20/0 soffit case, 20 cm diameter fuel pan, 1200 cm <sup>2</sup> exhaust vent. Average GER: 3.3, average total heat release rate of fires: 348 KW. Sample location: 5.1 cm from ceiling, center width. Normalizing concentrations given in legend. ....	80

3.15 THC Yield versus "Quasi" steady state GER. Soffit case: 20/0. The total heat release rate of fires ranged from 294 - 423 KW for low fuel rates, and 480 - 574 KW for high fuel rates. Each point represents a single experiment..... 82

3.16 CO Yield versus "Quasi" steady state GER. Soffit case: 20/20. The total heat release rate of fires ranged from 267 - 389 KW for low fuel rates, and 411 - 613 KW for high fuel rates. Each point represents a single experiment..... 84

3.17 THC Yield versus "Quasi" steady state GER. Soffit case: 20/20. The total heat release rate of fires ranged from 267 - 389 KW for low fuel rates, and 411 - 613 KW for high fuel rates. Each point represents a single experiment..... 86

## LIST OF TABLES

Table	page
3.1 Instantaneous ignition index for sustained external burning. 0 cm inlet soffit / 0 cm exit soffit. ....	63
3.2 Instantaneous ignition index for sustained external burning. 0 cm inlet soffit / 20 cm exit soffit.....	63
4.1 Post-compartment oxidation efficiency ranges for underventilated compartment fires. Data for hallway tests with various soffit heights and open jet tests [11,12].....	91

# CHAPTER 1

## INTRODUCTION

### 1.1 Motivation

In 1992, fires resulted in 4,730 deaths and 28,700 injuries as reported in the United States [1]. Approximately 2/3 of the deaths caused by fires are the direct result of inhaling the toxic fire exhaust gases [2,3]. Due to the obvious significance of exhaust gas inhalation in fire fatalities, the classification of environments in burning residential and commercial buildings, termed compartment fires, has become a major topic of investigation.

Prior studies have determined carbon monoxide (CO) to be the most significant fire exhaust gas, in terms of toxic levels, for a wide range of fuels [4,5]. The significance of CO is due to a combination of the high toxicity of CO, and the high concentrations typically found in post-flashover compartment fires. The next two significant gases that have been shown to make small contributions to the total toxicity of compartment fire exhaust gases are the aldehyde acrolein, and hydrogen cyanide [4,5]. The concentrations of these gases become significant when complex fuels are burned, such as plastics and textiles typically found in actual compartment fires [4,5].

CO is an odorless and colorless gas that acts as an asphyxiant when inhaled. CO interrupts the flow of oxygen through the blood stream by reacting with hemoglobin (Hb). Hemoglobin is a carrier in the blood stream that delivers oxygen throughout the body. Since CO has an affinity for hemoglobin about 300 times greater than that of oxygen, it forms the stable species carboxyhemoglobin (COHb) [6]. Therefore, small concentrations of inhaled CO can disable a significant percentage of hemoglobin in the body for an

extended period of time. CO concentrations as little as 2000 ppm are lethal within one hour of exposure [6]. Increasing the CO concentration to 1% decreases the lethal exposure period to one minute, which results in over 90% carboxyhemoglobin in the blood stream [6].

The concentrations of CO inside a burning compartment have been determined to reach up to 6% in a non-flammable compartment [7], and even higher, to concentrations greater than 14% with pyrolysis of a wood lined ceiling [8]. It is apparent that CO poses a serious threat inside a burning compartment. The effects of extreme heat and depletion of oxygen also contribute to the threat within a burning compartment. In addition, since CO is an odorless and colorless gas, the transport of this toxic gas to regions remote from the burning compartment poses a serious threat. Due to the inability of the human senses to detect CO, most deaths in compartment fires occur in rooms remote from the fire.

Some studies have been conducted to investigate the transport of exhaust gases to rooms other than the burning room, but there is still much more work to be done. These studies are summarized and discussed in section 1.3 on previous work. The transport of exhaust gases to other locations is a complex phenomenon due to the coupling between the chemical, thermodynamic, heat transfer, and fluid dynamic transport processes involved. Adding to the complexity of the problem, a large number of varied building geometries and orientations exist which significantly affect all of these processes in different ways.

Computer models that predict the behavior of compartment fires have been developed, and are continuing to be developed, refined, and upgraded. Again, the complex coupling of chemistry, heat transfer, thermodynamics, and fluid dynamics causes modeling compartment fires to be very difficult. This complexity of compartment fires

would result in models, based on first principles, requiring unacceptably long run times. Due to this obstacle, current computer fire models incorporate several simplifying assumptions. Experiments are required to determine what assumptions can be made in fire models with minimal loss of accuracy. Experiments allow simplified correlations to be developed, which may be used in place of solving many coupled, complex, fundamental equations. Experimental results are also required for validation of computer models once developed. One example of a developing computer model is given in Reference [9].

## **1.2 Background**

During the initial stage, most compartment fires begin as overventilated fires, with more than sufficient oxygen available for complete combustion of the fuel. Therefore, little or no production of toxic, incomplete products of combustion occurs, and no threat of toxic gases exists. If conditions exist such that the fire continues to develop, flashover occurs where every fuel source in the burning room becomes active in the fire. During this stage, fuel is vaporized faster than the room can be supplied with air, due to the limited number and sizes of ventilation paths. The fire during this stage is termed underventilated. With insufficient oxygen for complete combustion of the vaporizing fuel, generation of toxic, incomplete products of combustion results.

During the post-flashover stage of a fire, a layer of hot, buoyant, exhaust gases collects in the top of the compartment. The depth of this layer grows during the fire, and eventually drops below the height of the soffits of the room exits, i.e. doorways and windows. The exhaust gases then spill through the exit into the neighboring space to either the exterior of the building or another room or hallway. This causes the transport of toxic exhaust gases, posing a threat to anyone in an adjacent space. As the fuel rich exhaust gases escape from the compartment, ambient air in the adjacent space is entrained



into the exhausting gases. If the exhaust gas mixture entrains enough air to become flammable, and an ignition source is present, burning of the exhausting gases can occur. This phenomenon is termed external burning.

External burning can result in the complete oxidation of the toxic exhaust gases to less threatening carbon dioxide ( $\text{CO}_2$ ) and water provided the correct conditions exist. However, incomplete oxidation may occur if air entrainment is insufficient or unfavorable conditions exist, possibly resulting in a more toxic environment.

A useful concept of classifying the severity of a fire, and allowing development of correlations, is used in this work. This concept has been termed the global equivalence ratio (GER) concept [10]. The GER is defined as the overall equivalence ratio for the diffusion flame inside the burning compartment. Specifically, the GER is the ratio of the fuel vaporization rate to the air inlet rate into the compartment, normalized by the stoichiometric ratio. The GER concept was chosen to be used in this study because it has been successfully utilized for correlations of species generation rates inside a burning compartment and downstream of a burning compartment exhausting into the open atmosphere [11].

## **1.3 Previous Work**

### **1.3.1 Introduction**

Many studies have been performed to investigate the environment generated inside a burning compartment [7,8,11] and immediately outside of a burning compartment [4,5,11,12]. However, only a few experimental studies [4,5,13,14] have touched on the subject of exhaust gas transport from a burning compartment to other locations within the

confines of a building. These few studies have only begun to investigate the exhaust gas transport phenomenon.

The work that has been completed on exhaust gas transport has focused on two main areas. First, studies have been performed to investigate the characteristics of a flame as it impinges on a ceiling above the fire [13,14]. The second area of focus has been on the species environment produced in a remote location from the burning compartment within the same confined structure [4,5]. However, no studies have been conducted to investigate the detailed composition of the exhaust gases during transport to remote locations, including the effects of external burning on these exhaust gases.

This section provides a summary of one compartment fire study of the environment produced inside a burning compartment, and of the environment produced as a compartment exhausts into the open atmosphere. Those experimental results are later compared with results of this study for oxidation efficiency analysis. Also discussed in this section are the published transport studies from both focus areas so that the scope of this study may be distinguished to be unique compared to prior work.

### **1.3.2 In-Compartment and Open Jet Experiments**

The studies by Gottuk et al. [7,11,12] were used to compare with the data of the current experiment since both experimental studies utilized the same test compartment. Gottuk et al. [12] performed an investigation focused on the effect of open jet external burning, i.e. the burning of exhaust gases from a compartment fire as they vented to the open atmosphere, on destroying carbon monoxide and soot escaping from the burning compartment. These experiments were compared to the previous study of Gottuk et al. [7] on the exhaust gas composition inside a compartment, during similar fires, to

determine the efficiency of external burning in oxidizing CO and soot. A summary of these studies is given below.

Two distinct types of external flames were observed during compartment fires. Chronologically, external flame jets appeared first as ceiling jets extended from the main fire within the compartment, and out through the exhaust vent [11,12]. During significantly underventilated fires in the compartment, the second type of external flames occurred when the exhausting flammable gases from the compartment mixed with a sufficient amount of ambient air, and were ignited causing external burning [11,12]. Three different types of external burning were observed: 1) quick flashes, 2) short bursts lasting greater than one second, and 3) sustained external burning [11,12].

Overventilated fires never produced external burning due to the sufficient availability of oxygen in the compartment, resulting in complete combustion of the fuel inside the compartment. In this case, no flammable gases existed in the upper layer of the compartment to be exhausted and burned. For underventilated fires, there existed characteristic global equivalence ratios (CGER) that marked the onset of external flashes, and then sustained external burning.

Flashes were reported to occur at a CGER of  $1.4 \pm 0.4$  [11,12]. The CGER for sustained external burning showed a slight dependence on the exhaust vent area, reported as  $2.1 \pm 0.3$  for exhaust vents of 400 cm<sup>2</sup> area, and  $1.8 \pm 0.2$  for exhaust vents of area in the range of 800 to 1600 cm<sup>2</sup> [11,12]. This exhaust vent dependence was explained by the smaller flame jets observed with the smaller area exhaust vents, reducing the ability to ignite the exhausting gases [11,12]. Although the flammability of the exhaust gases mixing with ambient air was determined by the GER, the occurrence of sustained external burning was found to be controlled by the size of the ignition source.

Although an instantaneous GER of 1.8 (2.1 for small vents) was required for sustained external burning to begin, compartment fires that produced a "quasi-steady-state" average GER equal to or greater than 1.7 produced sustained external burning [11,12]. The occurrence of sustained external burning was the only form of external burning observed to reduce CO and soot levels significantly [11,12]. A species yield was defined as the ratio of grams of a given species produced to grams of fuel burned. The species yield for CO allowed determination of the oxidation efficiency. The downstream CO yields during sustained external burning were reduced to 10 - 25 % of the yield measured in the compartment, an average value of 0.22, for underventilated fires [11,12]. CO<sub>2</sub> yields downstream also approached their theoretical maximum during sustained external burning, indicating near complete oxidation of all carbon to CO<sub>2</sub> [11,12].

The effect of sustained external burning on soot yields was significant, following the same trends as CO oxidation, but with a larger amount of scatter in the data [11,12]. Soot was oxidized to 0 - 50% of levels observed just prior to sustained external burning [11,12]. On average, soot yields prior to sustained external burning reached about 0.015 [11].

### **1.3.3 Corridor Flame Experiments**

Hinkley et al. [13] performed an investigation of flames extending below both combustible and non-combustible ceilings. The focus of this study was to develop correlations for horizontal flame lengths and the downward radiation from the flame and gases. This study was performed with a town gas burner (and some wood crib experiments) to represent a fire at one end of a 7.3 m long, 1.2 m wide corridor. Flames from the burner were such that they extended to the ceiling and were deflected horizontally towards the open end of the unidirectional corridor. The corridor was not

completely enclosed, as the walls extended downward from the ceiling, located 1.8 m above the floor, roughly half way to the floor.

The measurements made included downward radiation (measured along the corridor with radiometers), ceiling surface temperature and heat flux, gas temperatures, gas velocity with both a pitot tube and "streak" photography, oxygen concentrations, and the mass burn rate of the combustible ceilings. Experiments were conducted with variable gas fuel supply rates (140-500 kW/m hall width) and variable heights of the burner from the ceiling (0.37 - 1.2 m) to vary the extension of the flame down the corridor. A constant flame was burned until heat transfer to the ceiling reached steady state before data was acquired. For the combustible ceiling experiments, different materials were tested.

The experiments of Hinkley et al. [13] indicated some interesting results. Correlations for the extended length of flames deflected below non-combustible ceilings were developed, and found to depend greatly on whether sufficient air for complete combustion was entrained in the vertical plume. This dependency was found to be related to the much reduced air entrainment rates for the horizontally flowing buoyant gases, about 12.5 times less efficient than for a vertical plume. Horizontal flames were found to have a significantly greater contribution to flame spread, compared to the vertical plume, due to the increased radiation downward for horizontal flames, and the transport of flames to other locations. The downward radiation from the horizontal flames was found to decay exponentially moving away from the source fire, with slightly more heat transfer to the ceiling than radiated downward.

For combustible ceilings, longer flames and more downward radiation was evident from the experiments. This was due to the additional fuel supplied to the flame by the

combustible ceiling. The downward radiation with combustible ceilings also behaved exponentially, however, with a slower rate of decay than for the non-combustible ceilings.

This study by Hinkley et al. [13] was not a direct study of the true transport of exhaust gases through an enclosure, mainly due to the lack of corridor walls extending completely to the floor. In true enclosed transport, the effect of the limited oxygen availability is expected to dominate in affecting the source flame and extension of the flame. Due to the open environment, the source flame not only burned in the overventilated mode, air entrainment into the horizontal flame was most likely greater than for full length corridor walls. Note that species sampling was limited to oxygen concentrations only, allowing no possibility for any kinetic oxidation analysis. Only one hallway configuration was used, without investigation of soffits in the hallway. Also, no investigation of turning the flame direction through a corner of the corridor was attempted. It is obvious that many additional interesting experiments could be performed.

A later study by Babrauskas [14] developed calculation procedures for estimating flame lengths under non-combustible ceilings for simple fuel geometries. Procedures for four cases were developed, comprised of an unbound ceiling and plume, a free plume in a room corner, a plume attached to walls in a room corner, and unidirectional corridor spread. The calculations were compared to experimental data, with only the experiments of Atallah [15] and Hinkley et al. [16] available on unidirectional corridor spread.

The calculated flame lengths were relatively accurate compared to the experimental results, being 10% low on average [14]. It was indicated that further experimental data was necessary for further development and confirmation of the correlation [14]. Limitations of the calculation procedures of Babrauskas [14] are the

same as indicated for the experiments of Hinkley et al. [16] since the correlations were based on that data.

### **1.3.4 Remote Environment Experiments**

Fardell et al. [4] conducted large scale experiments with a burning compartment exhausting perpendicular to the axial direction of an 11.4 m long, 1.2 m wide corridor with full height walls. This study investigated the environments produced just outside of the compartment, and at the end of the corridor by burning four fuels; wood (pine), polymethyl methacrylate (PMMA), polypropylene homopolymer (PP), and expanded polystyrene (EPS). Only two ventilation conditions were used with a 2 m high door between the burning compartment and the corridor, opened 0.76 and 0.2 m wide. The door provided the single ventilation path between the burning compartment and the corridor for both air flow into the compartment and exhaust gases flowing out of the compartment. Gas sampling was performed at two locations in the corridor, both 15 cm from the ceiling; one location just outside of the burning compartment, and the other at the end of the corridor. The gas samples were analyzed for carbon monoxide (CO), carbon dioxide (CO<sub>2</sub>), and oxygen (O<sub>2</sub>) continuously. Gas chromatography was used to analyze spot samples taken at three different stages of the fire; development, post-flashover, and decay. Between 20 and 40 hydrocarbon compounds were found in analysis of the spot samples. Other measurements made included gas temperatures, smoke measurements at the exit of the corridor, and crude air inlet velocity measurements at the open end of the corridor.

The main focus of the study by Fardell et al. [4] was to investigate the toxicity of the environment produced at the sampled locations, and the dependence on the fuel burned and the stage of the fire. Many types of hydrocarbons were found with spot

sampling, including oxygenated organics, saturated and unsaturated hydrocarbons, and aromatic hydrocarbons. The types of compounds found for each fuel were similar, although their concentrations varied between fuels, ventilation conditions, and stages of the fire. Overall, CO was found to be by far the most significant toxic gas, in concentration and toxicity, at both locations sampled. The next significant toxic gas found was acrolein, an aldehyde; however, a high concentration of CO was indicated whenever significantly high concentrations of acrolein were present. It was noted that most hydrocarbons analyzed did not pose an immediate lethal hazard at any time during the fire, although they would have contributed to the irritancy of the gases.

Morikawa et al. [5] performed experiments with a fire resistant two-story house with a first floor burning room vented to the open atmosphere and to a hallway attached to stairs leading to the second floor. A room on the second floor had a variable door size which was varied for different experiments. The burning room was equipped with typical room contents of furniture and draperies, representing a wide range of materials.

Continuous monitoring of CO, CO<sub>2</sub>, and O<sub>2</sub> was performed in the first floor hallway just outside of the burning room, and in the second floor room, at both high and low locations. Spot sampling of gases allowed chromatographic analysis of hydrogen cyanide (HCN) and acrolein concentrations at the same sampling locations. Other toxic gas concentrations were not analyzed since a previous study by the authors indicated these two to be the most significant toxic species other than CO [17]. Other measurements made included gas temperatures, smoke measurements, and gas velocities with bi-directional pitot tubes.

The results indicated, as in Hinkley et al. [13], that CO was the toxic gas with the most significant concentration in the fire exhaust. Figures 1.1 and 1.2 show reproductions



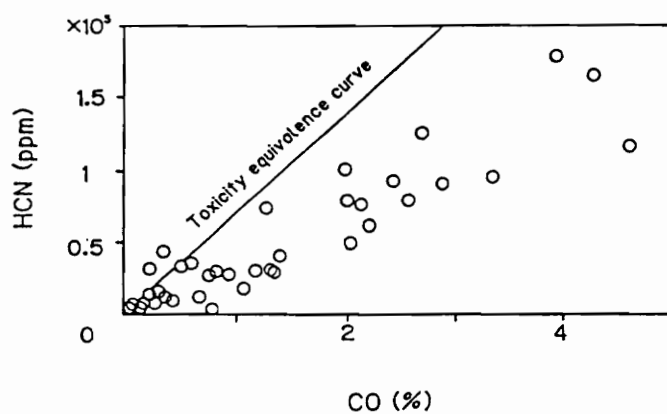


Figure 1.1 HCN concentrations versus CO concentrations measured at the exit from the burn room to the hallway leading to the second floor and in the second floor room for all tests. (Reproduced from Reference [5]).

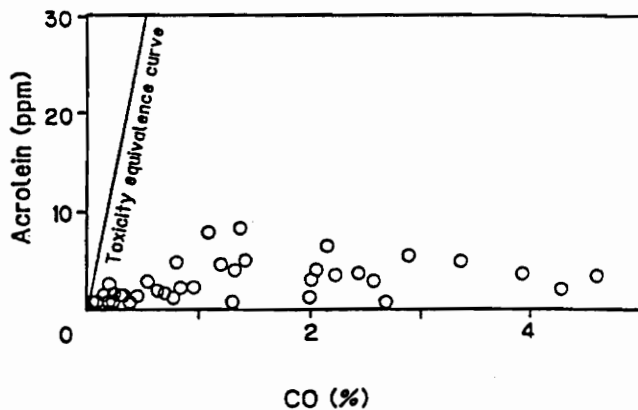


Figure 1.2 Acrolein concentrations versus CO concentrations measured in the second floor room for all tests. (Reproduced from Reference [5]).

from Reference [5] of a comparison of the toxicity of CO versus HCN and acrolein, respectively, for all of the sampled locations and for all experiments presented. The toxicity equivalence lines are based on lethal concentrations over a time period of 5 to 10 minutes, with these levels being 5000 ppm for CO, 350 ppm for HCN, and 30 ppm for acrolein. Note that the majority of the data points presented in these figures are located below the toxicity equivalence line, on the CO side, indicating that CO was the toxic gas with the most significant concentration for these experiments, and with a significant margin.

However, investigation indicated that the CO levels alone were not completely responsible for the lethal toxicity of the atmosphere in the second floor room, but that HCN had a significant contribution. HCN was found to be generated only during the burning of nitrogen containing fuels, which was highly dependent on how the fire spread within the burning compartment. The levels of acrolein in the second floor room were always found to be less than toxic on a 10 minute exposure time scale. One interesting point discovered indicated that a toxic environment in the second floor room was generated, even when the door was completely closed, leaving only small leaks around the door.

Both of the studies, by Fardell et al. [4] and Morikawa et al. [5], focused on the toxicological effects of the atmosphere generated. Neither study investigated the detailed chemical kinetics of how the composition of the gases exhausting from the burning compartment changed during transport to the other remote locations. Even though sampling was made in two locations, comparisons between these locations was not extensively discussed in either paper.

These studies only investigated a very limited number of ventilation cases, with no clear, well defined classification scheme for the different ventilation cases. Neither study indicated whether external burning of the exhaust gases occurred during transport. Both studies also picked a single building geometry for all experiments, with no systematic investigation of the effect of room and corridor geometry on the environments produced.

#### **1.4 Scope of Thesis**

The focus of this study was to investigate the evolution of compartment fire exhaust gases during transport through a hallway. The fuel rich plume exhausting from a compartment fire, into an adjacent enclosed space, mixed with ambient air allowing oxidation of incomplete products of combustion. Emphasis in this study was placed on investigation of the physical phenomena occurring during transport and oxidation of the exhaust gases, responsible for the overall species oxidation efficiencies. Related research reported prior to this study lacked key elements of this investigation.

The previous studies covered two main areas. First, some studies investigated the extension of flames below ceilings. These experiments were not concerned with the detailed chemical kinetics, but more on simple correlations for flame lengths. These experiments were also not conducted in spaces with fully enclosed walls, leaving out the important effects of restricted transport of air to the exhaust gases through the enclosed space.

The second area of investigation focused on the toxic environments produced in enclosed locations, remote from a burning compartment. These studies focused on the toxicity of the environments produced, and not on the details of how toxic gases were transported to, or produced in these environments. These studies only investigated fixed enclosure geometries with a limited number of ventilation cases.

The goal of this study was to investigate the efficiency of oxidation in the hallway and the relative effects of two aspects on the efficiency. These aspects included: 1) the chemical effects of different gas compositions in the compartment exhaust plumes, characterized by the GER, and 2) the fluid dynamic transport effects, determined by the compartment exhaust vent size, and the soffit heights at both the entrance to the hallway from the compartment, and at the exit of the hallway to the open atmosphere.

Experiments were performed with a compartment fire exhausting into a 3.7 m long hallway, with exhaust gases flowing directly along the hallway axis and exiting the hallway to the open atmosphere. Four soffit combinations, consisting of 0 and 20 cm soffit heights at both ends of the hallway, were investigated. For each soffit case, experiments were conducted for several different underventilated compartment fire cases. The design of the compartment allowed direct measurement of the GER by separating the air inlet and exhaust gas exit ventilation paths. Measuring both the air inlet mass flow rate and the fuel vaporization rate allowed the GER to be calculated.

Exhaust gases were sampled both well downstream of the hallway exit and inside the hallway. Downstream sampling allowed investigation of overall species levels exiting the hallway, where hallway sampling allowed detailed investigation of species consumption and production occurring in the hallway. Gas species concentrations measured included carbon monoxide, carbon dioxide, oxygen, and total hydrocarbons measured as ethylene. Soot measurements were taken downstream of the hallway only. Vertical gas temperature profile measurements were taken both in the compartment, and in the hallway at various locations.

## **CHAPTER 2**

### **EXPERIMENTAL APPARATUS AND PROCEDURE**

#### **2.1 Introduction**

This chapter describes the experimental apparatus and experimental procedure used for all of the experiments reported. This chapter is divided into three main sections: 1) description of the experimental apparatus and data acquisition equipment, 2) discussion of the experimental procedure, and 3) discussion of the data reduction calculations and procedure.

#### **2.2 Experimental Apparatus**

A schematic of the experimental apparatus used for experiments is given in Figure 2.1. Discussion of this apparatus has been separated into sections on: 1) the compartment and related instrumentation, 2) the hallway and related instrumentation, 3) the exhaust system and related instrumentation, 4) the gas sampling system, 5) the gas analysis system, and 6) the data acquisition system.

##### **2.2.1 Compartment**

A schematic of the main compartment structure with dimensions is given in Figure 2.2. This main structure consisted of two levels, a 1.2 m long x 1.5 m wide x 1.2 m tall fire compartment located above a 1.2 m long x 1.5 m wide x 0.4 m high air distribution plenum. The frame for the compartment consisted of welded 0.635 cm thick, 5.08 cm steel angle iron and 5.08 cm wide bar stock. The inside surface of the fire compartment

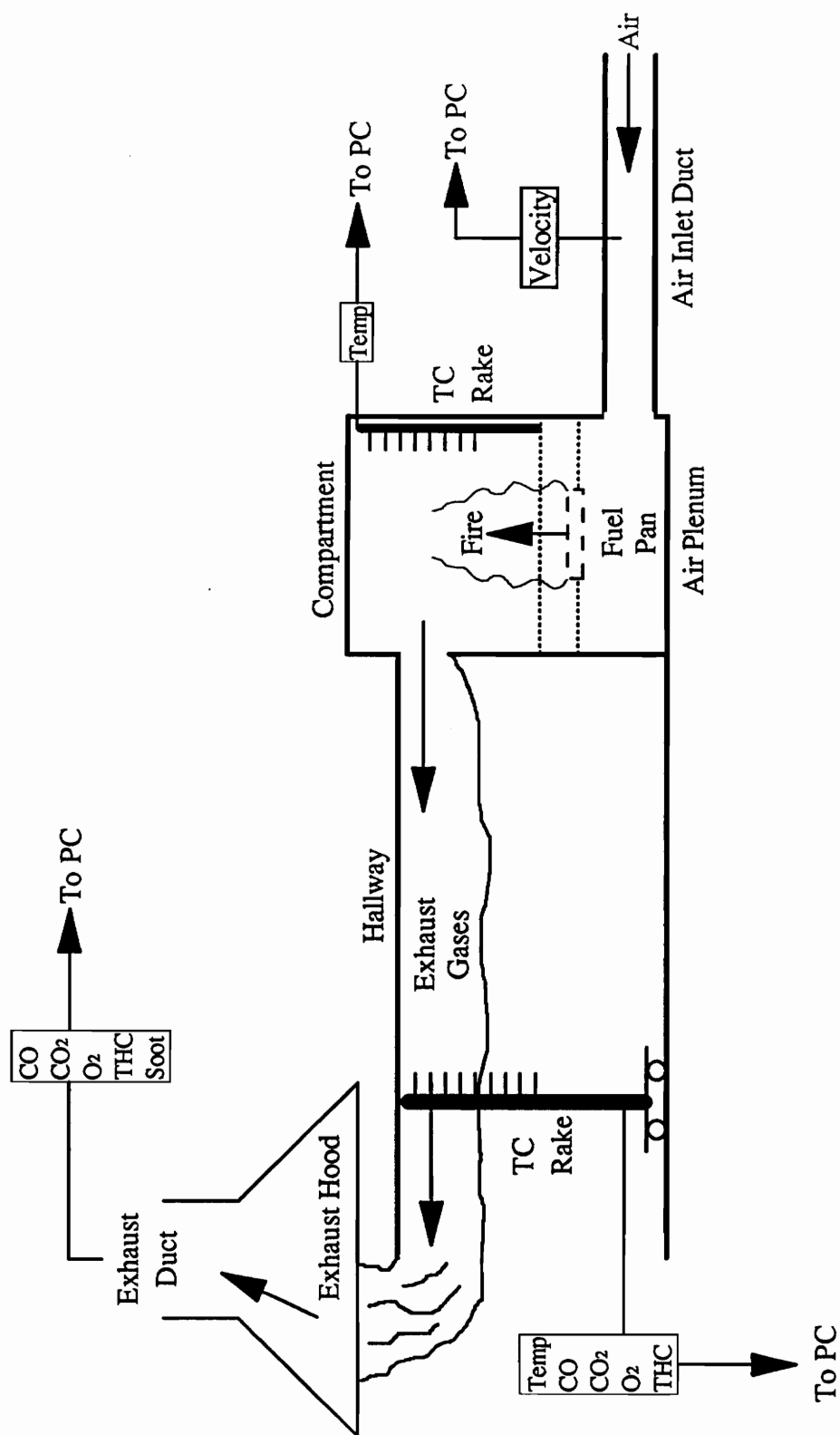


Figure 2.1 Schematic of experimental apparatus.

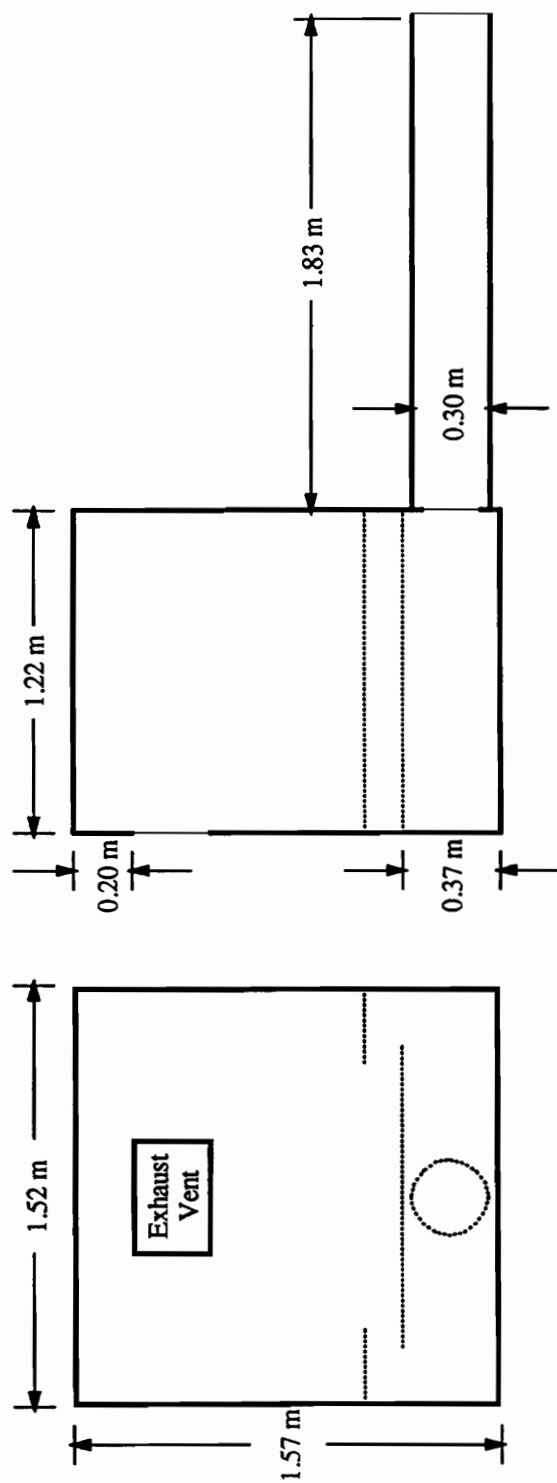


Figure 2.2 Schematic of fire compartment structure

consisted of 2.54 cm thick Fire Master, UL rated, fire insulation board. The inside surface of the air distribution plenum consisted of 0.3175 cm thick sheet steel.

A 1.83 m long, 30 cm diameter air inlet duct allowed air to be drawn naturally into the back of the air distribution plenum during experiments. Air was distributed uniformly to the bottom of the fire compartment through two thermally shielded vents, one on each side of the fire compartment floor. Each thermal shield extended 28 cm out from the side walls.

The air inlet duct was equipped with a Kurz model 415, hot film velocity probe and a bare type K thermocouple to allow measurement of the air velocity and temperature. From these measurements, the air mass flow rate into the compartment could be calculated. The velocity probe was calibrated for a range of 0-2 m/s. The velocity probe sensing element was located 0.9 m from the open end of the inlet duct, and 10.5 cm radially above the center line of the inlet duct. The radial position for the sensing element was selected by scanning the radial velocity profile, which was determined to be relatively flat due to the turbulent, underdeveloped flow. The velocity probe position was chosen as the location that provided the area averaged velocity.

Space limitations at the facilities restricted the inlet duct to a length shorter than recommended by the Kurz velocity probe installation guide. To compensate, the entrance of the air inlet duct was shielded by a wooden cubical housing, as shown in Figure 2.3, with an inner surface dimension of 0.76 m on all edges. The inner surface was covered with 0.635 cm thick finishing plywood, to allow smooth air flow through the housing into the duct. The inlet duct was centered in the single uncovered side of the box, and located at a depth of 0.305 m into the box. This housing provided considerable reduction in the noise levels measured by the velocity probe.



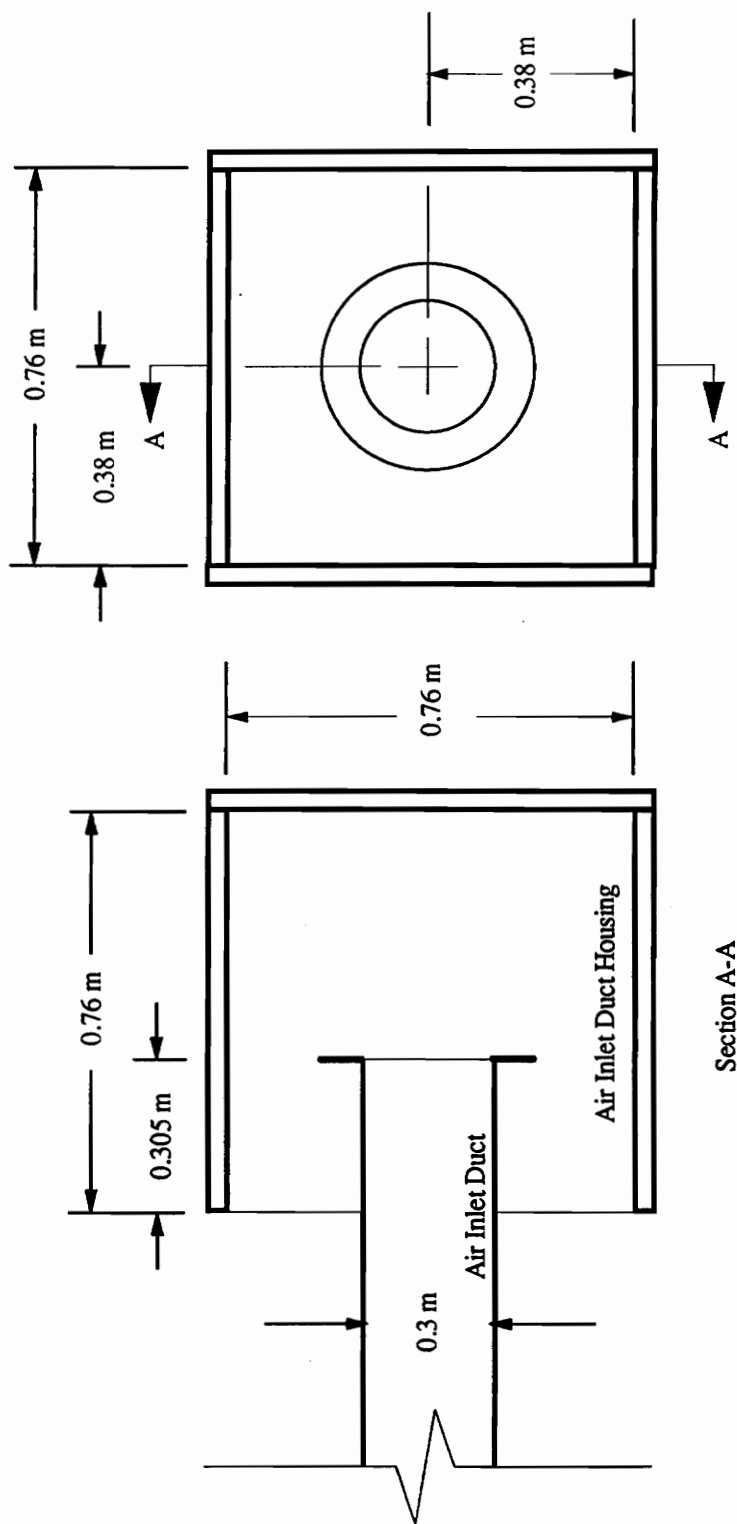


Figure 2.3. Schematic of air inlet duct housing

The installed velocity probe calibration was checked against the mass flow rate determined from a series of methane tracer dilution tests. The methane tracer tests involved injecting a measured flow rate of pure methane into the entrance of the air inlet duct. By measuring the uniform concentration of methane exiting the air inlet duct, into the air distribution plenum, the mass flow rate of air into the compartment could be calculated. The uncertainty of the velocity probe calculated mass flow rate, compared to the methane tracer tests, was determined to be within  $\pm 5\%$ .

A 15 kg A&D platform load cell, with 1 gm resolution, was located in the air distribution plenum. A 2.54 cm diameter aluminum rod connected a platform resting on the load cell to a platform in the fire compartment through a 3.2 cm diameter hole through the fire compartment floor. Both platforms were insulated with 2.54 cm thick fire insulation board to minimize the thermal effects on the load cell due to heat transfer from the fire in the fire compartment. A circular fuel pan was located on the platform in the fire compartment, which allowed measurement of the fuel weight during experiments. The fuel pans were constructed of 3.2 mm thick carbon steel, 6.4 cm deep with diameters ranging from 15 to 23 cm. The different fuel pan diameters allowed variation of the size of the compartment fire.

The fuel used for all experiments was reagent grade (99.9% purity) liquid hexane,  $C_6H_{14}$ . The liquid hexane was supplied by J. T. Baker, Inc. in 200 liter drums, and contained a mixture of isomers with an average molecular weight of 86.18.

The fire compartment was equipped with a stationary, aspirated, vertical rake holding 8 type K (nickel-chromium vs. nickel-aluminum), 30 gage thermocouples in the front corner of the compartment. The rake was constructed of 0.635 cm stainless steel tubing and Swagelok fittings, providing radiation shielding for the thermocouple beads. A

flow of gases through the thermocouple rake was induced by a Dayton Speedaire diaphragm vacuum pump, model #4Z024. Flow traveled through a water trap submerged in an ice bath, maintained at 0°C, and through a Gelman glass fiber filter before entering the pump. This allowed the gas to be cooled and filtered to avoid damaging the pump. The in-compartment thermocouples were spaced vertically 10 cm apart, starting at 10 cm from the ceiling, and spaced 10 cm from the walls to avoid wall jet effects.

A window style exhaust vent, centered with respect to the compartment width direction, was located in the front wall of the fire compartment. Exhaust vent sizes typically used in the hallway experiments included: 25 cm wide x 16 cm tall (400 cm<sup>2</sup>), 50 cm x 16 cm (800 cm<sup>2</sup>), and 50 cm x 24 cm (1200 cm<sup>2</sup>). The combination of exhaust vent size and fuel pan size used determined the steady-state global equivalence ratio produced in the compartment, which ranged from about 1.5 to 3.5 for the combinations used in the reported experiments. Exhaust vent sizes used assured only outward flow of exhaust gases from the compartment beginning shortly after ignition. For all exhaust vents, a soffit of 20 cm existed inside the compartment, between the compartment ceiling and the top of the exhaust vent.

### **2.2.2 Hallway**

The exhaust vent from the compartment opened into a 3.66 m long, 1.14 m wide, and 1.47 m tall hallway. The ceiling was lined with 2.54 cm Fire Master fire insulation board attached to a carbon steel frame, constructed with similar materials to that for the compartment frame. The walls of the hallway consisted of 6 modular sections. Each wall section consisted of gypsum board mounted on a steel self supporting frame. The complete inner surface of the assembled hallway walls were lined with Fiberfax fireproof insulating sheets.

A removable piece of the Fire Master insulation board allowed adjustment of the soffit at the exit of the hallway from 0 cm to 20 cm. The height of the hallway soffit at the inlet to the hallway, the distance between the hallway ceiling and the top of the compartment exhaust vent, was adjustable from 0 cm to 20 cm by raising the hallway ceiling, and extending the walls with insulation covered drywall.

A manually mobile, aspirated, vertical thermocouple rake holding 9 type K, 30 gage thermocouples was utilized in the hallway. The vertical spacing between thermocouples was 5.1 cm, typically starting 5.1 cm from the ceiling. The position of the thermocouple rake in the hallway was fully adjustable in three dimensions. The thermocouple rake was equipped with a sampling probe (see section 2.2.4), which had an adjustable height. The sampling probe was typically located so that one of the thermocouples was located at the same height and axial location, with a 5.1 cm width offset. For some experiments, a bare thermocouple was located at the same location as the sampling probe, but offset 2 cm in the width direction.

The rake was constructed of 0.635 cm diameter stainless steel tubes attached with Swagelok fittings to a 3.2 cm OD carbon steel pipe, with a wall thickness of 0.3 cm. The flow of gases through the thermocouple rake was forced by a Dayton Speedaire diaphragm vacuum pump, model #4Z024. Flow traveled in through the stainless steel tubes, into the steel pipe, out the bottom of the steel pipe through a high temperature (260°C max.), flexible Teflon tube. The dimensions of the Chem Pruf Teflon TFE tubing were 0.635 cm OD, with a 0.8 mm wall thickness. From the Teflon tube, the hot gases traveled through a water trap submerged in a 0°C ice bath, and through a Balston 915A, DX grade, glass fiber filter before entering the pump, again to avoid pump damage.

The thermocouple beads were located just inside the end of the aspirated stainless steel tubes for most experiments. This bead location allowed for the quickest time response and minimal radiation effects. For the early experiments with no hallway soffits, the thermocouple beads were recessed inside the aspiration tube about 3 to 4 cm. Comparison to a bare thermocouple indicated that the time response was very slow, due to heat transfer to the tubes. This caused the measured temperatures to be significantly lower than the true gas temperature. Temperatures measured with this thermocouple arrangement were approximately corrected as indicated in Appendix B.

### **2.2.3 Exhaust System**

A 1.5 x 1.5 m exhaust hood connected to a 45.7 cm diameter duct collected all exhaust gases exiting the end of the hallway. Flow through the hood was forced by a 9.3 kW, 142 m<sup>3</sup>/min blower downstream of the hood. An orifice plate arrangement in the exhaust duct allowed measurement of the volumetric flow rate through the duct. According to an A.S.T.M. standard design [18], a 30.5 cm inside diameter, sharp edged orifice plate was installed with two pressure taps, located one diameter downstream and one half diameter upstream of the orifice plate respectively. The pressure drop across the orifice plate was measured using a standard water manometer connected across the pressure taps. The measured pressure drop allowed calculation of the volumetric flow rate through the exhaust duct based on an equation provided in Reference [18] for the implemented design.

A laser extinction system in the exhaust duct, located 2.4 diameters downstream of the exhaust duct sampling probe and 3.7 diameters upstream from the orifice plate, enabled continuous measurement of the extinction coefficient, which allowed estimation of the smoke yield. A 670 nm, 5 mW diode laser, D. O. Industries model # LDA-1001, was

aligned along a path through small holes in the exhaust duct, perpendicular to the flow, and detected by a photo diode assembly. Oriel neutral density filters and diffusers were installed in the photo diode assembly to provide a signal in a detectable range with sufficient resolution.

#### **2.2.4 Gas Sampling System**

The gas sampling system, shown in Figure 2.4, allowed sampling from one of two different locations. One sample line drew gases from the exhaust duct, and another from the hallway. All of the plumbing lines for the sampling system consisted of 0.635 cm diameter stainless steel tubing. The sample lines were heated to about 120°C using Thermolyne electrical resistant heating tape, in order to keep water and high molecular weight hydrocarbons from condensing in the sample line.

The exhaust duct gas sampling probe was fixed in the center of the exhaust duct and well downstream of the exhaust hood. The probe was a 0.635 cm stainless steel tube with 0.3175 cm holes drilled every 2.54 cm perpendicular to the tube. Since the exhaust duct gas was fairly diluted, only a small Gelman glass fiber filter was required to trap out soot.

The hallway gas sampling probe was located inside the hallway mounted on the vertical thermocouple rake. The probe was a 0.635 cm diameter stainless steel tube attached to a heated stainless steel gas sample line at the exit of the hallway with high temperature (260°C), flexible Teflon tubing. The Chem Pruf Seamless Teflon TFE tubing had dimensions of 0.635 cm O.D., with a 0.8 mm wall thickness. This allowed three dimensional position adjustment of the gas sampling probe with the thermocouple rake. Since the soot loading in the hallway was much higher than in the diluted exhaust duct, a heavy duty glass fiber filter was used in series with the small Gelman filter. The Balston,

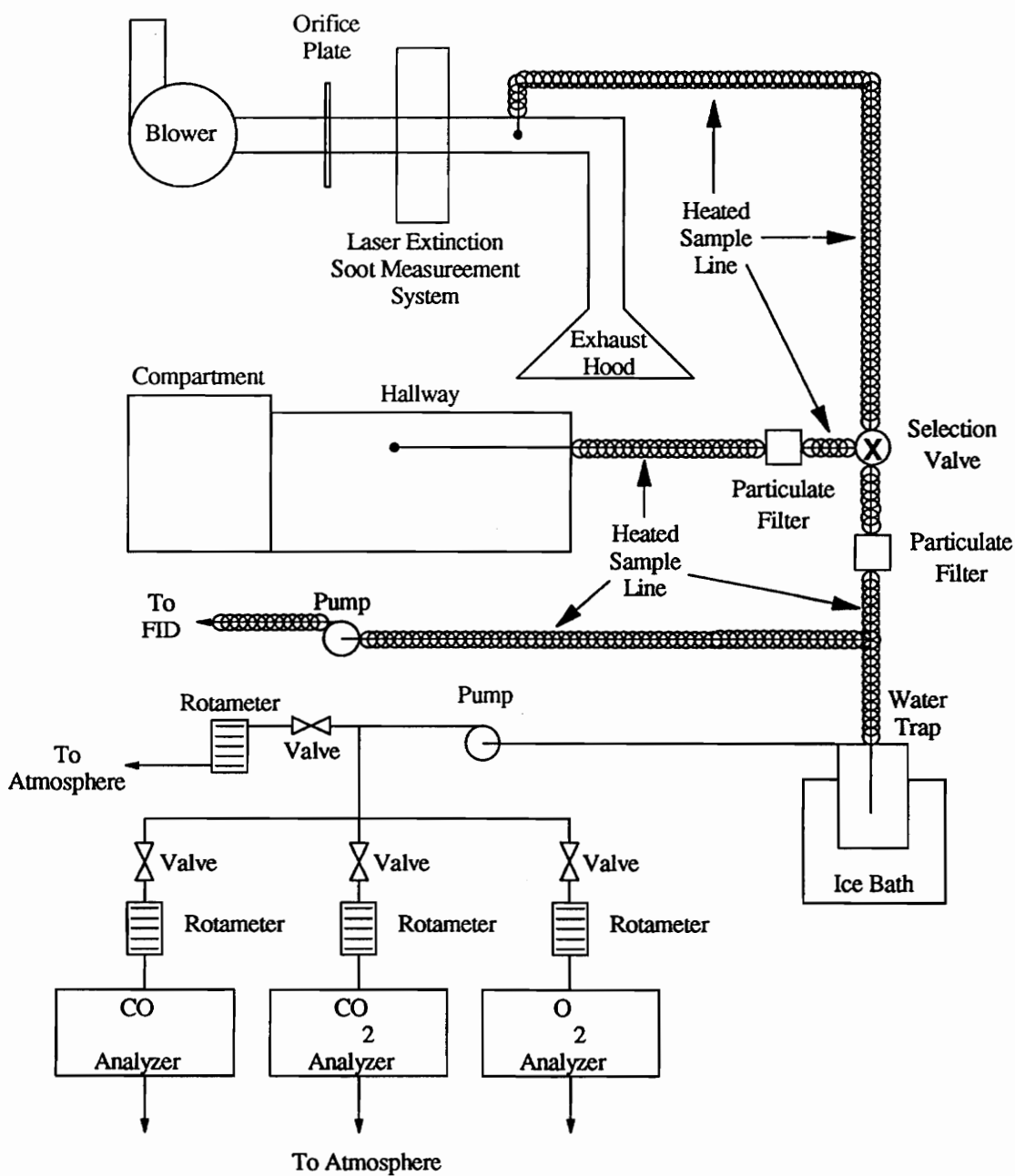


Figure 2.4. Schematic of gas sampling and analysis systems

DX rated, borosilica glass fiber filter, model #915A, was rated at 93% retention of 0.1 micron diameter particles.

### **2.2.5 Gas Analysis System**

A schematic of the gas analysis system, with the gas sampling system, is given in Figure 2.4. Both sample probe locations fed, through a selection valve, to a single gas analysis system. This system consisted of two Beckman NDIR model 880 analyzers to measure the CO and CO<sub>2</sub> concentrations, and a Siemens paramagnetic Oxymat 5E analyzer to measure O<sub>2</sub> concentrations. A Gow-Mac flame ionization detector (FID), model #12-800, was used with a Gow-Mac electrometer, model #40-900, to measure the unburned total hydrocarbon (THC) concentration, measured as ethylene, C<sub>2</sub>H<sub>4</sub>.

The sample gas was divided into two separate flow paths after passing through the filter, or filters, to trap out soot. One path delivered sample gas to the dry gas analyzers (CO, CO<sub>2</sub>, and O<sub>2</sub> analyzers), and the other delivered sample gas to the THC analyzer. Each path had a separate Thomas 2107 CA18 diaphragm vacuum pump to draw in the sample gases.

On the dry gas analyzer path, the sample gases passed through a water trap submerged in an isothermal refrigerated circulating bath, Fisher model #910, and held at a constant temperature of -10°C. The water trap cooled the gases allowing water to condense out of the sample. The trapping of water from the sample was required by the analyzers to avoid erroneous readings and damage due to water condensing in the sample cell. The dry concentrations were later converted to wet concentrations in the data reduction program (see section 2.4.1.1).

After passing through the pump, the flow was divided into an analyzed flow and a bypass flow. The bypass flow allowed a much higher sample flow rate than required for



the analyzers to reduce the delay time in the sampling system to 10 seconds or less. An optimal, constant, flow rate of 1 l/min to each of the dry analyzers was accomplished with a separate 0-3.5 SLPM range Matheson rotameter for each analyzer.

The CO and CO<sub>2</sub> analyzers had built in linearizers for a 0-5 volt output signal for all three sensitivity ranges. The three ranges for CO analyzer were 0 to 1000 ppm, 1%, and 10%. The three ranges for CO<sub>2</sub> analyzer were 0 to 2%, 15%, and 20%. When sampling in the exhaust duct, the lowest concentration ranges were used. The concentration range used for sampling in the hallway depended on the location and the experimental conditions. The highest concentration ranges were required closest to the compartment for fuel rich fires. Both analyzers were calibrated before each experiment using the automated routines to set the zero point (with pure nitrogen) and the span point. Certified and analyzed calibration gas mixtures of CO, and CO<sub>2</sub>, balanced with nitrogen, were used to set the span point of the analyzers. The calibration gases were typically 90% of the full scale of the given range.

The O<sub>2</sub> analyzer also had a built in linearizer for a 4-20 mA output. A 250 ohm resistor was used to convert the current signal to a measurable voltage signal between 1 and 5 volts. The oxygen analyzer range used for all experiments and sample locations was 22%, since oxygen levels could only decrease from the ambient concentration of 21%. The oxygen analyzer was calibrated before each experiment using automated routines to set the zero point with pure nitrogen, and set a span point with a mixture of 4.75% oxygen and a nitrogen balance. The low concentration span gas was used since the oxygen concentrations measured in the hallway during the times of interest were generally low, on the order of the span gas used. Oxygen concentrations were only measured in the hallway-sampled experiments.

A detailed schematic of the THC analyzer system is given in Figure 2.5. On the THC analyzer sample gas flow path, the tubing continued to be heated with heating tape, both before and after the sample pump. The heated sample tubing entered an oven that was maintained at a constant temperature of 105 °C. The sample gases then traveled through a 0-2 psig pressure regulator, Fairchild model #10. A valve and pressure gauge downstream of the regulator allowed the pressure to be monitored and set to a constant 1.5 psig. A 0-10 SLPM Matheson rotameter ensured that the THC bypass flow rate was also repeatable, usually 6 SLPM. The bypass flow was again used to reduce the delay time of the sampling system to within 10 seconds. Since the FID was unaffected by water in the sample, water was not trapped out and concentrations were measured wet to avoid loss of higher molecular weight hydrocarbons.

Connected to the 1.5 psig pressurized section of tubing was a capillary tube to allow a low flow of sample gas to be analyzed by the FID within the oven. With a fixed pressure across the fixed length of capillary tube, the flow through the capillary tube to the FID was constant and repeatable, at around the recommended flow rate of 20 to 40 cc/min. The length of the capillary tube, pressure, and flow rate were all selected for optimum performance of the FID.

The FID required a flame, produced by a constant flow of hydrogen and oxygen, to burn the hydrocarbons in the sample gas. The gas mixtures used were a 40/60 mixture of hydrogen and helium, and purified air, selected to provide optimal FID performance. Both flows were monitored by Matheson rotameters, with flow rates for optimum performance of 270 cc/min and 440 cc/min respectively. The analyzed sample flow and hydrogen flame products from the FID were vented into the oven, through a housing with a hydrogen detector, and to the open atmosphere.

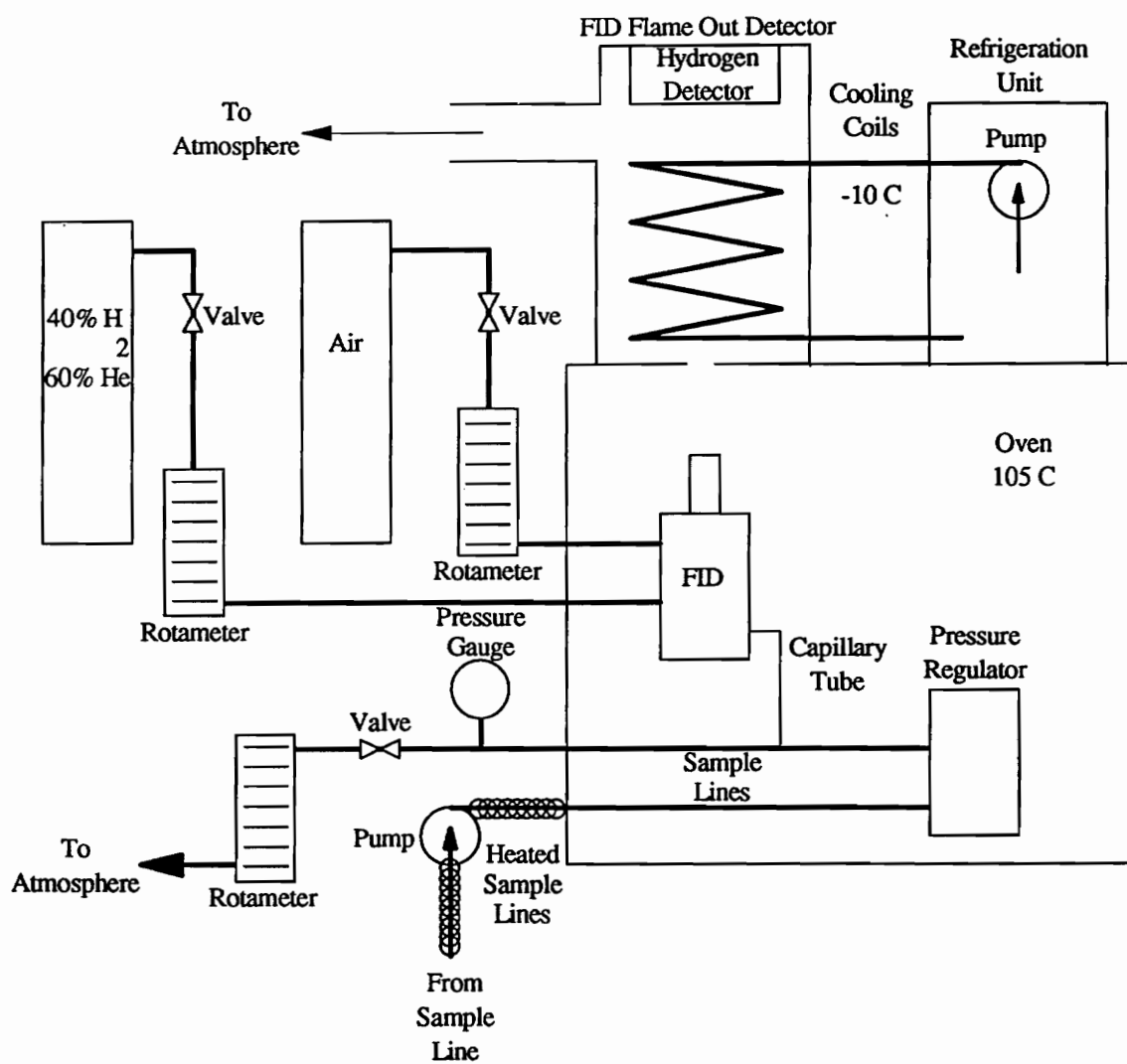


Figure 2.5 Schematic of total hydrocarbon (THC) analyzer

The hydrogen flame required by the FID posed a possible explosion hazard had the flame been extinguished. To avoid this hazard, the hydrogen detector was linked to a relay operating a solenoid valve to automatically interrupt the flow of hydrogen when excess amounts were detected. Since the hydrogen detector operating temperature was rated for a maximum operating temperature of 49°C, a -10°C cooling coil in the detector housing was required to cool the analyzed gases from the 105°C temperature in the oven.

The signal from the FID was conditioned by an electrometer with four different sensitivity ranges. The electrometer allowed the FID to be calibrated manually with pure nitrogen for the zero set point. The span point signal from the electrometer was recorded for manual calibration in the data reduction program. The span point was set with ethylene, C<sub>2</sub>H<sub>4</sub>, which was expected to be fairly representative of the unburned hydrocarbons present. Depending on the sampling location and the experimental conditions, concentrations of ethylene for calibration included 615 ppm, 5456 ppm and 4.71% for three different sensitivity ranges. When sampling in the exhaust duct, 615 ppm was used. When sampling in the hallway, the higher concentration calibration gases were required as the sample probe was moved closer to the compartment. The calibration of the FID was checked before each experiment.

### **2.2.6 Data Acquisition System**

The data was recorded using a 386 personal computer with Data Translations data acquisition boards. This computer was equipped with three internal DT 2801-A digital to analog (D/A) data acquisition boards with 12 bit resolution. One DT 2801-A board was linked to a standard DT 707 eight channel screw terminal board to measure the differential voltage outputs from the CO, CO<sub>2</sub>, O<sub>2</sub>, and THC analyzers, the air inlet duct velocity probe, the fuel load cell, and the laser extinction system. The other two DT 2801-A

boards were each connected to a separate DT 756-Y amplifying, multiplexing terminal board with cold junction compensation for thermocouple measurements. The multiplexing feature of these boards allowed measurement of a maximum of 16 differential signals, providing better signal accuracy as opposed to the standard 16 single ended signals. The board amplification enabled the low voltage thermocouple signals to be measured directly. One DT 756-Y board was allocated for each thermocouple rake, one in the compartment and one in the hallway, with additional thermocouples added to the remaining empty channels.

A program written in BASIC was used to control the actual data acquisition. This program called upon PCLAB subroutines, provided by Data Translations, to communicate with the data acquisition boards. The program allowed data collection to begin and end as the user desired, with data collection typically beginning with the ignition of the fire and ending 30 seconds after the compartment fire was extinguished. The additional 30 seconds of data at the end of each experiment allowed for compensation of the time delay in the gas sampling system during data reduction. Data was stored in a raw data file every 2 seconds, with each signal being averaged over  $\pm 1$  second of the recorded time. This averaging scheme resulted in averaging  $60 \pm 2$  measured values for each data point.

Data were collected and recorded to a user-titled raw data file where 28 signals, including time, were stored in serial form. The data signals for the DT 707 board were stored as 0-5 volt signals. The thermocouple voltage signals were converted to temperatures in degrees Celsius, using a PCLAB subroutine, before being stored in the raw data file. These raw data files were later reduced as explained in section 2.4.1.

## 2.3 Experimental Procedure

Two types of experiments were executed differing by the sampling location, each with a different goal. In the first type of experiments, termed **exhaust duct-sampled**, gas samples were withdrawn from the exhaust duct to provide overall species yields downstream of the hallway. These experiments were conducted for a wide variety of fuel rich (i.e. underventilated) global equivalence ratios, and allowed investigation of the corresponding changes in the species yields.

Comparison of exhaust duct-sampled data was made with the results of Gottuk et al. for in-compartment [7,11] and exhaust duct-sampled [11,12] species yields for open jet compartment fires. This comparison indicated the relative effect of exhaust gas transport through the hallway. The open jet experiments [7,11,12] were performed for a compartment fire exhausting through a window style vent into the open atmosphere. The open jet experimental results [7,11,12] were expected to bracket the results of the present investigation; data obtained from in the compartment defined the expected maximum yields without oxidation in the adjacent hallway, while measurements downstream of open jet burning defined the minimum attainable levels of species yields.

The second type of experiments, termed **hallway-sampled**, involved gas sampling and temperature measurements in the hallway at many different locations for fixed experimental conditions. This provided species concentration profiles within the hallway along different directions. These experiments allowed a more detailed investigation of the major parameters controlling oxidation in the hallway.

Before each experiment, the experimental apparatus was prepared with the appropriate experimental conditions, such as the fuel pan and exhaust vent sizes, hallway soffit heights, and the appropriate sampling location selected. The fuel pan was filled

completely with a fixed initial amount of liquid hexane, and placed on the load cell extension platform in the center of the compartment.

Recording with a video camera was initiated slightly before the experiment began. Manual ignition of the fire in the compartment was synchronized with the initiation of the data acquisition program. Each fire was allowed to burn until the initial amount of hexane fuel was completely depleted. The data acquisition program was allowed to record data for an additional 30 seconds after the compartment fire was extinguished, which allowed for compensation of the gas sampling system delay time in the data reduction program.

## **2.4 Data Reduction**

### **2.4.1 Data Reduction Program**

This section presents and discusses the fundamentals of the calculations performed by the data reduction program. The data reduction program read in the raw, serial data file created by the data acquisition program, converted the raw data signals to the desired dimensional variables, and calculated additional parameters as functions of the measured data. The data was then stored in seven reduced data files in tabular form so that the data could be plotted, manipulated, or averaged. The current working copy of this FORTRAN program, FIRERED2.FOR, is given in Appendix A.

#### **2.4.1.1 Species Concentrations and Yields**

The dry concentrations of CO, CO<sub>2</sub>, O<sub>2</sub>, and the wet concentration of THC<sub>s</sub> were all stored as voltage signals in the raw data file. The voltage signals were converted to the actual concentrations by indicating the range used for the dry gas analyzers. The THC signal required manual input of the span gas point for calibration during data reduction.

All gas concentrations were corrected for the time delay of the sampling system in the data reduction program. Since the sample system required a finite time to deliver the sampled gas to the analyzers, this delay time was accounted for so that the concentration measurements would be synchronized with the other instantaneously measured parameters, such as temperature, fuel vaporization rate, and air inlet rate.

These delay times were determined in a series of tests, in which a 2 second pulse of gas, containing either carbon dioxide (for the dry gas analyzers) or ethylene (for the THC analyzer), was used. The pulse of gas was injected directly into the hallway sample probe to determine the delay time for the hallway-sampled experiments, and into the exhaust hood over the hallway exit for the exhaust duct-sampled experiments. The delay times were determined by the difference between the time halfway through injection of the gas, and the time of the peak reading on the CO<sub>2</sub> or THC analyzer. The delay times were determined to be 6 and 8 seconds for the dry gas analyzers and the THC analyzer, respectively, when sampling in the exhaust duct. The delay times increased to 8 and 10 seconds, respectively, when sampling in the hallway due to the longer sample line.

The data reduction program also calculated the wet concentrations of CO, CO<sub>2</sub>, and O<sub>2</sub> from the measured dry concentrations. This calculation was based on the assumption that all of the water in the sample was produced from combustion of the fuel, and that the ratio of H<sub>2</sub>O to CO<sub>2</sub> was that of stoichiometric combustion. For hexane, this ratio is 7 parts of H<sub>2</sub>O for 6 parts of CO<sub>2</sub>. Using this assumption, the wet mole fractions,  $X_{sp, wet}$ , of the dry measured gases could be calculated from the derived equation:

$$X_{sp, wet} = X_{sp, dry} / (1 + (7/6) \cdot X_{CO_2, dry}), \quad (2.1)$$



where:

$X_{sp}$  dry - Dry mole fraction of the species of interest,

$X_{CO_2}$  dry - Dry  $CO_2$  mole fraction.

For the exhaust duct-sampled experiments, gas species yields were calculated. The yield of a species was defined as the ratio of the mass production rate of a given species to the mass vaporization rate of fuel. The mass production rate of the measured species was calculated from the wet concentrations measured in the exhaust duct and the molar flow rate through the exhaust duct. The equations used to calculate the species yields,  $Y_{sp}$  in Kg species / Kg fuel, were:

$$\dot{M}_{sp} = (X_{sp} \text{ wet} \cdot \dot{n}_{ed} \cdot MW_{sp}), \quad (2.2)$$

$$Y_{sp} = \dot{M}_{sp} / \dot{M}_{fuel}, \quad (2.3)$$

where:

$\dot{M}_{sp}$  - Mass production rate of the species of interest, Kg/sec,

$X_{sp} \text{ wet}$  - Mole fraction of the species of interest in the exhaust duct,

$\dot{n}_{ed}$  - Molar flow rate through exhaust duct, Kmol/sec,

$MW_{sp}$  - Molecular weight of the species of interest, Kg/Kmol,

$\dot{M}_{fuel}$  - Fuel vaporization rate, Kg/sec.

The measured pressure drop across the orifice plate was used to calculate the volumetric flow rate through the exhaust duct by the equation and coefficients found in Reference [18]. The assumption that the density and specific heat ratio of the gas passing through the exhaust duct was that of air did not introduce a significant error since the exhaust gases were diluted with ambient air in a ratio greater than 30:1. The molar flow rate was calculated from the ideal gas equation using the ideal gas constant for air, the gas temperature measured in the exhaust duct, and the atmospheric pressure. The pressure in

the exhaust duct was assumed to be approximately equal to the atmospheric pressure, which was measured and recorded before each experiment.

The hallway-sampled data lacked species yields due to the unknown entrainment rate of air into the exhaust gases inside the hallway. This air entrainment rate in the hallway would be difficult to measure directly, since mixing occurs across a dynamic interface and the rate of entrainment varies along the hallway axial direction.

#### **2.4.1.2 Smoke Extinction Coefficient and Yield**

The photo diode signal from the laser extinction system was stored in the raw data file as a voltage signal. Since negligible levels of smoke were produced during the beginning of the fire, the photo diode signal during the first ten seconds of the experiment was used as the reference signal with no attenuation. The photo diode signal was left as a voltage signal, since the ratio of the attenuated signal to the reference signal was used in the calculations. The extinction coefficient was calculated directly from the photo diode signal ratio, from which the smoke yield was estimated as explained below.

The extinction coefficient,  $\sigma$ , in units of  $[m^{-1}]$  was calculated from the measured photo diode signal ratio as given by Tewarson [19]:

$$\sigma = - (1/L) \cdot \ln (I/I_0), \quad (2.4)$$

with:

L - Optically attenuated laser path length, m,

I - Attenuated laser intensity, arbitrary units,

$I_0$  - Unattenuated reference laser intensity, arbitrary units.

Based on the work of Tewarson [19], the mass optical density per unit length, MOD', in units of  $[m^2/g]$  and the smoke yield,  $Y_{\text{smoke}}$ , in units of  $[Kg \text{ smoke} / Kg \text{ fuel}]$

were calculated from the extinction coefficient using:

$$\text{MOD}' = (\sigma / 2.303) \cdot \dot{Q}_{\text{ed}} / \dot{M}_{\text{fuel}}, \quad (2.5)$$

$$Y_{\text{smoke}} = \text{MOD}' / \xi, \quad (2.6)$$

with:

$\dot{Q}_{\text{ed}}$  - Volumetric flow rate through exhaust duct, m<sup>3</sup>/sec,

$\dot{M}_{\text{fuel}}$  - Fuel vaporization rate, g/sec,

$\xi$  - Specific extinction coefficient of smoke, m<sup>2</sup>/g,

The specific extinction coefficient was not a simple coefficient, in that it was a function of the size distribution of the smoke particles attenuating the laser signal. The specific extinction coefficient typically varies during different stages of a fire, especially for underventilated fires. However, since no accurate correlation was available for underventilated fires, a simple relation suggested by Tewarson [19] for well ventilated fires was used to allow relative comparisons between experiments:

$$\xi = 3.213 / (\lambda \cdot \rho), \quad (2.7)$$

with:

$\lambda$  - Incident laser light wavelength,  $\mu\text{m}$ ,

$\rho$  - Density of smoke, g/cm<sup>3</sup>.

The density of smoke also typically changes during the fire, but a suggested value of 1.1 g/cm<sup>3</sup> from References [19,20] was used. This calculation was the same method used by Gottuk et al. [7,11,12], so that relative comparisons with his reported data could also be made with confidence.

### 2.4.1.3 Global Equivalence Ratio

The fuel weight signal recorded in the raw data file represented a 1-5 volt signal corresponding to 0-10 Kg weight. The data reduction program made this conversion. The first derivative of the fuel weight was calculated numerically to estimate the fuel vaporization rate. The numerical derivative was estimated from the ratio of the drop in the fuel weight between  $\pm 10$  seconds from the point estimated, to the time between these two points. The second derivative of the fuel weight with respect to time was estimated by the same procedure performed on the fuel vaporization rate.

An alternative way of estimating the size of the fire was to calculate the maximum theoretical heat release rate. This parameter assumed complete combustion of the vaporized fuel, and was calculated simply by multiplying the fuel vaporization rate by the heat of combustion. The actual heat release rate inside the compartment for underventilated fires was less than this calculated value since combustion was not complete.

A method of providing a check on the species measurements involved a carbon mass balance between the carbon supply rate of the vaporizing fuel, and the carbon exhaust rate measured from the exhaust products in the exhaust duct. A carbon error was calculated, defined as the percent over prediction (negative error for under prediction) of carbon from the measured  $\text{CO}_2$ , CO, and THC yields in the exhaust duct gases. The carbon error was generally less than  $\pm 10\%$  during the averaging period.

The signal for the rate of air flow into the compartment was recorded as a 0-5 volt signal from the velocity probe in the raw data file. The reduction program converted this signal to the corresponding 0-2 m/s velocity, correcting for ambient atmospheric pressure and the gas temperature in the inlet duct. Since the velocity probe was positioned to

measure the area averaged velocity, the mass air flow rate through the inlet duct was simply calculated by multiplying the measured gas velocity by the inlet duct cross sectional area and the density of the air.

The global equivalence ratio (GER) was calculated as the ratio of the fuel mass vaporization rate, to the compartment air mass inlet rate, and normalized by the stoichiometric ratio. The experimental apparatus was designed specifically to separate the flow paths, one exclusively for air flow into the compartment, and the other exclusively for exhaust flow out of the compartment. This allowed a direct measurement of the GER in the compartment from the air inlet flow rate and the fuel vaporization rate.

The dilution ratio, on a molar basis, of exhaust from the compartment to the total flow of gases through the exhaust duct was calculated. This ratio, which indicated that the exhaust gases were highly diluted in the exhaust duct, varied between 30:1 and 80:1 during the averaging time for different experiments.

#### **2.4.1.4 Temperatures**

The temperatures recorded by the data acquisition program in the raw data file were stored in units of degrees Celsius. The data reduction program converted all temperatures to degrees Kelvin for calculation purposes and for storage in the reduced data files.

#### **2.4.1.5 Ignition Index**

An ignition index, based on classical empirical relations for lean flammability limits, was calculated as a function of time by the data reduction program. The ignition index was calculated based on measured and estimated flammable gas concentrations, indicating a flammable mixture for values greater than one. The detailed development and derivation

of the ignition index is given by Beyler in Reference [21]. The general equation used to calculate the ignition index, I.I., was:

$$I.I. = \sum_i (X_{i \text{ wet}} \cdot \Delta H_{c_i} / n_p \cdot C_p \cdot \Delta T), \quad (2.8)$$

where:

$i$  - Summation variable, for CO, THC<sub>s</sub>, and H<sub>2</sub>,

$X_{i \text{ wet}}$  - Wet mole fraction of species  $i$ ,

$\Delta H_{c_i}$  - Heat of combustion of species  $i$ , KJ/mole,

$n_p$  - Total moles of products after complete combustion of one mole of reactants, mole,

$C_p$  - Specific heat of products of complete combustion, KJ/mole K,

$\Delta T$  - Temperature difference between initial gas temperature and adiabatic flame temperature.

The ignition index calculation utilized the hallway-sampled CO, CO<sub>2</sub>, THC, and O<sub>2</sub> concentrations, and the gas temperature measurements taken in the compartment. The calculation of the ignition index also required two assumptions to determine the concentrations of unmeasured gases. The first assumption (made previously for converting the measured dry gas concentrations to wet concentrations) involved the existence of a stoichiometric ratio between CO<sub>2</sub> and H<sub>2</sub>O. This allowed calculation of the water concentration in the sample gas, and of the wet concentrations of the measured dry gases. A second assumption was made to calculate the hydrogen gas (H<sub>2</sub>) concentration. According to Beyler [22], the ratio of H<sub>2</sub> to CO varied between 0.26 and 0.67 for underventilated fires. Analysis performed by Gottuk [11] indicated that using a representative value of 0.5 for the ratio of H<sub>2</sub> to CO resulted in an error of less than  $\pm 10\%$  in the ignition index.

The nitrogen ( $N_2$ ) concentration was then calculated by a mole balance assuming no other species existed in the sampled gas other than  $CO_2$ ,  $CO$ ,  $O_2$ , THC<sub>s</sub> (as  $C_2H_4$ ),  $H_2O$ ,  $H_2$ , and  $N_2$ . The temperature of the gas mixture was taken to be the same temperature as the upper layer in the compartment. This temperature value was quantified as the average of the top three compartment thermocouples.

The ignition index calculation indicated the flammability of the mixture of carbon monoxide, total hydrocarbons (measured as  $C_2H_4$ ), and hydrogen gases, and included the effect of the gas temperature. The ignition index calculations required values for specific heats of the products of complete combustion, taken from Reference [23], values for heats of combustion for the flammable gases, taken from References [21,24], and values for the adiabatic flame temperatures of the flammable gases, taken from Reference [21].

#### **2.4.2 Video Data Reduction**

A VHS video camera was used to record the development and burning of the exhaust gas upper layer in the hallway during each experiment. The video camera was typically placed outside of the open end of the hallway, back about 0.75 m, and about 0.50 m below the height of the hallway ceiling. From this position, the exhaust gas flow through the hallway was viewed from below, allowing observation of sustained external burning along the entire length of the hallway.

The video record of each experiment served two main functions. First, the taping of each experiment allowed for determination of the times when important events occurred, such as sustained external burning. This allowed the determination of characteristic global equivalence ratios for such events. Second, the video provided a permanent record of each experiment, when further evaluation was required. When any of the numerical data appeared questionable or indicated unexpected results, the video was

available to determine whether it was the result of a strange occurrence or invalid data. The video tape also allowed close visual investigation of the mixing behavior of the exhaust gases with the hallway air, and characterization of the external flame structure, size, and geometry.

The video recording was started slightly before the experiment began. The ignition of the fire was used as a reference for the beginning of the experiment, time equal to zero, which coincided with the initiation of the data acquisition system. Ignition was easily observable in the video recordings, marked by highly visible radiation reflecting off of the walls from inside the compartment. From ignition, the time of each important event was recorded. The standard events typically observed during experiments, in chronological order, included flame jets extending from the exhaust vent, quick flashes of external burning in the hallway, the initiation and completion of sustained external burning, and the extinguishment of the compartment fire. However, all of these events did not occur for every experiment. Any other events that appeared unusual or interesting were also noted.

The times for flashes and the beginning of sustained external burning were then used to obtain the instantaneous global equivalence ratios from the reduced data files, defined as the characteristic global equivalence ratios. The time over which sustained external burning occurred was used to indicate a time frame over which averaging of the data would be appropriate.

### **2.4.3 Data Averaging**

Experiments for both sampling locations were averaged during sustained external burning to allow comparison of the data to other experiments. A simple FORTRAN averaging program, FIREAVG2.FOR, was used to average the reduced data. This program read the reduced data files and averaged them over a user-prompted averaging



period. The program then printed the statistical average and the 95% confidence interval limits ( $\pm 2$  standard deviations) for the data over the indicated time interval.

Data for the exhaust duct-sampled experiments were averaged over a "quasi" steady state period. This allowed comparison not only to other experiments of this study, but also to the open jet experiments of Gottuk et al. [7,11]. This period was defined as a time span during sustained external burning in which the GER and CO, CO<sub>2</sub>, THC, and smoke yields remained fairly constant. Other measured quantities, such as the fuel rate, temperatures, and carbon error were checked for reasonable values and trends during the averaging period. For all of the exhaust duct species-sampled experiments, the "quasi" steady state period chosen for averaging lasted between 30 and 80 seconds (16 and 41 data points), although 30 seconds was most commonly used.

For the hallway-sampled experiments, species yields were not available due to an unknown air entrainment rate into the hallway. Therefore, it was necessary to compare species concentrations, measured at different locations, to understand the evolution of the exhaust gases in the hallway. However, unlike the species yields, the species concentrations were found not to be constant during sustained external burning, but steadily changed as the result of a steadily decreasing fuel vaporization rate. When calculating yields in the exhaust duct, this unsteadiness was eliminated due to the definition of the species yield. Incorporated into the definition of the species yield was the fuel vaporization rate, thus producing constant species yields during most of sustained external burning.

In order to average measured quantities for hallway-sampled experiments over time, a repeatable reference point was required. The reference point used was the earliest peak of CO, THCs, and CO<sub>2</sub> concentrations, which occurred shortly after sustained

external burning began. THC's usually peaked first, although all peaks typically occurred within 6 to 10 seconds of each other. This allowed averaging to include all of the carbon species peaks, indicating the worst case scenario. Oxygen also usually reached a minimum concentration shortly after the carbon species peaked. Additional parameters besides the species concentrations were also checked for reasonable behavior during the averaging period. These parameters included the GER, the second derivative of fuel weight, and the compartment and hallway temperature profiles.

The chosen point of reference essentially allowed the same volume of exhaust gases to be evaluated, independent of the axial location of the sample probe in the hallway. This eliminated comparing different gas samples at different sampling locations, which would not accurately represent a meaningful comparison.

A reasonable duration for the averaging period was selected to be 20 seconds (10 data points) for all hallway species-sampled experiments. This value was chosen, by inspection of the data, to be long enough to include enough data points so that a single bad data point would not invalidate the averaged value. However, the averaging time had to be short enough to avoid averaging over a wide span of decreasing values, resulting in a significant error.

## CHAPTER 3

### RESULTS AND DISCUSSION

#### 3.1 Introduction

This chapter presents the results of experiments performed for this study. The results presented are also analyzed and discussed within this chapter. This chapter is organized into four main sections: 1) introduction to the variables investigated, 2) results and discussion on characteristic global equivalence ratios, 3) results and discussion on ignition index calculations, and 4) results and discussion on species-sampled experiments. The final section is further divided into sections by the soffit cases examined. The soffit cases are presented in the order of: 0 cm inlet and exit soffits (0 / 0), 0 cm inlet soffit and 20 cm exit soffit (0 / 20), 20 cm inlet soffit and 0 cm exit soffit (20 / 0), and 20 cm inlet and exit soffits (20 / 20).

The experiments of this study focused on two main variables. The first variable was the global equivalence ratio (GER), or the ratio of the fuel vaporization rate to the air induction rate into the compartment. The GER provided a method for classifying the fire in the compartment. The compartment fires chosen for investigation were all sufficiently underventilated ( $GER > 1$ ) so that sustained external burning would occur in the hallway. Gottuk et al. [11,12] had determined previously that overventilated compartment fires did not produce sustained external burning due to complete combustion of the fuel within the compartment. The downstream yields of compartment fires without sustained external burning, including overventilated fires and slightly underventilated fires, have also been characterized by Gottuk et al. [11,12] in the open jet tests to remained unchanged from in-compartment levels.

The second variable investigated was the soffit heights in the hallway, at both the inlet from the compartment and the open end. All four combinations of 0 cm and 20 cm soffits at both end of the hallway were investigated. This allowed investigation of the fluid dynamic effects of soffits. The four different cases of soffit combinations are identified for discussion by indicating first the inlet soffit height, and then the exit soffit height in centimeters, separated by a slash. For example, the case with a 0 cm inlet soffit and a 20 cm exit soffit would be referred to as the 0 / 20 soffit case.

Two types of experiments were conducted during this investigation of each soffit case, differing by the sampling location. In the first type of experiments, gas samples were withdrawn from the exhaust duct to provide overall species yields downstream of the hallway. Experiments of this type were conducted for a wide range of underventilated global equivalence ratios. Comparison of data for these experiments was made with the results of Gottuk et al. for in-compartment [7,11] and exhaust duct-sampled [11,12] species yields for open jet compartment fires. The open jet experiments [11,12] were performed for a compartment fire exhausting through a window style vent into the open atmosphere. The open jet experiments [11,12] were expected to bracket the results of the present investigation; data obtained from in the compartment defined the expected maximum yields without oxidation in the adjacent hallway, while measurements downstream of open jet burning defined the minimum attainable levels of species yields should air entrainment be sufficient for complete combustion.

The second type of experiments involved gas and temperature sampling in the hallway, at many different locations. The results of these experiments provided more detailed information about the major parameters controlling oxidation in the hallway. Species concentrations measured in the hallway were normalized by the concentrations

measured entering the hallway for product species, and by the ambient atmospheric level for oxygen, to allow for comparison between sample locations in the hallway.

### 3.2 Characteristic Equivalence Ratios

In order to characterize when sustained external burning would occur, the global equivalence ratio was investigated. Two characteristic global equivalence ratios (CGER) were utilized.  $\Phi_{\text{flash}}$  was defined as the instantaneous global equivalence ratio when quick external flashes began to occur in the hallway, and  $\Phi_{\text{seb}}$  was defined as the instantaneous global equivalence ratio when sustained external burning began. These CGERs were examined for a dependence on the inlet and exit soffits, the exhaust vent size, and the fuel pan size.

In the data presented, the CGERs of all tests with the same conditions, i.e. soffits, exhaust vent and fuel pan size, were averaged to produce a single data point. Each of the average data points for the CGERs displayed the 95% statistical confidence intervals. Data points presented without the confidence interval indicate points represented by a single experiment, in which a statistical confidence interval could not be calculated.

The statistical confidence intervals for the CGERs were relatively large due to the fact that flashes and the initiation of sustained external burning both occur during an unsteady, transient stage of the fire. The global equivalence ratio changed very rapidly during this stage of the fire, amplifying the uncertainties in the time selected for the given events.

As mentioned in the related literature section, Gottuk et al. [11,12] also investigated CGERs for compartment fires exhausting to the open atmosphere. These studies reported CGERs of  $\Phi_{\text{flash}} = 1.4$  for all exhaust vent sizes investigated,  $\Phi_{\text{seb}} = 2.1$

for 400 cm<sup>2</sup> exhaust vents, and  $\Phi_{seb} = 1.8$  for 800 and 1200 cm<sup>2</sup> exhaust vents. The fuel pan size was determined not to have a significant effect on either characteristic equivalence ratio.

Experiments conducted with a 0 cm inlet soffit followed a typical series of events leading to sustained external burning. First, as the source fire in the compartment developed and grew in size, flame jets were deflected by the compartment ceiling and extended through the exhaust vent into the hallway as a visible flame. Quick external flashes followed, lasting less than 1 second and distinguishable by flames detached from any extensions of the flame jet. Eventually, sustained external burning occurred in the hallway, filling the entire hall width with flames and typically extending anywhere from 3/4 of the hallway length to extending beyond the exit of the hallway into the exhaust hood. Sustained external burning appeared as a turbulent sheet of flames, occurring at the interface between the hot exhaust gas upper layer in the hallway and the air below. The exhaust gas upper layer height decreased slightly, and with it the flame approached closer to the ceiling, as the gases moved downstream toward the open end of the hallway. Although this series of events was typical of experiments conducted without an inlet soffit, all events did not always occur.

Figure 3.1 and 3.2 show data for both  $\Phi_{flash}$  and  $\Phi_{seb}$  versus the exhaust vent area for the 0 / 0 soffit case experiments with a 23 cm and 20 cm fuel pan, respectively. For both fuel pan sizes,  $\Phi_{flash}$  demonstrated exponential behavior with respect to the exhaust vent area, increasing as the exhaust vent area decreased. This dependence can be explained by the fact that the exhaust vent size controls the possibility of igniting the exhausting gases. As the exhaust vent size decreased, less heat transfer occurred from the compartment to the hallway, and the flow of hot exhaust gases from the compartment decreased. This allowed the relatively cold air entrained to decrease the temperature of

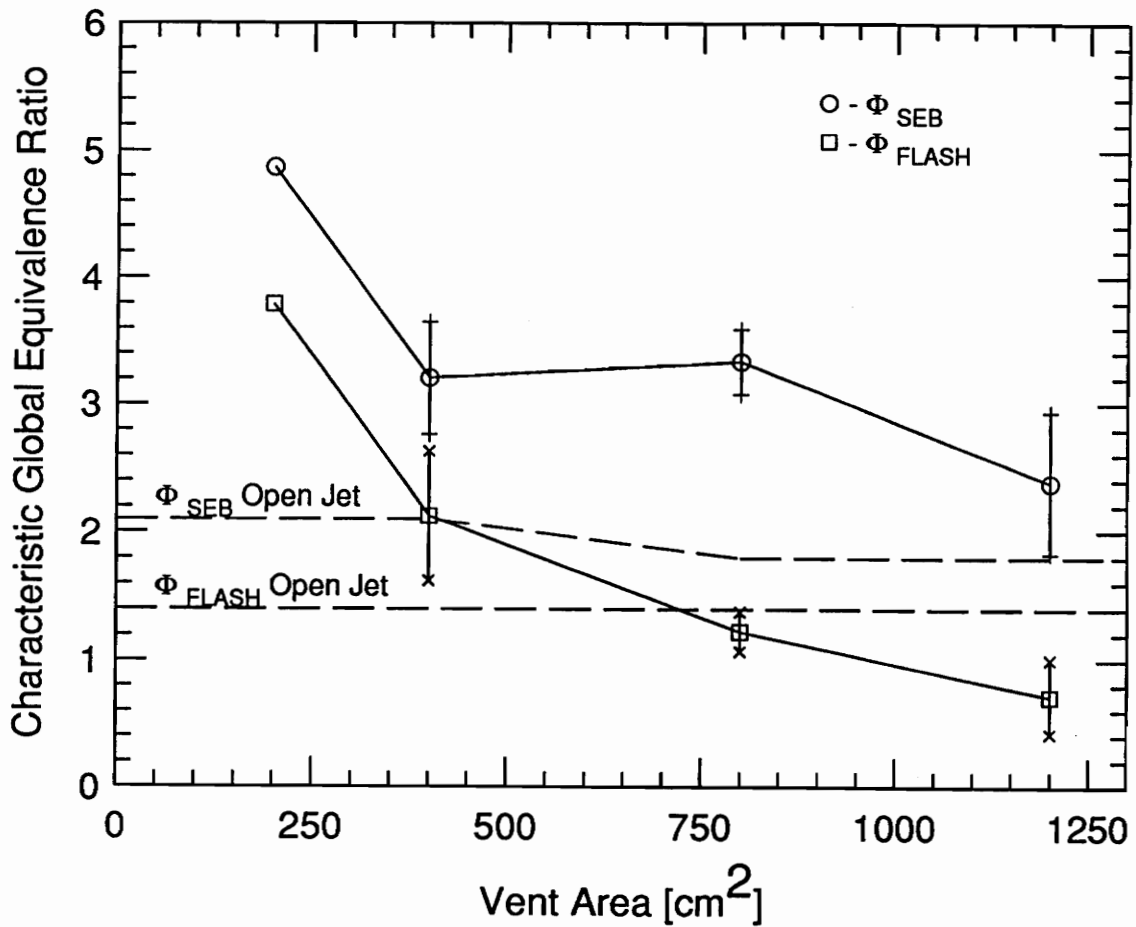


Figure 3.1 Characteristic global equivalence ratios versus exhaust vent area. Experimental conditions: **0/0 soffit case, 23 cm diameter fuel pan**. Each point represents the average of many tests, 95% confidence intervals shown except for single test data points. Data from open jet experiments of Gottuk et al. [11,12] shown as dashed lines for comparison.

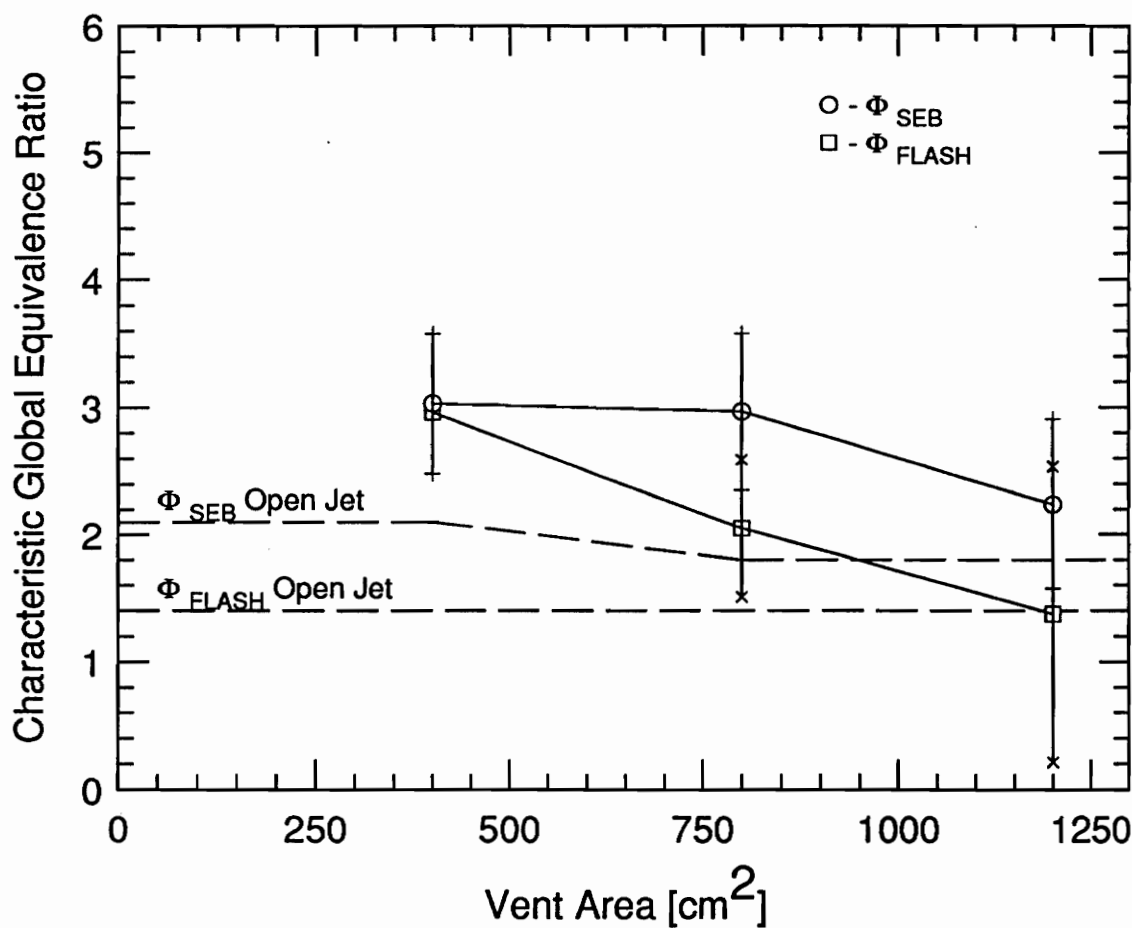


Figure 3.2 Characteristic global equivalence ratios versus exhaust vent area. Experimental conditions: 0/0 soffit case, 20 cm diameter fuel pan. Each point represents the average of many tests, 95% confidence intervals shown except for single test data points. Data from open jet experiments of Gottuk et al. [11,12] shown as dashed lines for comparison.



the exhaust gas - air mixture. Decreasing the exhaust vent size also reduced the probability, and size, of flame jets exiting the compartment through the exhaust vent, thus reducing the chance for ignition.

Comparing  $\Phi_{\text{flash}}$  for different fuel pan sizes in Figures 3.1 and 3.2 shows that decreasing the fuel pan diameter also increased the CGER for flashes. Decreasing the fuel pan size affects  $\Phi_{\text{flash}}$  by decreasing the heat generated in compartment, again reducing the heat transfer to the hallway. The size of the source fire also decreased with the fuel pan size, again reducing the probability, and size, of flame jets extending into the hallway.

Compared to the results of Gottuk et al. [11,12] for open jet experiments, also shown in Figures 3.1 and 3.2,  $\Phi_{\text{flash}}$  was shifted to higher values for the smaller exhaust vents. This can be explained by the reduced air entrainment efficiency in the hallway compared to the compartment exhausting to the open atmosphere. However, the bigger exhaust vents show equivalent or lower values to that of Gottuk et al. [11,12] for  $\Phi_{\text{flash}}$ . This indicates that with larger exhaust vents, and thus higher hot exhaust gas flow rates into the hallway, the advantage of the increased retention of heat due to the confinement of the hallway dominated the disadvantage of less efficient air entrainment. These results indicate that  $\Phi_{\text{flash}}$  was much more sensitive to variations in the exhaust vent and fuel pan sizes for compartment fires exhausting into a hallway, compared to the open atmosphere. This increased sensitivity for the hallway experiments resulted from the trade off between the increased heat retention and the reduced air entrainment efficiency.

The CGERs for sustained external burning are also shown in Figures 3.1 and 3.2. This data indicates that  $\Phi_{\text{seb}}$  does not demonstrate simple exponential behavior as was observed with  $\Phi_{\text{flash}}$ , but displays a more complex dependency on the exhaust vent geometry. Changing from the 1200 cm<sup>2</sup> vent to the 800 cm<sup>2</sup> vent represented a decrease

in height, producing a significant increase in  $\Phi_{seb}$ . In contrast, changing from the 800 cm<sup>2</sup> vent to the 400 cm<sup>2</sup> vent represented a decrease in width, with no significant change in  $\Phi_{seb}$  within the limits of the 95% confidence interval. A further decrease in the vent width, from 400 cm<sup>2</sup> to 200 cm<sup>2</sup>, showed a significant effect.

This behavior suggests that  $\Phi_{seb}$  may possibly be correlated as a function of both the exhaust vent area, and the exhaust vent height to width ratio. An attempt was made to correlate  $\Phi_{seb}$  with the common flow parameter of  $\text{Area} \cdot (\text{Height})^{1/2}$ . This correlating parameter resulted in a curve similar to that in Figure 3.1 since all of the exhaust vents had the same height except for the largest vent. Determining an accurate correlation for this complex dependence would require additional experiments with a much wider range of exhaust vent sizes. One additional interesting point that should be noted was that, unlike  $\Phi_{flash}$ ,  $\Phi_{seb}$  was fairly independent of the fuel pan size within the limits of the statistical confidence intervals.

Comparing data for  $\Phi_{seb}$  to that of the open jet experiments of Gottuk et al. [11,12], again shown in Figures 3.1 and 3.2, indicated a shift to considerably higher values for any vent or pan size. This can be explained by the stronger dependence of sustained external burning on continuously efficient air entrainment compared to the phenomenon of flashes. Sustained external burning required a steady supply of air with sufficient mixing in the hallway, where as flashes did not require constant air replenishment due to their transient behavior. Note that similar to  $\Phi_{flash}$ ,  $\Phi_{seb}$  was more sensitive to variations in the exhaust vent size compared to the results of Gottuk et al. [11,12] for open jet experiments. This was likely due to the reduced air entrainment efficiency and limited air supply in the hallway.

Figure 3.3 shows the CGERs for the experimental case of no inlet soffit, a 20 cm exit soffit, and a 20 cm diameter fuel pan. Compared to Figure 3.2, the data shown in Figure 3.3 indicated that the CGERs did not appear to be dramatically different from the trends and values presented for the experiments without any soffits, although less data was available. The data that was produced showed significantly more variability, especially with  $\Phi_{\text{flash}}$ , which was most likely due to the less stable flow pattern generated with the 20 cm exit soffit.

For all experiments with a 20 cm inlet soffit, the sequence of events differed from the experiments without an inlet soffit. The occurrence of flame jets did not change significantly, however, no distinct flashes were observable. Sustained external burning required anywhere from 0 to 20 seconds to fully develop, beginning with a short sustained flame, typically detached from the exhaust vent. Once sustained external burning became fully developed, the flame base attached to the exhaust vent and usually engulfed the entire upper layer of exhaust gases before reaching the end of the hallway.

The appearance of the flames during sustained external burning also differed from that for the experiments with no inlet soffit. Without an inlet soffit, the exhaust gases flowed horizontally through the exhaust vent from the compartment, spread out to the walls and horizontally down the hallway. During sustained external burning, this allowed the flames to spread across the width of the hall and extended anywhere from 3/4 to just beyond the hallway exit in the form of a turbulent sheet of fire. With a 20 cm inlet soffit, the exhausting gases formed a vertical exhaust plume that rose into the upper layer of buoyant exhaust gases. During sustained external burning, flames encompassed the entire exhaust gas vertical plume. The flame in this region was very luminous, and as shown later, was efficient in entraining air.

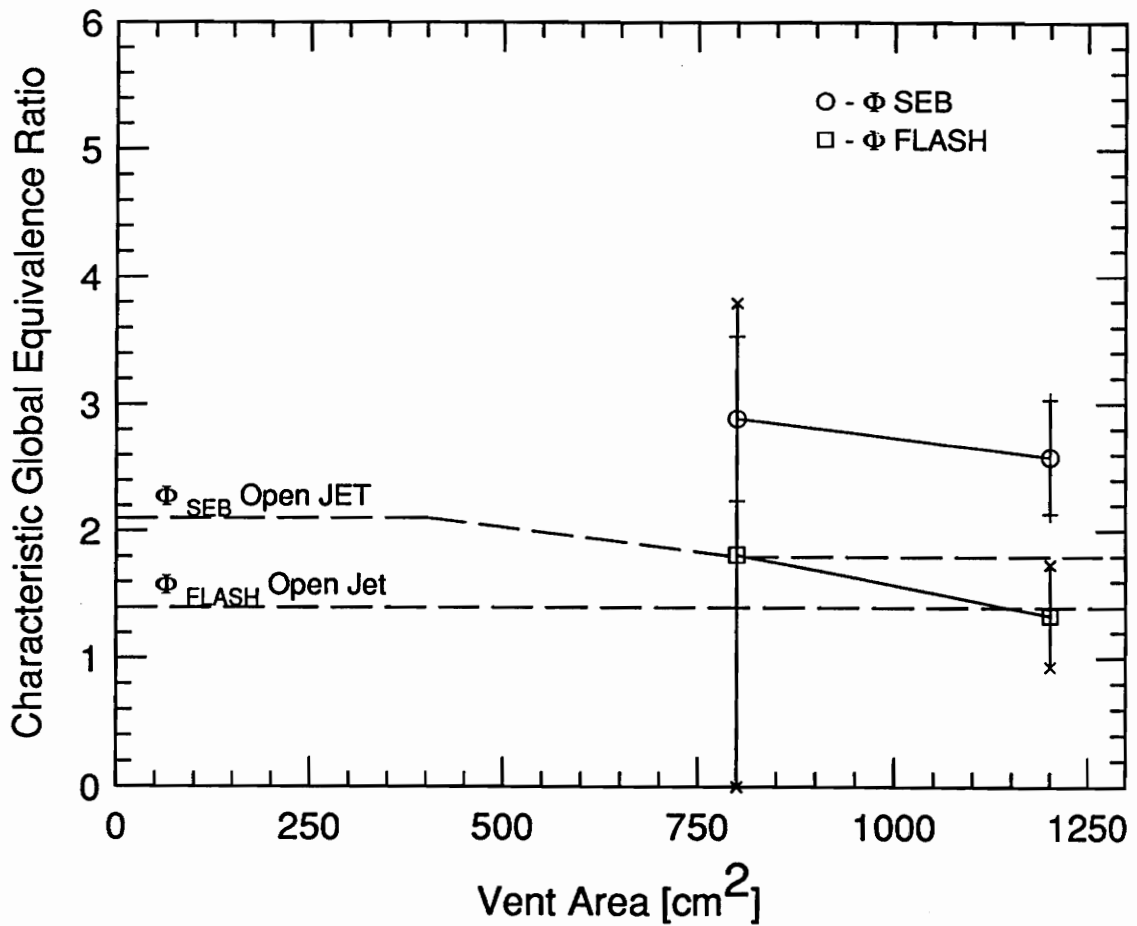


Figure 3.3 Characteristic global equivalence ratios versus exhaust vent area. Experimental conditions: 0/20 soffit case, 20 cm diameter fuel pan. Each point represents the average of many tests, 95% confidence intervals shown except for single test data points. Data from open jet experiments of Gottuk et al. [11,12] shown as dashed lines for comparison.

As the vertical plume entered the exhaust gas upper layer and gas flow was deflected horizontally, the flame continued along the interface between the upper layer exhaust gases and the air below. The flames beyond this region resembled that observed for experiments without an inlet soffit, but did not extend as far along the hallway. The flames reached very close to the ceiling at the farthest extension, indicating complete combustion of the entire upper layer of exhaust gases.

The characterization of  $\Phi_{\text{flash}}$  was not investigated for experiments conducted with a 20 cm inlet soffit since no flashes were observed during these experiments. The time used to determine  $\Phi_{\text{seb}}$  was taken when sustained external burning became fully developed. Investigation of the time when the transient phase of sustained external burning first occurred revealed no repeatable trends.

Figure 3.4 shows  $\Phi_{\text{seb}}$  as a function of the exhaust vent area for experiments conducted with a 20 cm inlet soffit, no exit soffit, and a 20 cm diameter fuel pan. The data displays an increasing  $\Phi_{\text{seb}}$  as the exhaust vent area decreased. For large vents equal to or greater than 800 cm<sup>2</sup>,  $\Phi_{\text{seb}}$  was slightly lower than for the case without any soffits. This behavior was most likely due to the increased air entrainment efficiency with the 20 cm inlet soffit. However, unlike for the 0 cm inlet soffit case, decreasing the vent size to 400 cm<sup>2</sup> caused  $\Phi_{\text{seb}}$  to continue to increase.

This phenomenon can be explained by the high efficiency air entrainment combined with a decrease in the flow rate of flammable exhaust gases. The flow rate of exhaust gases into the hallway decreased with a decreasing exhaust vent size, while the efficiency of the cold air entrainment by the exhaust plume remained relatively unchanged. This combination caused the temperature of the exhaust gas - air mixture to decrease with a decreasing exhaust vent size, thus requiring a higher GER for sustained

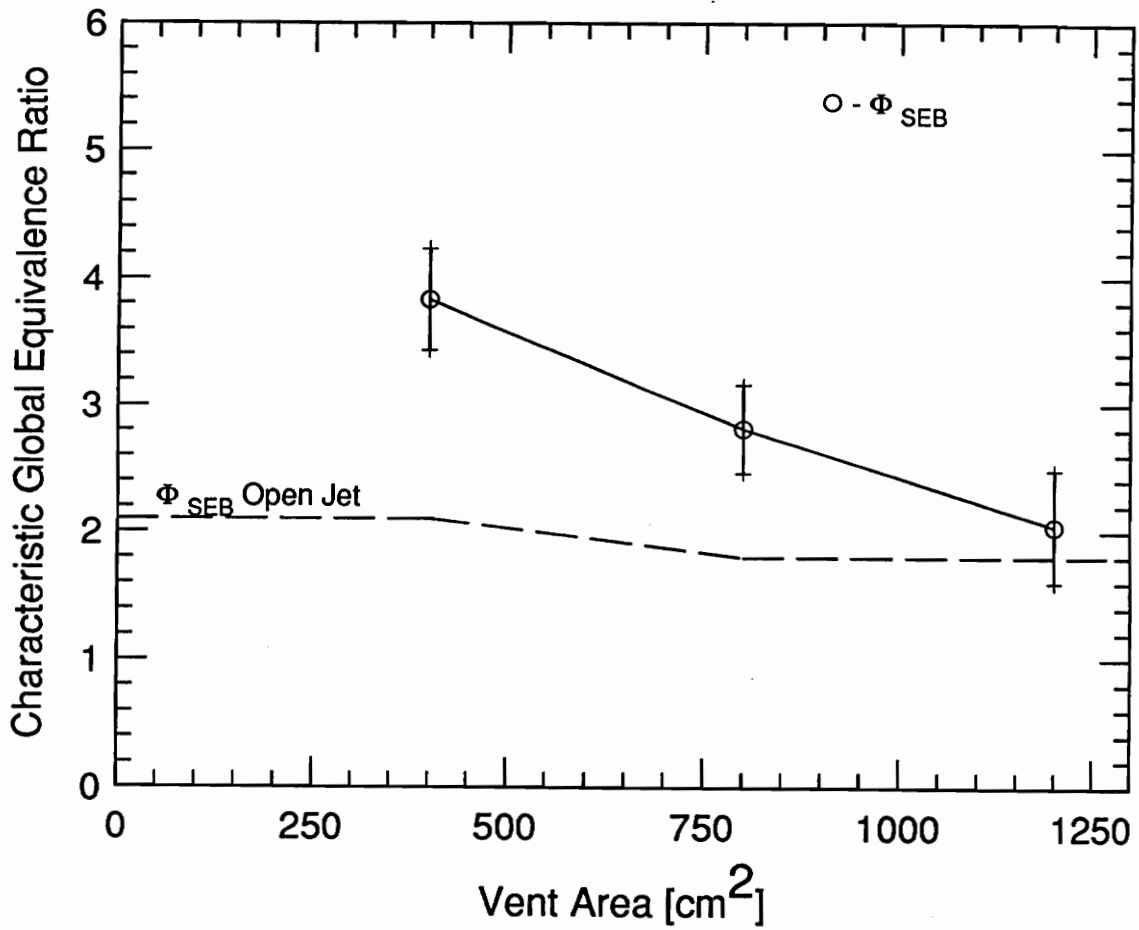


Figure 3.4 Characteristic global equivalence ratios versus exhaust vent area. Experimental conditions: **20/0 soffit case, 20 cm diameter fuel pan**. Each point represents the average of many tests, 95% confidence intervals shown except for single test data points. Data from open jet experiments of Gottuk et al. [11,12] shown as dashed lines for comparison.

external burning to occur. The air entrainment was not as efficient in experiments with the 0 cm inlet soffit under similar conditions. The lower air entrainment rate resulted in less of a temperature drop, but enough entrained air to support sustained external burning. This behavior caused  $\Phi_{seb}$  to be dependent simply on the exhaust vent area for the 20 cm inlet soffit, where as a more complex dependence was apparent without an inlet soffit.

Comparing the 20 cm inlet soffit experiments to the open jet experiments of Gottuk et al. [11,12], shown in Figure 3.4,  $\Phi_{seb}$  was shifted to higher values, as was the case for experiments with no inlet soffit. This indicates that air entrainment in the hallway, for the vent sizes investigated, was still not quite as efficient, near the compartment, as in the open jet. Observing the trend for  $\Phi_{seb}$  with respect to vent size indicates that increasing the exhaust vent slightly beyond 1200 cm<sup>2</sup> may produce a value close to 1.9, the value reported for the open jet experiments [11,12]. Again note that  $\Phi_{seb}$  was more sensitive to variations in the exhaust vent size compared to the results of Gottuk et al. [11,12] for open jet experiments. This again was likely due to the reduced air entrainment efficiency and limited air supply in the hallway.

Figure 3.5 shows  $\Phi_{seb}$  versus the exhaust vent area for experiments with 20 cm soffits at both the inlet and exit to the hallway, and a 20 cm fuel pan. Comparing this data to that for a 0 cm exit soffit with other conditions unchanged, shown previously in Figure 3.4, very little variation in either values or trends was present between the two cases. This indicates that the added 20 cm exit soffit had a negligible effect on the entrainment of air in the gas plume exhausting from the compartment.

In conclusion, although the composition of the flammable gases exhausting from the compartment was controlled by the global equivalence ratio, the entrainment and

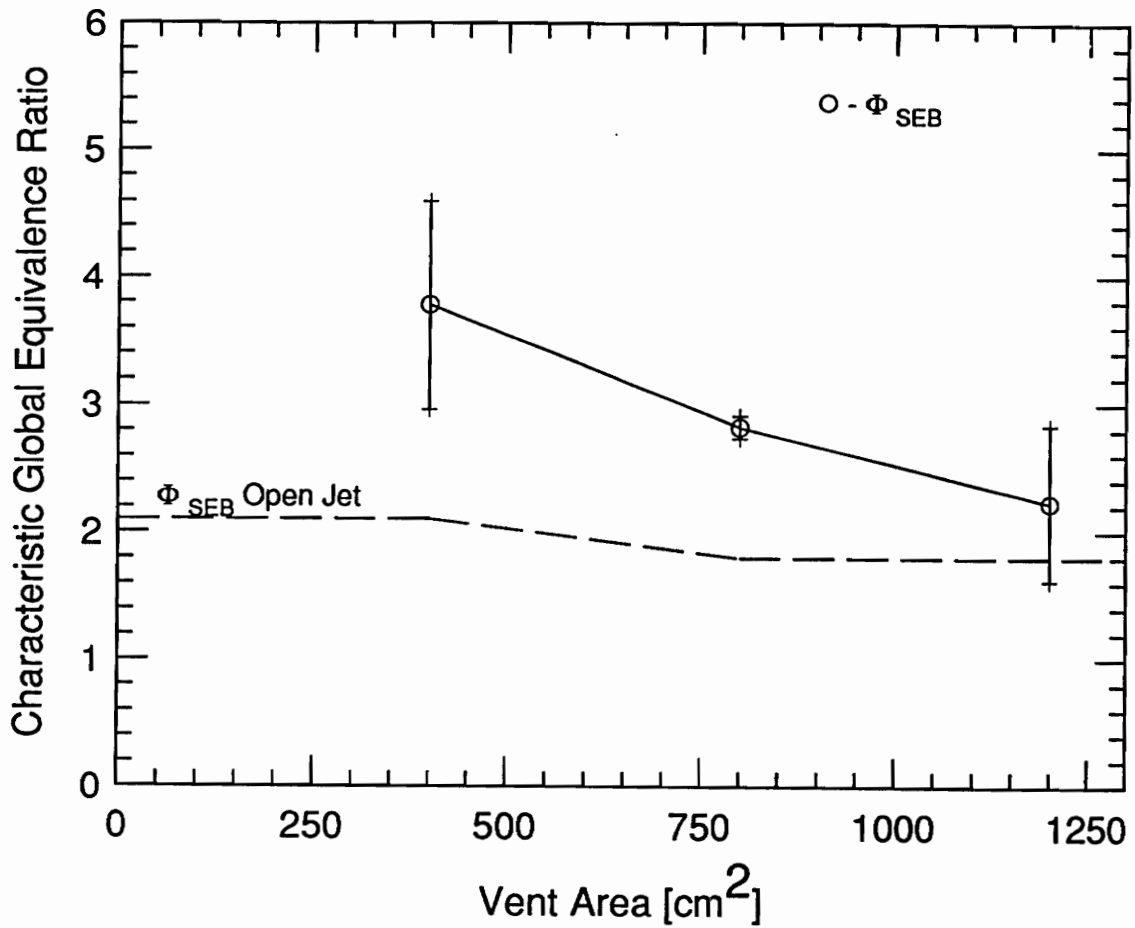


Figure 3.5 Characteristic global equivalence ratios versus exhaust vent area. Experimental conditions: **20/20 soffit case, 20 cm diameter fuel pan**. Each point represents the average of many tests, 95% confidence intervals shown except for single test data points. Data from open jet experiments of Gottuk et al. [11,12] shown as dashed lines for comparison.



mixing of ambient air with the exhausting gases to produce an ignitable mixture, and then ignition of this mixture was strongly influenced by the exhaust vent and fuel pan sizes.

### 3.3 Ignition Index

A second method to characterize when sustained external burning occurred, termed the ignition index, was also investigated. This method was developed by Beyler [21] to predict layer burning in hood experiments, and also showed promise for predicting the occurrence of sustained external burning in the open jet experiments by Gottuk et al. [11,12]. The ignition index is based on classical empirical relations for lean flammability limits of flammable gases. An ignition index greater than one indicates a flammable mixture of gases capable of sustaining a flame.

In this study, the ignition index was based on the flammable gases typically produced in compartment fires, i.e. carbon monoxide (CO), unburned hydrocarbons (THC), and hydrogen (H<sub>2</sub>). The ignition index is similar to the global equivalence ratio, since the concentrations of the gases produced in compartment fires has been correlated to the global equivalence ratio by Gottuk [11]. However, the ignition index also accounts for the temperature of the gases.

Discussion of the equation used to calculate the ignition index was given in Section 2.4.1.5. Calculation of the ignition index required concentrations of carbon monoxide, unburned hydrocarbons, hydrogen, oxygen, carbon dioxide, water and nitrogen. The temperature of these gases was also required. In this study, since the hydrogen and water concentrations could not be measured, they were estimated from correlations based on assumptions. The concentration of nitrogen was calculated from a mole balance.

In the studies by Gottuk et al. [11,12], the ignition index was calculated based on the gas concentrations measured in the upper layer inside the burning compartment. This was an ideal sampling location since ignition of the exhausting gases occurs just outside the exhaust vent of the compartment, and Gottuk et al. [11,12] reported fairly uniform concentrations in the upper layer. However, sampling in the current study was performed in the hallway. The sampled locations used for calculating the ignition index were taken 5 cm below the hallway ceiling, at the center width of the hallway, and either 11 or 46 cm down the hallway axis from the compartment.

Before sustained external burning occurred, sampling in the hallway at these locations provided a reasonable measurement of the composition of the exhaust gases just outside of the compartment, where ignition for sustained external burning occurs. The only difference between the gas composition at these two locations would have been due to dilution with air, which was minimal at this location in the hallway. During sustained external burning, however, the ignition index calculated based on these concentrations significantly under-predicted the actual ignition index due to the sampling of partially oxidized gases.

The temperatures used for calculating the ignition index were measured in the compartment. The compartment temperatures were more likely to be representative of the temperature of the gases exhausting from the compartment, compared to the hallway gas temperatures. The difference in temperatures at the two locations was due to heat losses in the hallway by convection, conduction, and radiation to the surroundings.

The calculated ignition index was determined to peak slightly after sustained external burning occurred. This peak value of the ignition index was used in this analysis. The instantaneous value of the ignition index when sustained external burning occurred

was highly variable between experiments, due to the rapidly changing ignition index during this period. In most of the experiments, the time where the ignition index peaked occurred within 5 seconds of the time when sustained external burning occurred, as determined by the video recording. For a few experiments, the difference in the time between these events was less than 20 seconds.

Tables 3.1 and 3.2 show the ignition index for sustained external burning determined for single experiments, the average, and the 95% statistical confidence interval for 0 / 0 and 0 / 20 soffit cases respectively. For both soffit cases, the average was calculated as 1.2. Since the average ignition index was the same for both soffit cases, this indicates that the effect of the exit soffit on ignition of sustained external burning was minimal.

These values were averaged regardless of the exhaust vent and fuel pan size used since a limited amount of data was available. The ignition index varied between 1.0 and 1.5 for different experiments, with the higher values typically found for experiments conducted with a smaller exhaust vent and fuel pan. However, due to the limited amount of data available and the estimations used for some species concentrations, a detailed investigation of the dependence of the ignition index on the exhaust vent and fuel pan sizes was not possible.

The value determined for the ignition index was slightly lower than the value reported for open jet experiments of Gottuk et al. [11,12] of 1.3. This difference was within the 95% confidence interval bounds, indicating that it may be attributed to the limited amount of data. The difference may also be attributed to dilution of the sampled gases with air since sampling was performed slightly downstream of the compartment in the hallway. More data should be obtained for confirmation, preferably sampled in the

**TABLE 3.1**

Instantaneous ignition index for sustained external burning.  
0 cm inlet soffit / 0 cm exit soffit

Entry #	Ignition Index
1	1.1
2	1.3
3	1.0
4	1.3
5	1.3
6	1.5
7	1.3
8	1.3
9	1.0
Average	1.2
95% confidence interval	$\pm 0.33$

**TABLE 3.2**

Instantaneous ignition index for sustained external burning.  
0 cm inlet soffit / 20 cm exit soffit

Entry #	Ignition Index
1	1.2
2	1.2
3	1.3
Average	1.2
95% confidence interval	$\pm 0.06$

compartment, and with more detailed species composition analysis to eliminate assumptions used in this study.

Experiments sampled in the appropriate locations for both the 20 / 0 and 20 / 20 soffit cases were too limited to indicate any solid conclusions about the ignition index with these configurations. In addition, the few tests that were sampled in appropriate locations for calculation of the ignition index provided significantly varied results. However, the calculated ignition index for all experiments did obtain values between 1.0 and 1.5, indicating a possible correlation when accounting for different exhaust vent and fuel pan sizes.

### **3.4 Species-Sampled Results**

This section presents the actual results of species measurements to determine how the different soffit configurations affected the oxidation of exhaust gases in the hallway. Both types of experiments conducted, sampled downstream in the exhaust duct and sampled in the hallway, are presented. Exhaust duct-sampled experiments determined the overall oxidation efficiencies, where the hallway-sampled results were investigated to determine the phenomena responsible for producing the overall results.

Again, the results are presented and discussed in separate sections for each soffit case. The order of presentation of the soffit cases is: 0 cm inlet and exit soffits (0 / 0), 0 cm inlet soffit and 20 cm exit soffit (0 / 20), 20 cm inlet soffit and 0 cm exit soffit (20 / 0), and 20 cm inlet and exit soffits (20 / 20).

#### **3.4.1 Hallway Soffits: 0 cm inlet / 0 cm exit**

Figure 3.6 shows carbon monoxide (CO) yields versus the GER for the 0 / 0 soffit case. Data from the open jet experiments of Gottuk et al. [7,11,12] are shown for

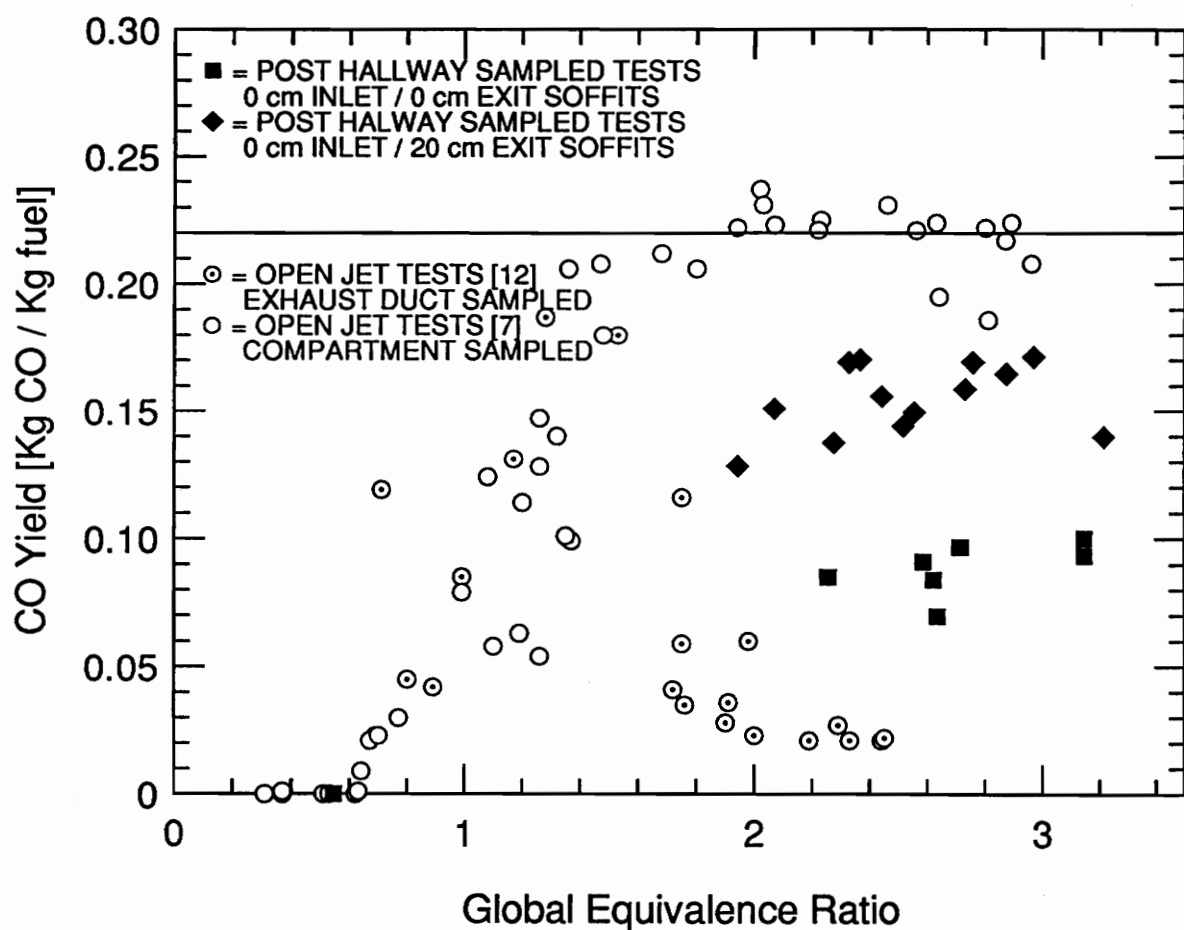


Figure 3.6 CO Yield versus "Quasi" steady state GER. Soffit case: 0/0, 0/20. The total heat release rate of the underventilated fires ranged from 254 - 562 KW for the 0/0 soffit case, and 360 - 554 KW for the 0/20 soffit case. Each point represents a single experiment.

comparison, with an average in-compartment CO yield of 0.22 for sufficiently underventilated compartment fires. Gottuk et al. [11,12] reported a reduction in downstream CO yields for open jet experiments of 75 - 90% of the in-compartment yields when sustained external burning occurred. The post hallway CO yields for this soffit case varied between 0.100 and 0.070, with an average of 0.089. These levels indicate a 54 - 68% reduction from in-compartment levels, averaging 60%. These results demonstrate that oxidation of CO did occur in the hallway, but less efficiently than for the open jet experiments.

Figure 3.7 shows total unburned hydrocarbon (THC) yields versus the GER for the 0 / 0 soffit case. In-compartment data from the open jet experiments of Gottuk et al. [7,11] are shown for comparison, with an average in-compartment THC yield of 0.33 for sufficiently underventilated compartment fires. The post-hallway THC yields for this soffit case varied from 0.022 to 0.055, a reduction of 83 - 93% from in-compartment levels. The average THC yield was 0.033, or a 90% reduction. Compared to CO, THCs were oxidized very efficiently in the hallway.

The low CO oxidation efficiency in the hallway can be attributed to a combination of limited air entrainment, the large amount of hydrocarbons present, and thermal quenching. It was observed at the compartment end of the hallway for experiments without an inlet soffit that buoyancy forced the hot exhaust gases to spread across the full hallway width, thus developing an upper layer as deep as the compartment exhaust vent height before sustained external burning occurred. This situation of hot exhaust gases flowing above cool air was a thermally stable configuration, resulting in limited mixing between the layers. The flame during sustained external burning was observed to be a turbulent sheet at the layer interface, stretching the full hall width and extending between 2/3 to the full length of the hallway.

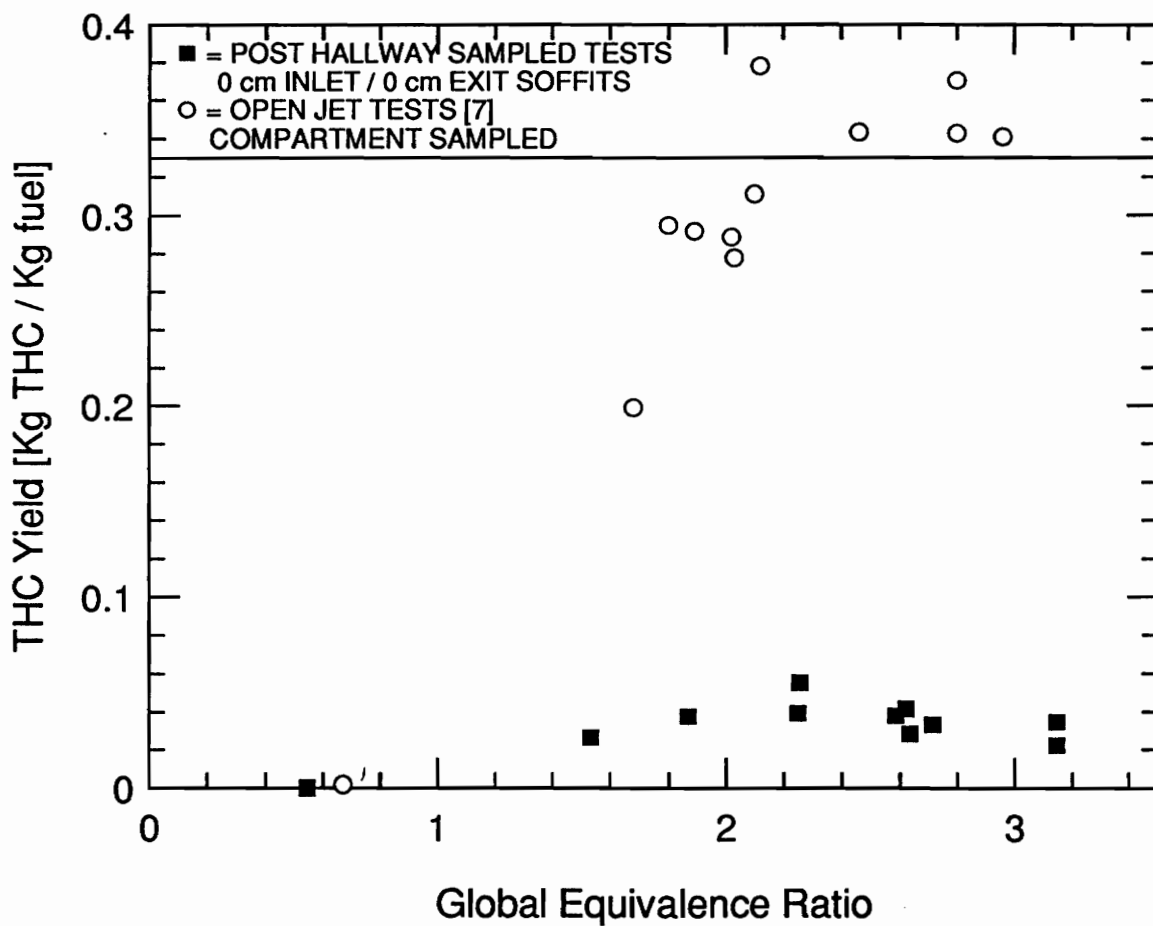


Figure 3.7 THC Yield versus "Quasi" steady state GER. Soffit case: 0/0. The total heat release rate of underventilated fires ranged from 254 - 562 KW. Each point represents a single experiment.



The effect of hydrocarbons on carbon monoxide oxidation was determined by conducting hallway-sampled experiments to provide a detailed map of normalized species concentrations along the hallway axis, shown in Figure 3.8. These hallway-sampled experiments were conducted for the conditions of a 20 cm diameter fuel pan and a 1200 cm<sup>2</sup> exhaust vent, producing an average global equivalence ratio of 2.0. The sampling probe was located 5 cm below the hallway ceiling, sampling in the hallway upper layer of exhaust gases, and along the center width of the hallway.

The THC concentration, initially 3.9%, displayed the behavior of a first order reaction, decaying exponentially along the hallway and reaching near complete oxidation by the end of the hallway, in agreement with the exhaust duct-sampled results. Carbon monoxide, initially at 8800 ppm, experienced a delay before a net reduction occurred in the hallway, and did not oxidize as completely by the end of the hallway. This is also in good agreement with the exhaust duct-sampled results. The concentrations for THCs and CO at the end of the hallway were about 1900 ppm and 3100 ppm respectively, a ratio of about 0.6.

The observed CO profile can be explained by separating the hallway into three regions. In approximately the first third of the hallway, no net CO oxidation was observed due to two main factors. First, THC oxidation occurs much faster than CO oxidation at the measured local temperatures, i.e. up to 1100 K, as indicated in the literature [10,11,25]. The reaction rate of the primary reaction responsible for the high temperature oxidation of CO ( $\text{CO} + \text{OH} \rightarrow \text{CO}_2 + \text{H}$ ) is less than that for the primary hydrocarbon oxidation reactions with OH [25]. At 1000 K, the rates for the reactions of OH with the majority of hydrocarbon species, formaldehyde up to propane, are between 1 and 2 orders of magnitude greater than the primary CO-OH reaction [25]. As the gas temperature

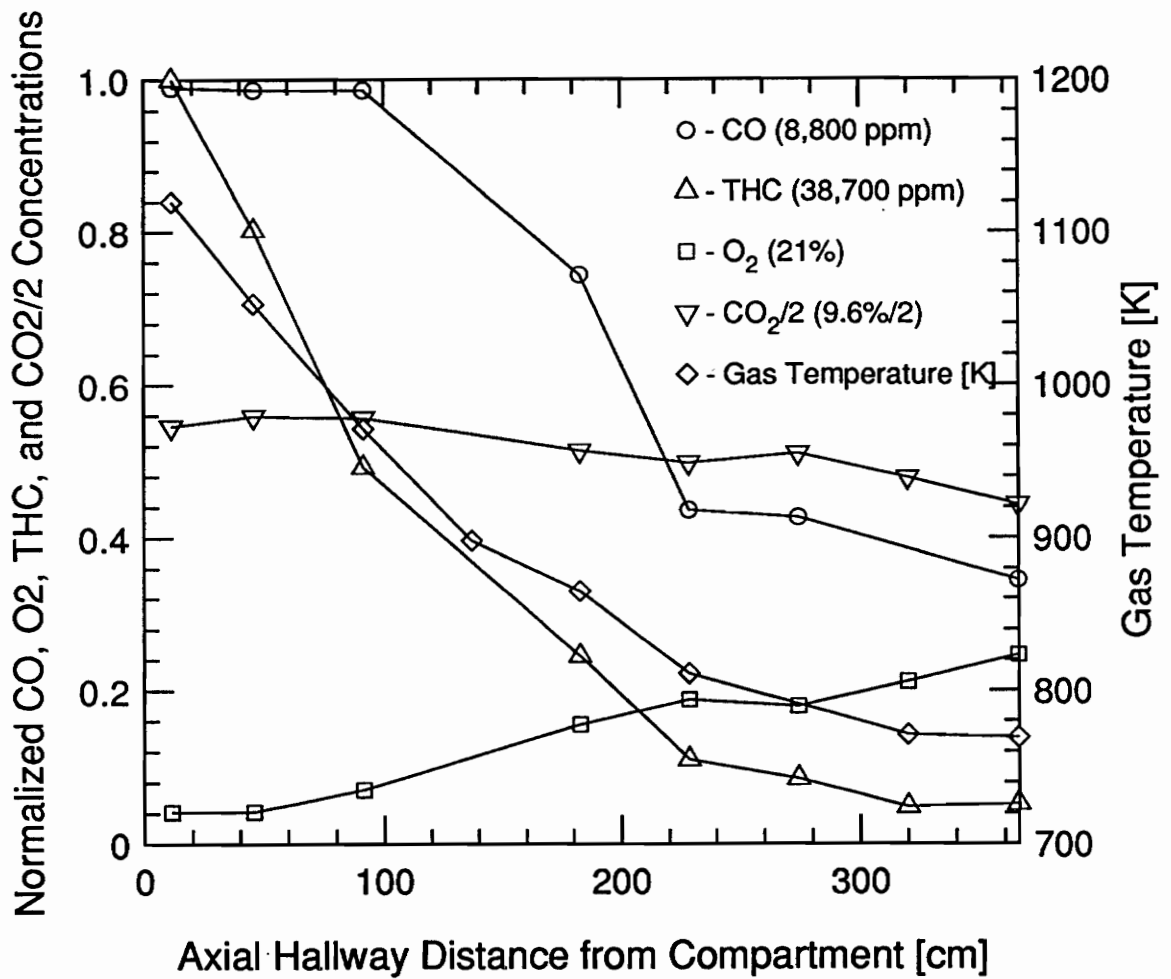


Figure 3.8 Normalized species concentrations and gas temperature versus hallway axial distance. Experimental conditions: **0/0 soffit case, 20 cm diameter fuel pan, 1200 cm<sup>2</sup> exhaust vent. Average GER: 2.0, average total heat release rate of fires: 413 KW. Sample location: 5.1 cm from ceiling, center width.** Normalizing concentrations given in legend.

drops below 950 K, the CO-OH reaction rate decreases rapidly due to a substantial drop in OH concentrations with temperature. At the lower temperatures, the CO reaction with HO<sub>2</sub> ( $\text{CO} + \text{HO}_2 \rightarrow \text{CO}_2 + \text{OH}$ ) soon becomes the most significant CO oxidation reaction [26]. However, at these low temperatures, the important free radicals, including HO<sub>2</sub>, are still more reactive with hydrocarbons. Thus, the presence of hydrocarbons continue to inhibit CO oxidation.

Due to the high reactivity of the free radicals important in combustion of organic fuels (i.e. O, H, OH, and HO<sub>2</sub>) with most hydrocarbons, the concentrations of these radicals remain low during hydrocarbon oxidation [10,25]. Once the hydrocarbons (unburned fuel and intermediate fragments) are oxidized to a significant degree, the radical pool grows enabling in the oxidation of CO [10,25]. This effect is magnified in this study due to the limited oxygen availability in the hallway and the poor air entrainment into the exhaust gas upper layer. The second factor affecting CO oxidation is the fact that CO is a product of THC oxidation, acting to decrease the net CO oxidation rate. In studies of CO oxidation in closed systems [10,11,25], this effect was noted as significant and was indicated by an increase in the concentration of CO during the oxidation of hydrocarbons.

As the exhaust gases traveled through roughly the second third of the hallway, a net oxidation of CO was observed as shown in Figure 3.8. In this section of the hallway, the bulk of the THC's had been oxidized, again resulting in a two fold effect on CO oxidation. First, the reduced THC concentration allowed the free radical pool to grow, resulting in an increase in the oxidation of CO. Second, a decrease in THC's, and so in the THC oxidation rate, reduced the amount of CO produced.

As the exhaust gases proceeded into the final third of the hallway, heat losses due to dilution with ambient air and greater radiation losses to the atmosphere through the

open end of the hallway caused a significant drop in the hallway gas temperature. The flames in experiments with a 0 cm inlet soffit were visibly observed to extend only about two thirds of the length of the hallway. The corrected gas temperatures at the point of flame extinction indicated a temperature in the neighborhood of 800 to 700 K. According to the chemical kinetic modeling studies of Pitts [10] and Gottuk [11], this temperature range was identified as that where the oxidation rate of CO to CO<sub>2</sub> decreases very rapidly. Since the bulk of the THC's were oxidized by this stage, and the CO oxidation rate was decreasing, a flame could no longer be sustained.

Any decrease in the concentrations of CO and THC's past the flame extinction point was attributed to dilution by transport of air into the upper layer, and of exhaust gases into the lower air layer. This was evident by the increasing oxygen concentration in the upper layer toward the end of the hallway. The carbon dioxide (CO<sub>2</sub>) concentration in the upper layer also decreased toward the end of the hall. Since CO<sub>2</sub> was a final product of combustion, the decreasing concentration was only possible by dilution.

The height profile of species concentrations was also investigated halfway down the hallway axis, along the center width, for the same conditions of the axial profile. This profile is given in Figure 3.9. At this axial location, the turbulent flame was located between 5 and 10 cm below the ceiling, as determined from the location of steep CO, THC, and O<sub>2</sub> concentration gradients, and the drop in the temperature profile. This profile also shows that compared to THC's, more CO survives through the flame front into the air layer below. The concentrations of CO and THC's level off at 970 ppm and 390 ppm respectively, a ratio of 2.5 as compared to 0.23 at the compartment exit. This provides evidence that hydrocarbons do oxidize faster than CO.

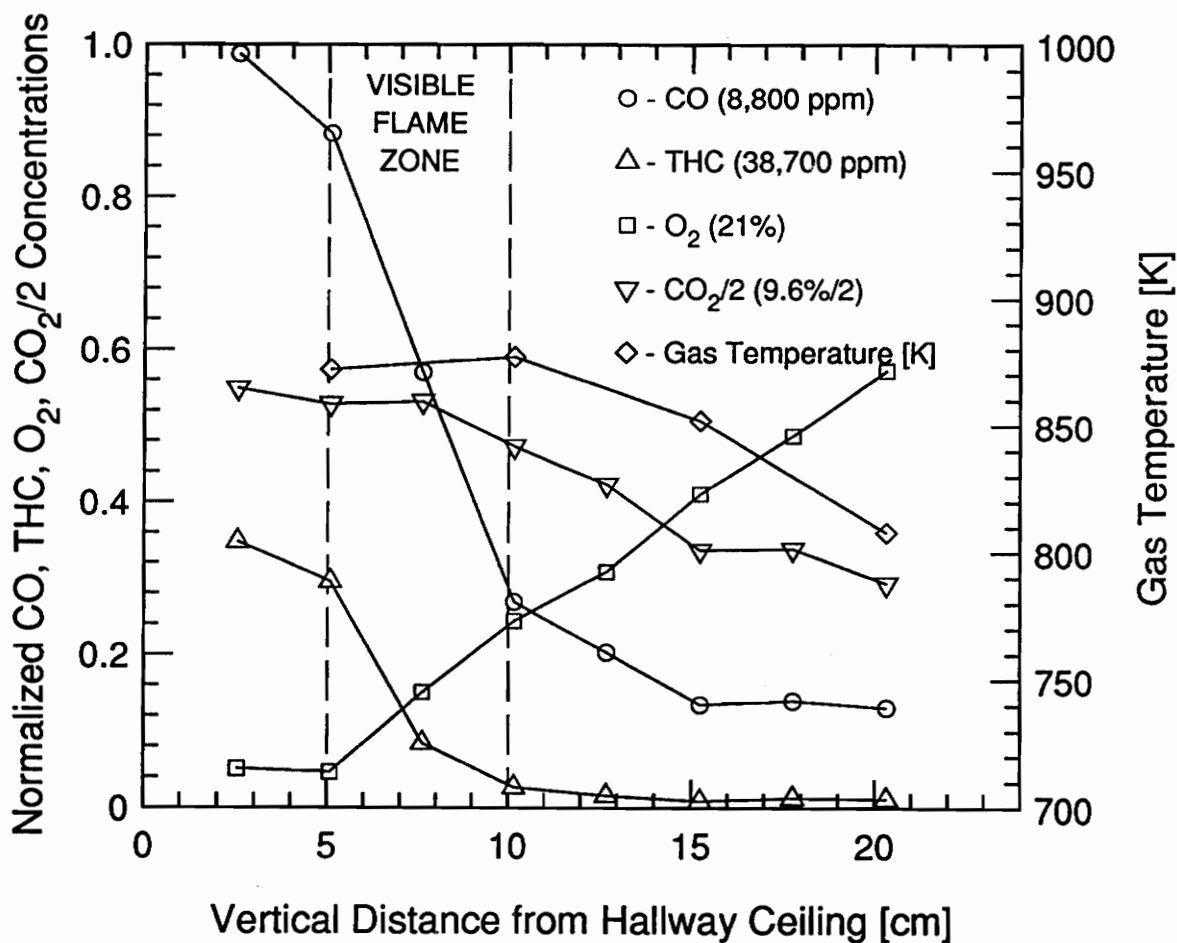


Figure 3.9 Normalized species concentrations and gas temperature versus hallway distance from ceiling. Experimental conditions: 0/0 soffit case, 20 cm diameter fuel pan, 1200 cm<sup>2</sup> exhaust vent. Average GER: 2.3, average total heat release rate of fires: 434 KW. Sample location: 1.83 m axially from compartment, center width. Normalizing concentrations given in legend.

Smoke yields were also investigated downstream of the hallway. The open jet experiments of Gottuk et al. [11,12] demonstrated an average smoke yield of 0.015 shortly before sustained external burning occurred. During sustained external burning, Gottuk et al. [11,12] reported a reduction of 50 - 100% in the smoke yield. The smoke yields have the same general trends seen with the CO and THC yields; however, with a greater amount of scatter. The smoke yields measured in this study for the 0 / 0 soffit case varied between 0.0077 and 0.0021 with an average of 0.0051. Compared to the average smoke yield before sustained external burning, this translates to a reduction of 48 - 86%, with an average of 66%. This was as efficient as the open jet experiments.

#### **3.4.2 Hallway Soffits: 0 cm inlet / 20 cm exit**

Figure 3.6 also shows the post hallway CO yields versus the GER for the 0 / 20 soffit case. These CO yields varied between 0.171 to 0.128, a reduction of 22 - 57% from in-compartment levels. Averages were 0.155 and 40% respectively. Compared to the 0 / 0 soffit case, CO oxidation was obviously less efficient. The post hallway THC yields for this soffit case are given in Figure 3.10. These THC yields ranged from 0.082 to 0.037, producing a 75 - 89% reduction from in-compartment yields. The yield average for THC was 0.063, a reduction of 81%. The THC yields for this soffit case were not significantly different from that for the 0 / 0 soffit case, with oxidation only slightly less efficient. The relative difference between the magnitudes of the effect of the exit soffit on CO and THC oxidation demonstrates the quicker net oxidation rate of THC compared with CO.

The further reduction of the CO and THC oxidation efficiencies with the 20 cm exit soffit, compared with the already inefficient 0 / 0 soffit case, can be explained from the blockage to exhaust flow by the exit soffit. Blockage of the exit soffit causes an increased depth of the hallway exhaust gas upper layer. Since the interfacial area where the mixing-

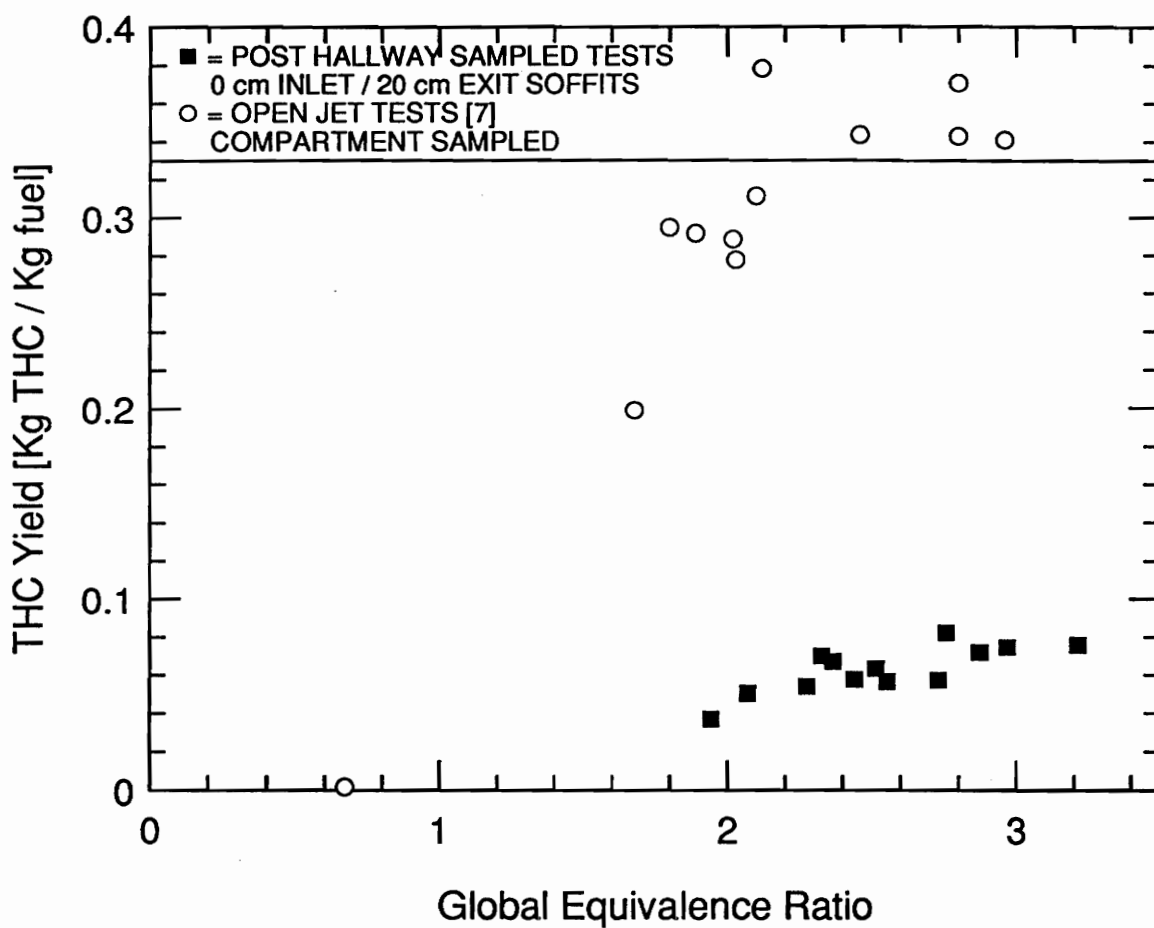


Figure 3.10 THC Yield versus "Quasi" steady state GER. Soffit case: 0/20. The total heat release rate of fires ranged from 360 - 554 KW. Each point represents a single experiment.

limited flame existed remained close to the same, determined by the hallway width, increasing the upper layer volume allowed more exhaust gases to escape unburned in the upper layer as the flame was quenched toward the end of the hallway. As with the 0 / 0 soffit case, sustained external burning extended anywhere from 2/3 to the full length of the hallway.

The increased upper layer depth in the hallway was confirmed by visual observation, since the flame was not able to penetrate as deep into the upper layer as for the 0 / 0 soffit case. Confirmation was also indicated by a series of height profile experiments where species and temperature profiles were acquired halfway down the hallway, as a function of distance from the ceiling. This profile is given in Figure 3.11 for the 0 / 20 soffit case. The same experimental conditions were used as was for the height profile with the 0 / 0 soffit case, given in Figure 3.9, for comparison purposes. The height profile for the 0 / 20 soffit case showed the flame occurring between 13 to 18 cm from the ceiling, again determined by the concentration gradients and temperature drop. This represents a doubling of the 0 / 0 soffit case upper layer height of 5 to 10 cm.

Other than the increase in the upper layer depth, the height profile trends for the 0 / 20 soffit case remained unchanged from the 0 / 0 soffit case. The trends of the axial profile in the hallway also behaved similar to the 0 / 0 soffit case, of course, with higher CO and THC concentrations at the exit of the hallway.

The smoke yields investigated for the 0 / 20 soffit case had the same general trends seen with the CO and THC yields. The smoke yields for the 0 / 20 soffit case varied between 0.0117 and 0.0065, with an average of 0.0090. Based on Gottuks results of 0.015 smoke yield before sustained external burning, this translates to a reduction of 22 -



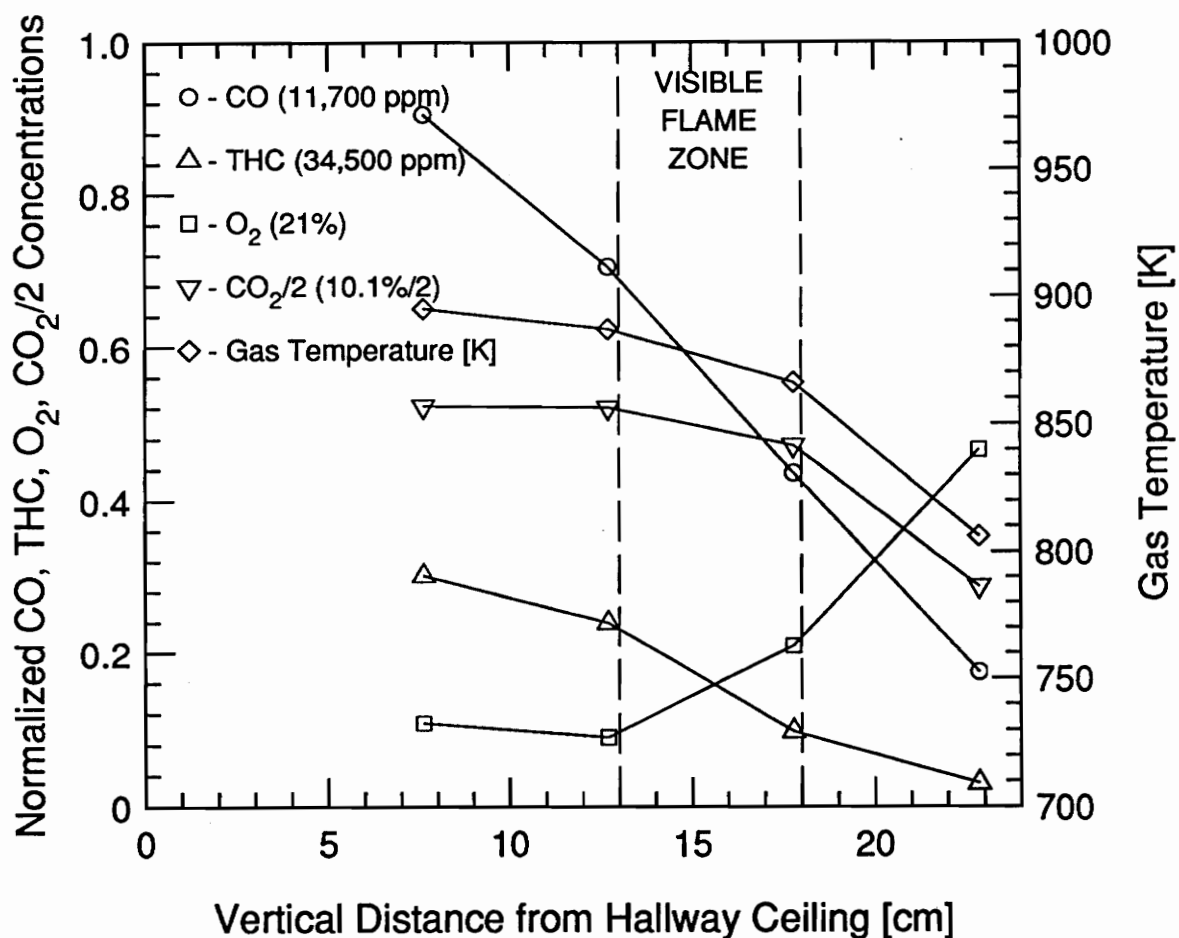


Figure 3.11 Normalized species concentrations and gas temperature versus hallway distance from ceiling. Experimental conditions: 0/20 soffit case, 20 cm diameter fuel pan, 1200 cm<sup>2</sup> exhaust vent. Average GER: 2.8, average total heat release rate of fires: 444 KW. Sample location: 1.83 m axially from compartment, center width. Normalizing concentrations given in legend.

57%, with an average of 40%. This was much less efficient than without an exit soffit, which can also attributed to the deeper upper layer.

### **3.4.3 Hallway Soffits: 20 cm inlet / 0 cm exit**

Figure 3.12 shows the CO yield versus the GER for the 20 / 0 soffit case. The CO yield for this soffit case displayed a different trend than for either of the cases without an inlet soffit. Two regions of different CO oxidation efficiency existed which could not be distinguished based on the GER alone. Further investigation revealed the fuel vaporization rate to be the strongest parameter responsible for the given behavior. Figure 3.13 shows this dependency compared for all soffit cases. At low fuel rates, below 10 g/s, CO oxidation was as efficient as open jet burning [11,12], with the CO yield varying between 0.049 and 0.024, a reduction of 78 - 89% from in-compartment levels. Average values were 0.039 and 82% respectively. It is interesting to note that an inlet soffit as small as 20 cm produced a significant change in the fluid mechanics and provided oxidation as efficient as an open jet.

During these experiments, a buoyant jet was observed exhausting from the compartment. The 20 cm inlet soffit allowed the upper layer in the hallway to form above the exhaust vent, allowing a buoyant jet of hot exhaust gases to enter the hallway in the lower air layer, and rise into the upper layer. This occurred in contrast to spilling horizontally directly into the upper layer, which was what happened without the inlet soffit. This turbulent jet resulted in enhanced mixing and an increased interfacial area with air.

An axial profile of normalized species concentrations for a low fuel rate case, with the same experimental conditions for the 0 / 0 soffit axial profile, is given in Figure 3.14. From the data it is obvious that CO, as well as THCs, are completely oxidized within the

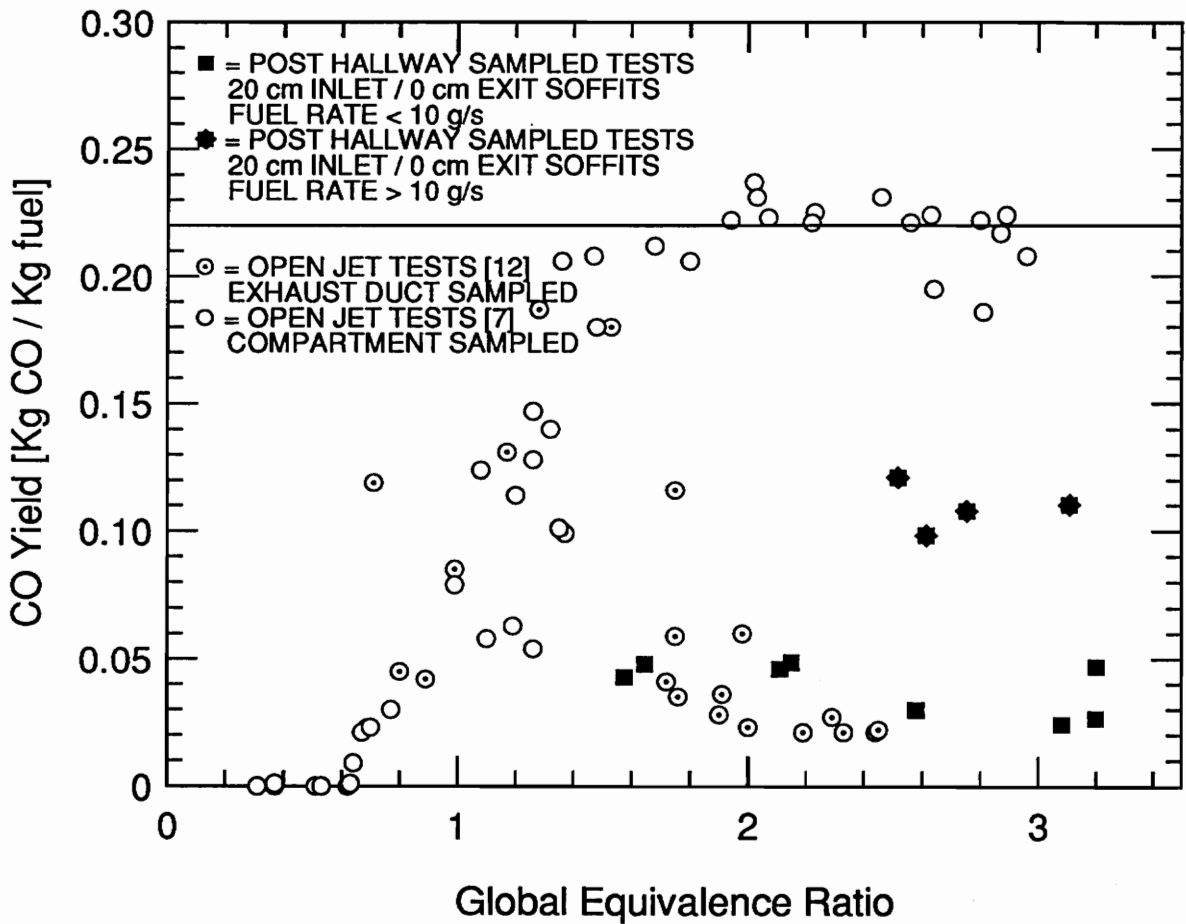


Figure 3.12 CO Yield versus "Quasi" steady state GER. Soffit case: 20/0. The total heat release rate of fires ranged from 294 - 423 KW for low fuel rates, and 480 - 574 KW for high fuel rates. Each point represents a single experiment.

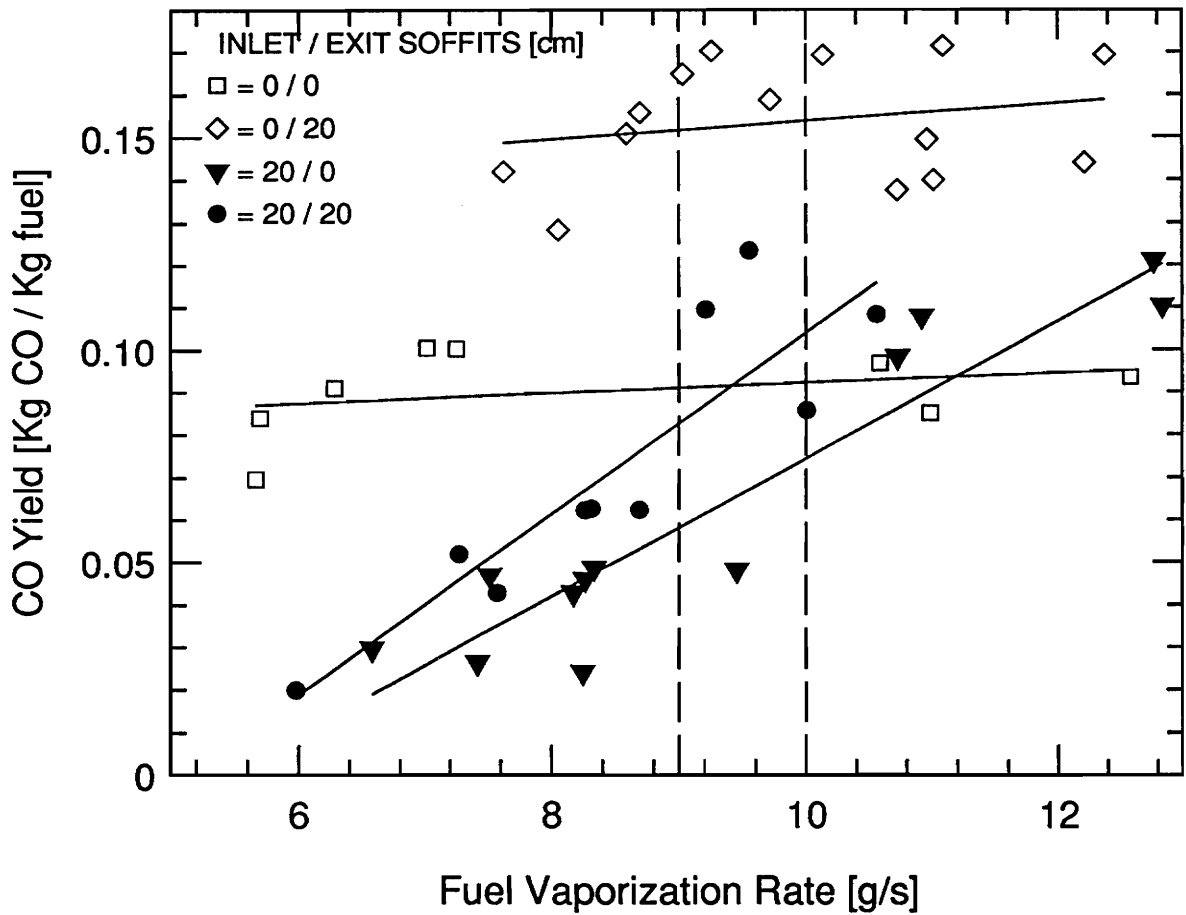


Figure 3.13 CO Yields versus fuel vaporization rate for all soffit combinations. GER range: 1.5 to 3.5 for all tests. Range of total heat release rate of fires: 254 to 574 KW for all tests.

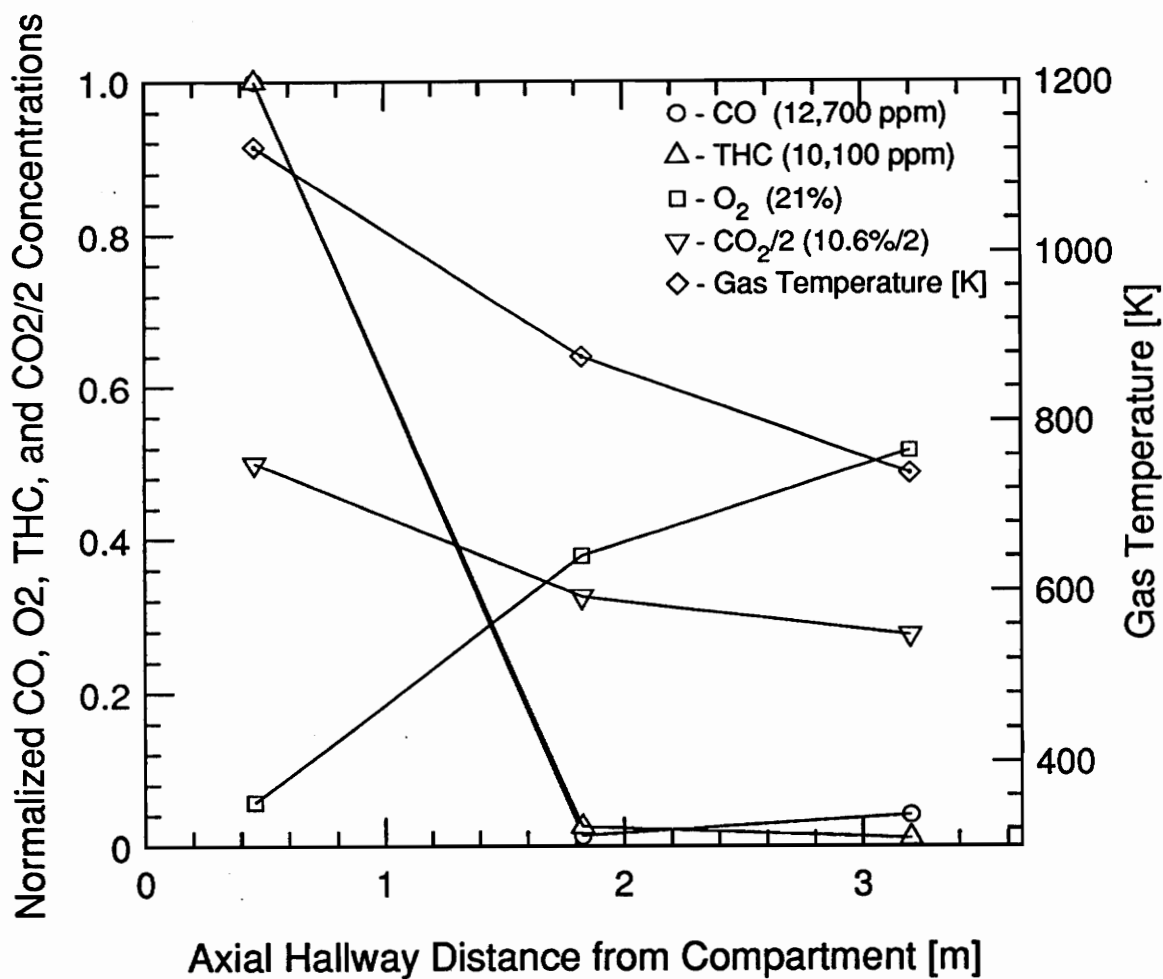


Figure 3.14 Normalized species concentrations and gas temperature versus hallway axial distance. Experimental conditions: 0/20 soffit case, 20 cm diameter fuel pan, 1200 cm<sup>2</sup> exhaust vent. Average GER: 3.3, average total heat release of fires: 348 KW. Sample location: 5.1 cm from ceiling, center width. Normalizing concentrations given in legend.

first half of the hallway. A height profile halfway down the hallway also indicated very little CO at any height. The flame jet was also visibly observed to extend halfway along the hallway, with the flame burning along the ceiling surface toward the furthest extension of the flame. This indicated that air entrained in this case was sufficient for sustained external burning to result in complete oxidation of the exhaust gas upper layer. An added advantage of the enhanced air entrainment and oxidation close to the compartment was to oxidize CO in a higher temperature region where the kinetic oxidation rate was faster.

As the fuel vaporization rate increased beyond about 10 g/s, the post hallway CO yield began to increase. The CO yields for the experiments with high fuel rates varied from 0.121 to 0.098, with an average of 0.109. This resulted in a 45 - 55% reduction from in-compartment levels, with an average of 50%. The efficiency of air entrainment induced by the buoyant jet was relatively insensitive to the fuel vaporization rate. However, increasing the fuel vaporization rate produced higher concentrations of THC<sub>s</sub> and CO in the exhausting gases from the compartment, requiring the flame to extend further down the hall to entrain sufficient oxygen. This extension of the flame in experiments with higher fuel rates was visually observed. Eventually the flame reached a point where again the decreasing gas temperature caused the oxidation of CO to freeze out, quenching the flame.

Due to the faster oxidation rate of THC<sub>s</sub> compared to CO, the THC<sub>s</sub> exhibited only a slight effect due to increasing the fuel vaporization rate. For either fuel rate regime tested, THC oxidation was very efficient as is shown in Figure 3.15. For fuel rates below 10 g/s, the THC yield varied from 0.026 to 0.009, averaging 0.016. This represented a 92 - 97% reduction from in-compartment levels, averaging an efficient 95%. The THC yields with fuel rates greater than 10 g/s varied between 0.038 to 0.029, an 88 - 91% reduction

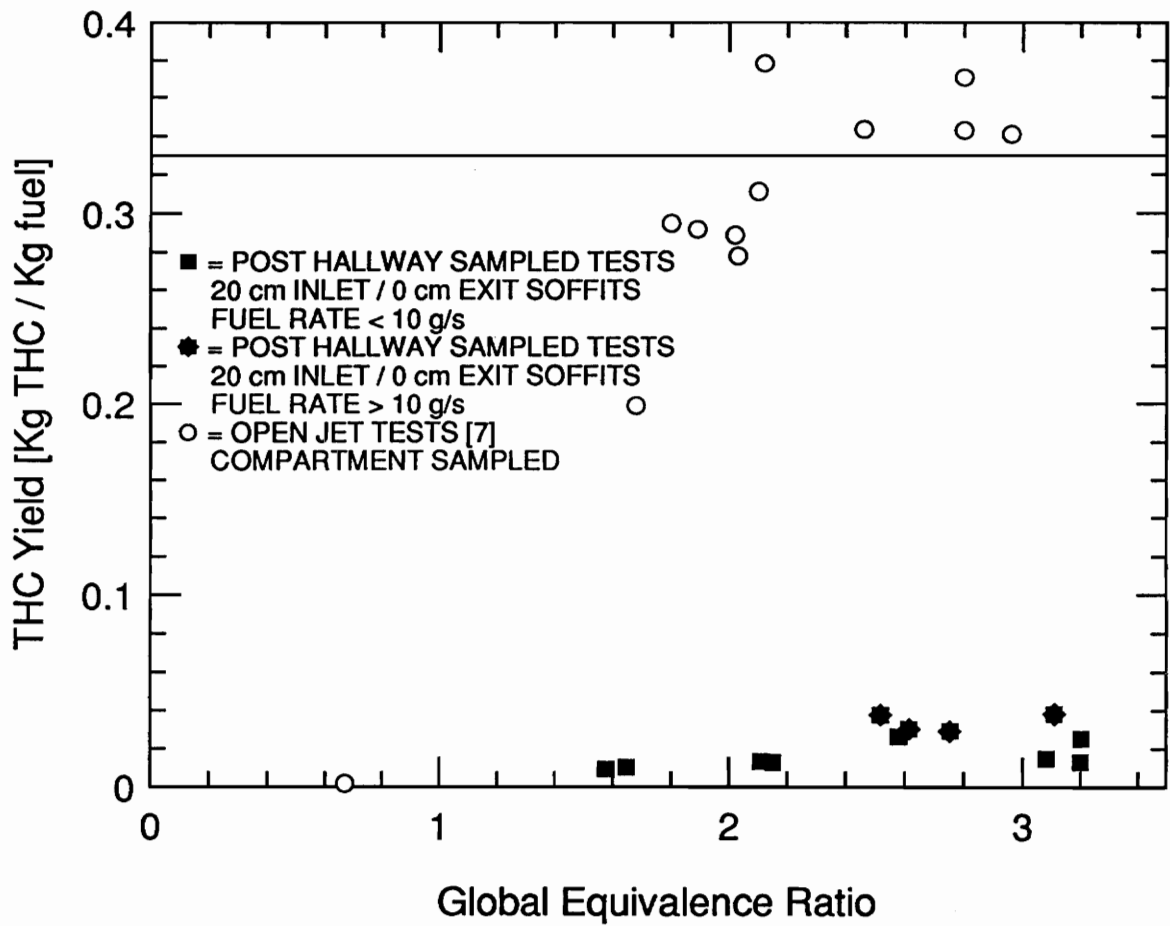


Figure 3.15 THC Yield versus "Quasi" steady state GER. **Soffit case: 20/0.** The total heat release rate of fires ranged from 294 - 423 KW for low fuel rates, and 480 - 574 KW for high fuel rates. Each point represents a single experiment.

from in-compartment levels. The average yield was 0.034, or a 90% reduction. From this data, it is expected that the THC yield would not increase dramatically by increasing the fuel rate until the CO yield approached in-compartment levels.

The smoke yields also demonstrated a dependency on the fuel vaporization rate, although not as sensitive as CO yields, but more sensitive than THC's. The smoke yields with a fuel vaporization rate below 10 g/s varied between 0.0059 and 0.0012 with an average of 0.0036. Based on the smoke yield before sustained external burning, this translates to a reduction of 61 - 92%, with an average of 76%. This was as efficient as the open jet experiments of Gottuk et al. [11,12], and more efficient than experiments with a 0 cm inlet soffit and either exit soffit. Again, this was attributed to the enhanced air entrainment of the jet of gases exhausting from the compartment.

For the higher fuel vaporization rate, the smoke yields varied between 0.0087 and 0.0067 with an average of 0.0078. These yields translate to a reduction of 42 - 56% from the in-compartment levels, with an average of 48%. This was, as expected, less efficient than with the lower fuel rate. It was also slightly less efficient than the open jet experiments of Gottuk et al. [11,12].

#### **3.4.4 Hallway Soffits: 20 cm inlet / 20 cm exit**

The CO yields versus the GER for the case of 20 cm soffits at the inlet and exit are shown in Figure 3.16. The fuel vaporization rate dependency observed without the exit soffit was again evident, as shown previously in Figure 3.13. In the low fuel rate region, below 9 g/s, the CO yield varied between 0.063 and 0.020, a 71 to 91% reduction from in-compartment levels. Averages were 0.049 and 78%. For this region, CO oxidation was as efficient as the 20 / 0 soffit case, and the open jet experiments [11,12]. The flame jets for these tests were again visibly observed to oxidize by the first half of the hallway, as



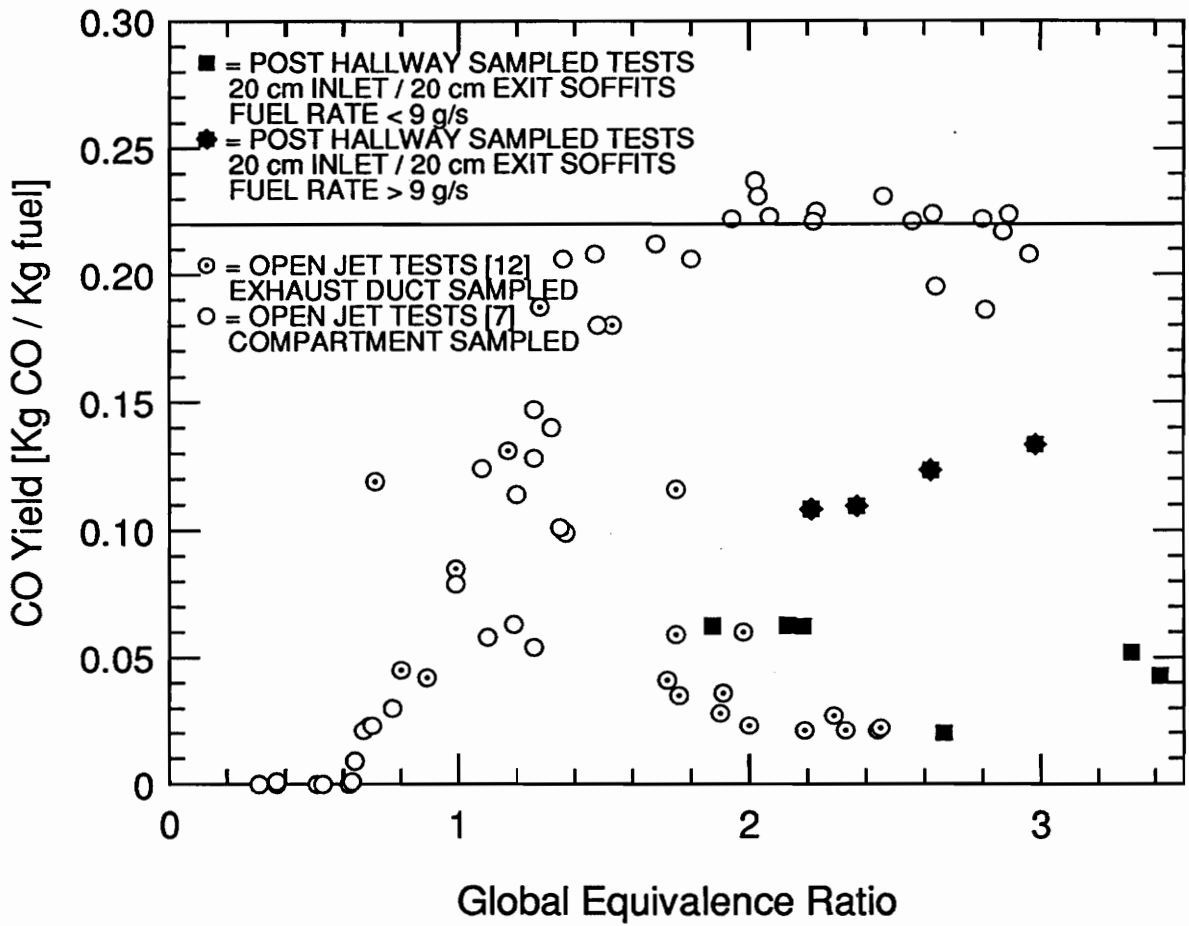


Figure 3.16 CO Yield versus "Quasi" steady state GER. Soffit case: 20/20. The total heat release rate of fires ranged from 267 - 389 KW for low fuel rates, and 411 - 613 KW for high fuel rates. Each point represents a single experiment.

was confirmed by an axial concentration profile, resembling the profile for the 20 / 0 soffit case. Since oxidation of the exhausting gases was complete well before the exit of the hallway was reached, the exit soffit had no significant effect on oxidation.

As the fuel vaporization rate increased, the hallway flame extended further towards the exit soffit, and therefore began to be affected by the altered flow pattern. The efficiency of CO oxidation decreased as the fuel vaporization rate increased beyond 9 g/s. The lower fuel rate of 9 g/s where inefficient oxidation began, compared to 10 g/s with the 20 / 0 soffit case, demonstrates a sensitivity to the exit soffit. As the fuel rate increased further and the effect of the exit soffit became more significant, the transition from efficient CO oxidation to inefficient oxidation occurred much more quickly than without the exit soffit. This was due to the increased upper layer depth in the hallway, similar to the effects seen by varying the exit soffit in the absence of an inlet soffit. For experiments conducted with fuel rates above 9 g/s, the CO yield varied between 0.134 and 0.108, and averaged 0.119. This represents a 39 - 51% reduction, 46% on average, from in-compartment levels.

The THC yields exhibited similar behavior to the case without an exit soffit, as shown in Figure 3.17. With fuel rates below 9 g/s, the THC yields varied from 0.029 to 0.006, averaging 0.015. Compared to in-compartment levels, this represents a 91 - 98% reduction from in-compartment levels, with an average of 95%. For experiments with fuel rates greater than 9 g/s, the THC yield varied between 0.045 and 0.024, a 86 - 93% reduction from in-compartment levels. Averages were 0.033 and 90% respectively. Again, the difference in THC yields at different fuel rates was small compared to the CO yields. The variation of THC yields for this case, compared to without an exit soffit, was insignificant even for the higher fuel rates. This shows very little affect of the exit soffit on THC yields for the given 20 cm height.

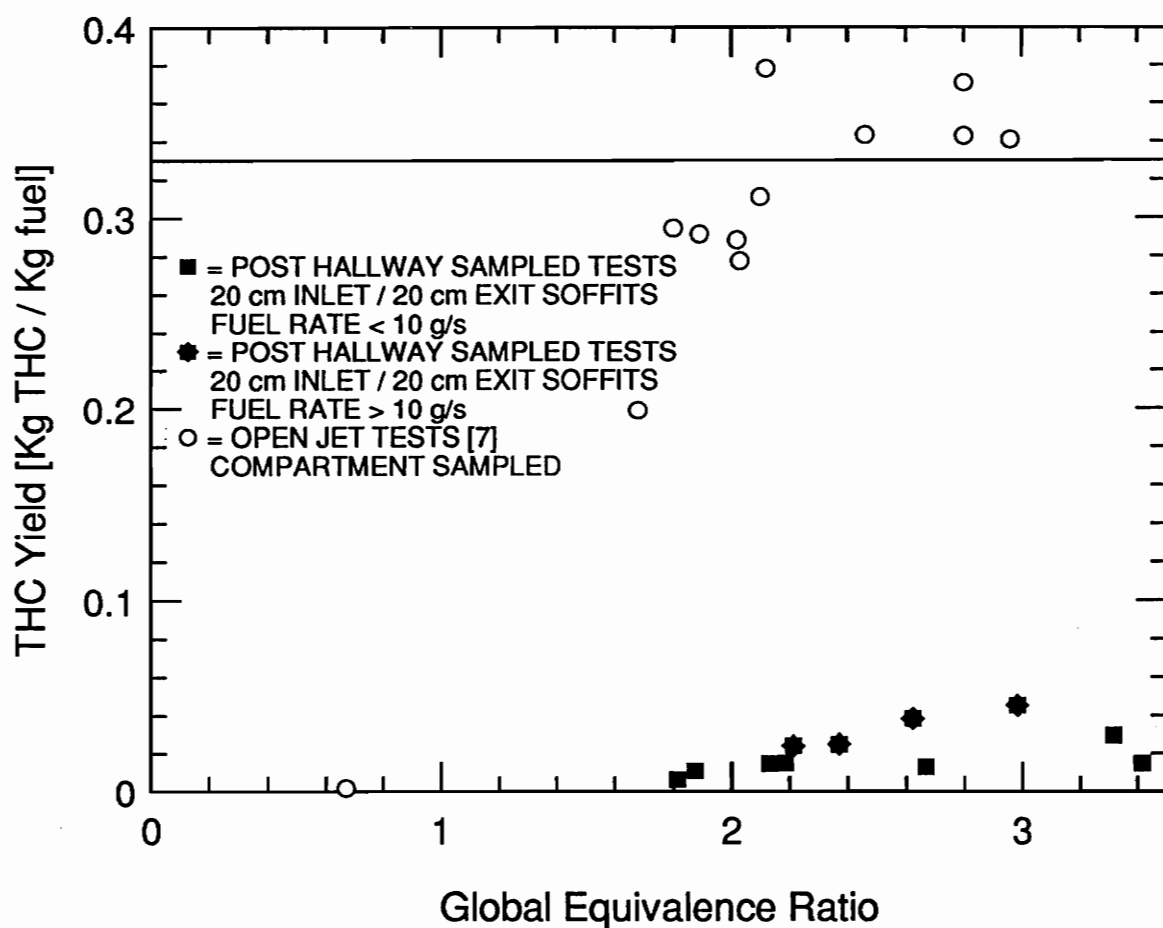


Figure 3.17 THC Yield versus "Quasi" steady state GER. Soffit case: 20/20. The total heat release rate of fires ranged from 267 - 389 KW for low fuel rates, and 411 - 613 KW for high fuel rates. Each point represents a single experiment.

The smoke yields again demonstrated a dependency on the fuel vaporization rate, although not as sensitive as CO, but more sensitive than THC<sub>s</sub>. The smoke yields with a fuel vaporization rate below 9 g/s varied between 0.0066 and 0.0017 with an average of 0.0042. This demonstrates a reduction of 56 - 88%, with an average of 72%. This was not much different from the case without the exit soffit, again since oxidation was complete by the end of the hallway. For the higher fuel vaporization rate, the smoke yields varied between 0.0109 and 0.0081 with an average of 0.0092. Translated to percent reduction before sustained external burning indicates a 28 - 46% reduction, with an average of 39%. This was again less efficient than with the lower fuel rate. It is also obvious that with the 20 cm exit soffit, the smoke yields were much more sensitive to the higher fuel rates, as was also seen with the CO yields.

## CHAPTER 4

### SUMMARY AND CONCLUSIONS

#### 4.1 Summary

Underventilated compartment fire experiments were performed with a compartment exhausting along the axis of a 3.7 m long hallway to examine the composition of the exhausting gases during sustained external burning. Sustained external burning occurred when fuel rich exhaust gases from the compartment mixed with air in the hallway, ignited and produced sustained burning of this mixture in the hallway. The emphasis of this study was to investigate the effects of the hallway, and the soffit heights at both ends of the hallway, on the efficiency of sustained external burning in oxidizing the toxic gases from the compartment.

The design of the compartment allowed direct measurement of the global equivalence ratio (GER), the fuel to air ratio in the compartment, which was used as a main correlating parameter. Gas sampling was performed downstream of the hallway to determine the overall efficiency of sustained external burning for a variety of global equivalence ratios. Gas sampling was also performed in the hallway to provide a detailed investigation of the processes occurring in the hallway that generated the overall results.

In order to determine when sustained external burning would occur, two characteristic global equivalence ratios (CGERs) were investigated. The CGERs were defined as the instantaneous global equivalence ratios when short flashes and sustained external burning began in the hallway, termed  $\Phi_{\text{flash}}$  and  $\Phi_{\text{seb}}$  respectively. In general, the exit soffit had very little effect on the CGERs relative to the inlet soffit. In the absence of an inlet soffit,  $\Phi_{\text{flash}}$  demonstrated exponential behavior with respect to the exhaust

vent size, with larger exhaust vents and fuel pans producing flashes at lower GERs.  $\Phi_{seb}$  showed more complex behavior, dependent on both the exhaust vent area and the height to width ratio, again decreasing with larger vents. A 20 cm inlet soffit eliminated any occurrences of short flashes due to enhanced air entrainment, which was caused by the improved exhaust gas plume exiting the compartment into the hallway.  $\Phi_{seb}$  for a 20 cm inlet soffit displayed a simple dependence on the exhaust vent area, and no dependence on the fuel pan size.

Compared to the open jet experiments of Gottuk et al. [11,12], which characterized a compartment fire exhausting into the open atmosphere, the CGERs were much more sensitive to the exhaust vent and fuel pan sizes due to the competing effects of the reduced air entrainment and the increased heat retention in the hallway. The CGERs for the hallway were also higher than determined for the open jet experiments due to the reduced air entrainment in the hallway, although cases with larger vents approached values obtained for open jet experiments. Although the flammability of the exhaust gases was determined by the global equivalence ratio in the compartment, the occurrence of ignition and sustained external burning of the exhausting gases was dictated by the exhaust vent and fuel pan sizes, which controlled the heat transfer from the compartment and the availability of an ignition source.

Another method investigated to classify when sustained external burning occurred was the ignition index developed by Beyler [21]. The ignition index was based on the flammability limits of carbon monoxide, hydrocarbons, and hydrogen, and included the effects of temperature to classify the flammability of the exhaust gas mixture supplied with a stoichiometric amount of air. The results indicated an average ignition index of 1.2 when sustained external burning occurred without an inlet soffit. Values for the ignition index of all experiments varied between 1.0 and 1.5, indicating a dependence on the

exhaust vent and fuel pan size. Additional experiments are required with a more complete analysis of the flammable exhaust gases present to determine a correlation for the effect of different exhaust vent and fuel pan sizes on the ignition index.

The oxidation of the exhaust gases, leaving an underventilated compartment fire to an adjacent hallway was shown to vary among different species, and also to be very sensitive to the hydrodynamic mixing between the rich exhaust plume and the cooler ambient air in the hallway. The gas temperatures in the hallway and fuel vaporization rate were also determined to affect oxidation in the hallway. Variations in the hallway inlet and exit soffits produced significant effects on the hydrodynamic structure of the exhaust plume and oxidation efficiencies. A summary of the oxidation efficiencies obtained for experiments of different soffit arrangements, and for the open jet experiments of Gottuk et al. [11,12], is given in Table 4.1.

For all soffit configurations, the overall oxidation of THC<sub>s</sub> was much more complete than for CO. This result was explained by two effects. First, at the local temperatures measured in the hallway, the oxidation rate of THC<sub>s</sub> is much faster than that for CO, causing the entrained oxygen to be depleted by THC<sub>s</sub>. Second, oxidation of THC<sub>s</sub> produced CO, which decreased the net CO oxidation rate. The oxidation of THC<sub>s</sub> essentially inhibited the oxidation of CO with the oxygen limited environment in the hallway. Due to this favorable chemical kinetic situation, THC oxidation was very insensitive to changes in soffit heights, whereas the oxidation of CO was dramatically affected. The oxidation efficiency of soot displayed a sensitivity to soffit heights similar to that of CO.

The inlet soffit exhibited the strongest effect on the oxidation of all exhaust gases in the hallway due to the effect on air entrainment of the plume exhausting from the

**TABLE 4.1**

Post-compartment oxidation efficiency ranges for underventilated compartment fires.  
 Data for hallway tests with various soffit heights and open jet tests [11,12].

Species	Open Jet Experiments [11,12]	Hallway Experiments			
		Soffits: 0 cm inlet 0 cm exit	Soffits: 0 cm inlet 20 cm exit	Soffits <sup>a</sup> 20 cm inlet 0 cm exit	Soffits <sup>b</sup> 20 cm inlet 20 cm exit
CO	75 - 90%	54 - 68%	22 - 42%	78 - 89% (45 - 55%)	71 - 91% (39 - 51%)
THCs	N/A	83 - 93%	75 - 89%	92 - 97% (88 - 91%)	91 - 98% (86 - 93%)
Soot	50 - 100%	48 - 86%	22 - 57%	61 - 92% (42 - 56%)	56 - 88% (28 - 46%)

<sup>a</sup> values in parenthesis are for fuel rate > 10 g/s

<sup>b</sup> values in parenthesis are for fuel rate > 9 g/s



compartment. In the absence of an inlet soffit, the hallway exhaust gas upper layer formed with a depth equal to the compartment exhaust vent height. The buoyant gases exhausting from the compartment entered the hallway upper layer directly without a vertical plume. This caused a density-stratified configuration opposed to mixing, consisting of an upper layer of hot exhaust gases flowing above cool air. Complete CO oxidation was not realized with the 0 cm inlet soffit due to the inhibiting effects of THC oxidation combined with the poor air entrainment in the beginning of the hallway, and due to quenching of the flame toward the end of the hallway. The inefficient air entrainment of this configuration also resulted in relatively poor soot oxidation.

The 20 cm inlet soffit provided enhanced mixing by allowing a jet of buoyant gases to exhaust from the compartment into the lower air layer and rise into the upper layer. With a low enough fuel vaporization rate, the improved air entrainment allowed near complete oxidation of CO, soot, and THCs within the first half of the hallway. However, with higher fuel vaporization rates producing higher concentrations of unburned exhaust gases, the enhanced air entrainment was not sufficient for complete combustion, causing the flame to extend further down the hallway. Eventually, as the fuel vaporization rate was increased, the oxidation efficiencies of CO and soot decreased significantly to levels comparable to without an inlet soffit, where as THC oxidation was only slightly affected.

The presence of an exit soffit had an opposite, though less significant, effect on exhaust gas oxidation. Without an exit soffit, exhaust gases flowed freely out of the end of the hallway, whereas a 20 cm exit soffit obstructed the flow causing a deeper upper layer to develop in the hallway. The deeper upper layer resulted in reduced oxidation efficiencies for all species by allowing a larger volume of gases to escape in the unburned upper layer. However, the exit soffit only produced an effect on oxidation efficiencies

with the 20 cm inlet soffit during high fuel rates, when the external flame approached the end of the hallway.

## 4.2 Conclusions

The main result of this study indicated that entrainment of ambient air into the exhaust gas plume coming out of a burning compartment is dramatically reduced when discharged into an enclosed hallway, as compared to an open environment. As a result, the oxidation of exhaust gases in the hallway is mixing limited and, in general, less efficient. The results of this study show that the inlet soffit, i.e. the distance from the hallway ceiling to the top of the compartment exhaust vent, has the most significant effect on enhancing air entrainment. This enhancement of air entrainment translates to a significant increase in the oxidation efficiency of the exhaust gas plume in the hallway. Some of the results also suggest that the increased heat retention in the enclosed hallway, again compared to a plume exhausting to the open atmosphere, also has a significant, though less prominent, effect on exhaust gas oxidation.

The effect of the inlet soffit on enhancing mixing of the exhaust gases with ambient air is the result of two primary factors. First, a larger inlet soffit results in a larger vertical distance between the exhausting gases and the exhaust gas upper layer in the hallway. This geometry provides an increase in the interface area between the exhaust gases and the ambient air, thus increasing mixing. Second, the higher upward velocity of the exhaust gases due to the buoyancy-driven acceleration for larger inlet soffits also results in enhanced mixing.

As is typical in fluid dynamics, the Reynolds number ( $\rho UL/\mu$ ) is expected to be an important dimensionless group for scaling the viscous entrainment of air into the exhaust plume. The gas properties should be evaluated for the exhausting gases and the velocity

taken as that of the exhausting gases. The exhaust gas velocity could be calculated from the exhaust gas flow rate divided by the exhaust vent area. The characteristic length should be taken as the inlet soffit height, since this study indicated it to be the most important length parameter. Inefficient mixing is expected for high values of the Reynolds number since this would indicate high inertia (small residence times) relative to low viscosity (poor mixing). This situation is expected to allow little vertical gas motion, producing the poor air entrainment configuration of hot exhaust gases flowing horizontally over cold air. However, the importance of large scale vortical structures at high Reynolds numbers will be significant by enhancing air entrainment. In this range, the Reynolds number is expected to be the strongest correlating parameter.

For low Reynolds numbers, the residence times will be high due to the relatively slow flow rate. In this flow regime, the efficiency of mixing is expected to be controlled by the buoyant forces and display a strong dependence on the inlet soffit height. In this situation, the Froude number ( $U^2/gL$ ) is expected to display a stronger relationship with the air entrainment rate since it relates the magnitudes of inertia to buoyancy. Again, the same velocity and length scales suggested for the Reynolds number should be used. Efficient mixing should be expected for low Froude numbers, indicating buoyancy dominated vertical flow. This situation with a vertical plume was shown to result in more efficient air entrainment compared to a thermally stable horizontal flow of hot exhaust gases over cold air. Increasing the inlet soffit height will also decrease the Froude number, which was shown to enhance mixing. At intermediate values of the Reynolds number, both of these dimensionless parameters are expected to display similar magnitudes of importance. More controlled experiments, over a wide range of conditions, are required to develop accurate scaling correlations.

As observed in the results for experiments with an inlet soffit, the oxidation efficiency depends on the fuel vaporization rate. This dependency relates to whether the increased air entrainment rate, due to the inlet soffit, is sufficient for complete oxidation of the unburned exhaust gases at a given exhaust rate. During insufficient air entrainment, the efficiency of CO oxidation suffers. Insufficient air entrainment in the initial exhaust plume requires air to be entrained into the exhaust gas upper layer. As previously noted, this thermally stable configuration of hot exhaust gases flowing over cool air results in poor air entrainment and inefficient CO oxidation.

The results of this study could easily be applied to other fuels with respect to the fuel vaporization rate at which the enhanced air entrainment becomes insufficient. Again, the important factor is the amount of air entrained into the exhaust plume. The basis for equivalency between the fuel used in this study (hexane) and a different fuel, should be made on the mass ratios of stoichiometry. For example, with a different fuel requiring more air for complete oxidation (i.e. a lower stoichiometric fuel to air ratio), the transition from efficient oxidation to inefficient oxidation would occur at a lower fuel rate.

Another important aspect of compartment fires apparent in this study was the importance of the relationship between hydrocarbon and carbon monoxide (CO) oxidation. Several previous studies on hydrocarbon oxidation [10,11,25] have shown that typical hydrocarbons oxidize much faster than CO. This was observed in this study by a delay in CO oxidation until hydrocarbons were oxidized significantly. This was shown to be one of the key phenomenon responsible for poor CO oxidation in the hallway, especially in combination with an oxygen limited environment. This effect would be amplified in a more realistic building fire, where the ceilings and walls would typically be flammable. During sustained external burning, this would feed additional unburned hydrocarbons into the upper layer as they vaporized off of the flammable surfaces. This

situation would result in the continuous threat of high CO concentrations, since CO oxidation would be impeded by the constant supply of gaseous hydrocarbons.

The other key phenomenon found responsible for poor CO oxidation in the hallway was the rapid temperature drop in the hallway. Typical building materials are likely to have less efficient insulating properties compared to the materials used in this study. This would result in more heat transfer through the walls, a quicker gas temperature drop in the hallway, and again less efficient CO oxidation.

## CHAPTER 5

### RECOMMENDATIONS

This study investigated the transport of exhausting gases from a burning compartment exhausting along the axis of a hallway. Although the results of these experiments have been interesting, they have not exhausted the possibilities for further investigation. By comparison, the situation of a burning compartment exhausting perpendicular to the hallway axis is one of the many variations expected to differ significantly from this study. The alteration of the flow dynamics in the hallway should be significant enough to affect the air entrainment and, as a result, display an effect on the oxidation efficiencies of the exhausting gases. Continuing efforts to investigate this case are currently being pursued at Virginia Tech during the writing of this Thesis.

In order to accurately scale the results of this study to other soffit heights and flow conditions, experiments with more control over key parameters are required. As discussed in section 4.2, both the Reynolds number and the Froude number are expected to be important parameters for scaling the results of this study. The important experimental variables that define these dimensionless groups are the exhaust gas flow rate from the compartment, the compartment exhaust vent size, the hallway inlet soffit height, and the compartment exhaust gas physical properties. Experiments to determine these scaling relations should be designed to vary these parameters easily and over a wide range of values.

The agreement between the behavior observed for the evolution of exhaust gases in the hallway with the chemical kinetic modeling studies of Pitts [10] and Gottuk [11] was very encouraging. This agreement indicated the possibility of a feasible model for the

transport and remote oxidation of exhaust gases traveling through a burning building. The study by Pitts [10] concluded that the gas temperature was the most significant property for accurate modeling. Had the air entrainment rate into the exhausting gases been known in this investigation, modeling with a plug flow reactor code could have been performed based on the axial temperature profile, initial concentrations entering the hallway, and the flow rate of the exhausting gases. Comparison of the model results to the data presented in this study could be used to determine the accuracy of this model.

Several variations of the chemical kinetic model could also be studied. Comparison of these different models with the data presented in this study, and combined with knowledge of the complexity of each model, would allow determination of the most efficient model. Heat transfer will obviously affect the results of the model. Instead of using the axial temperature profile, as it will not always be available, the two extreme cases of an adiabatic hallway (no heat transfer) and an isothermal hallway (total heat transfer) could be investigated given the initial gas temperature. The cooling effect by entrainment of cold air was observed to be significant, since the gas temperatures decreased significantly along the hallway axis, and should be accounted for in each case. With the air entrainment rate and ambient temperature of the air known, the temperature could be adjusted for the cooling effect at each step after the adiabatic or isothermal condition was imposed.

In order to extend any model to actual compartment fires, the heat transfer would have to be quantified for typical building materials. The insulating material used for the ceiling and walls in this study was more resistant to heat transfer than typical building materials, possibly causing a significant difference between the results of this study and the expected results with typical building materials. Typical building materials are flammable,

which would also have to be accounted for in any model expecting to predict the behavior of real compartment fires.

Another simplifying variation could be to use the air entrainment correlations of Hinkley et al. [16]. Air entrainment in the buoyant plume observed with an inlet soffit, could be estimated by correlations for vertical plume entrainment, and the correlations for ceiling deflected flames could be utilized to estimate the air entrainment into the horizontally flowing exhaust gas upper layer.

The investigation of the ignition index in this study, and in the studies by Gottuk et al. [11,12], indicated potential for this method in predicting when sustained external burning would occur. A more detailed study of the ignition index with both of these configurations would prove interesting. However, future studies should attempt to perform a more detailed analysis of the flammable gas composition, including direct measurement of the concentration of diatomic hydrogen gas. Sampling should be performed inside the burning compartment upper layer for a more complete study of the ignition index concept.

During this investigation, the determination of the air entrainment into the hallway, through the end open to the atmosphere, was determined to be a measurement that would provide useful and complementary information to this study. By measuring the air entrainment rate into the hallway, the efficiency of the air entrainment by the exhaust gases in the hallway could be characterized in more detail, as well as allowing the calculation of species yields in the hallway. A global equivalence ratio could also be defined for the gases in the hallway and investigated as a correlating parameter. The description of one successful method that could be utilized is given in Reference [27]. This method determines the one-dimensional, non-uniform velocity profile across a finite vertical exit



plane from a burning compartment using a full temperature height profile in the plane of interest, and another temperature profile in the compartment. This method also uses some simplifying assumptions and a mass balance equation.

A few other experimental apparatus additions were investigated during this study for implementation to improve the capability of the apparatus. Implementing a continuous fuel supply system, instead of testing with a fixed initial mass of fuel as used in this study, would allow experiments to be conducted with longer "quasi" steady state periods. Combined with an automated hallway sampling system, gas sampling could be performed at several different locations within the hallway during a single test. Compared to the method used in this study, time would be saved by increasing the information obtained from each experiment, and improved repeatability of results would be accomplished.

Measurement of soot in the hallway with a laser extinction system was also investigated during this study. These measurements would enhance the apparatus, allowing a more detailed investigation of the soot production and/or oxidation rates within the hallway. However, collection of soot on optical access windows in the hallway was determined to provide difficulty for laser extinction measurements. One possible solution would require a recessed optical window with a nitrogen-purged plenum volume to prevent soot from coming in contact with the windows. Radiation emission measurements from the hallway flame would also enhance analysis of the processes occurring in the hallway, as oxidation of soot has been shown to radiate a significant amount of energy from the reacting flow, decreasing the gas temperature.

## REFERENCES

1. Karter, M. J., "Fire Loss in the United States in 1992", *NFPA Journal*, 78-87, 1993.
2. Harwood, B. and Hall, J. R., "What Kills in Fires: Smoke Inhalation or Burns?", *Fire Journal*, 83, 29-34, 1989.
3. Harland, W. A. and Anderson, R. A., "Causes of Death in Fires", Proceedings, smoke and toxic gases from Burning Plastics, London England, 15/1-15/19, 1982.
4. Fardell, P. J., Murell, J. M., and Murell, J. V., "Chemical 'Fingerprint' Studies of Fire Atmospheres", *Fire and Materials*, 10, 21-28, 1986.
5. Morikawa, T., Yanai, E., Okada, T., and Sato, K., "Toxicity of the Atmosphere in an Upstairs Room Caused by Inflow of Fire Effluent Gases Rising from a Burn Room", *Journal of Fire Sciences*, 11, 195-209, 1993.
6. Meyer, E., Chemistry of Hazardous Materials, Prentice-Hall, Inc., Englewood Cliffs, NJ, 1977.
7. Gottuk, D. T., Roby, R. J., and Peatross, M. J., "Carbon Monoxide Production in Compartment Fires", *Journal of Fire Protection Engineering*, 4, 133-150, 1992.
8. Pitts, W. M., Johnsson, E. L., and Bryner, N. P., "Carbon Monoxide Production in Compartment Fires by Wood Pyrolysis", *1993 Annual Conference on Fire Research: Book of Abstracts*, NISTIR 5280, 123-124, 1993.
9. Jones, W. W., "Modeling Smoke Movement through Compartment Structures", *Journal of Fire Sciences*, 11, 172-183, 1993.
10. Pitts, W. M., "Reactivity of Product Gases Generated in Idealized Enclosure Fire Environments", Twenty-Forth Symposium (International) on Combustion, The Combustion Institute, Pittsburgh, 1737-1746, 1992.
11. Gottuk, D. T., "The Generation of Carbon Monoxide in Compartment Fires," Ph.D. Dissertation, Virginia Polytechnic Institute & State University, Department of Mechanical Engineering, 1992.
12. Gottuk, D. T., and Roby, R. J., "A Study of Carbon Monoxide and Smoke Yields from Compartment Fires with External Burning", Twenty-Forth Symposium (International) on Combustion, The Combustion Institute, Pittsburgh, 1729-1735, 1992.

13. Hinkley, P. L., Wraight, H. G. H., and Theobald, C. R., "The contribution of flames under ceilings to fire spread in compartments", *Fire Safety Journal* , 7, 227-242, 1984.
14. Babrauskas, V., "Flame Lengths Under Ceilings", *Fire and Materials*, 4, 119-126, 1980.
15. Attallah, S., "Fires in a Model Corridor with a Simulated Combustible Ceiling, Part I - Radiation, Temperature and Emissivity Measurements", *Fire Research Note 628*, Fire Station, Borehamwood, 1966.
16. Hinkley, P. L., Wraight, H. G. H., and Theobald, C. R., "The Contribution of Flames Under Ceilings to Fire Spread in Compartments, Part I Incombustible Ceilings", *Fire Research Note 712*, Fire Research Station, Borehamwood, 1968.
17. Morikawa, T., Yanai, E., Watanabe, T., Okada, T., and Sato, Y., "Toxic Gases from House Fires of Natural Polymers or Both Synthetic and Natural Polymers Under Different Conditions", *Proceedings of Interflam '90*, 249-255, 1990.
18. Fluid Meters: Their Theory and Application, Report of A.S.M.E. Research Committee on Fluid Meters, Sixth edition, Ed. Bean, H. S., A.S.M.E., NY, 1971.
19. Tewarson, A., "Generation of Heat and Chemical Compounds in Fires" from The SFPE Handbook of Fire Protection Engineering, Ed, DiNenno, P. J., National Fire Protection Association, Quincy, MA, 1988.
20. Newman, J. S. and Steciak, J., "Characterization of Particulates from Diffusion Flames", *Combustion and Flame*, 67, 55-64, 1987.
21. Beyler, C. L., "Ignition and Burning of a Layer of Incomplete Combustion Products", *Combustion Science and Technology*, 39, 287-303, 1984.
22. Beyler, C. L., "Development and Burning of a Layer of Products of Incomplete Combustion Generated by a Buoyant Diffusion Flame", Ph.D. Dissertation, Harvard University, 1983.
23. Van Wylen, G. J., Sonntag, R. E., Fundamentals of Classical Thermodynamics, 3rd Edition, John Wiley & Sons, Inc., NY, 1986.
24. Drysdale, D., An Introduction to Fire Dynamics, John Wiley & Sons, 1985.
25. Westbrook, C. K. and Dryer, F. L. "Chemical Kinetic Modeling of Hydrocarbon Combustion", *Progress in Energy and Combustion Science*, 10, 1-57, 1984.

26. Yetter, R. A., Dryer, F. L., and Rabitz, H., "A Comprehensive Reaction Mechanism for Carbon Monoxide / Hydrogen / Oxygen Kinetics", *Combustion Science and Technology*, 79, 97-128, 1991.
27. Janssens, M. and Tran, H. C., "Data Reduction of Room Tests for Zone Model Validation", *Journal of Fire Sciences*, 10, 528-555, 1992.

**APPENDIX A**  
**DATA REDUCTION PROGRAM**

The FORTRAN program given below, FIRERED2.FOR, was used to reduce the raw serial data files produced by the BASIC data acquisition program, FIRE5.BAS. Output includes 7 tabular files (8 for ignition index calculations) containing the reduced measured parameters, as well as parameters calculated from the measured data.

```

C  PROGRAM: FIRERED2.FOR
C
C  ORIGINAL AUTHOR: D. GOTTUK
C  MODIFIED VERSION AUTHOR: D. EWENS
C
C  PURPOSE:
C  THIS PROGRAM REDUCES THE EXPERIMENTAL DATA FROM THE RAW
C  DATA FILE CREATED BY PROGRAM FIRE5.BAS.
C  THE REDUCED DATA MAY BE AVERAGED USING FIREAVG2.FOR
C
C  VARIABLES:
C
C  AIRRAT    - INLET DUCT AIR MASS FLOW RATE [Kg AIR/S]
C  AIRVEL(I) - INLET DUCT AIR VELOCITY [M/S]
C  AREA      - AREA OF AIR INLET DUCT [M^2]
C  CCT       - CARBON COUNT, # OF CARBON ATOMS IN FUEL MOLECULE [#]
C  CERROR    - RELATIVE CARBON ERROR [%] (Cout-Cin)/Cin
C  CMOLIN    - # OF CARBON MOLES IN FROM FUEL [KMOLES]
C  CMOLOT    - # OF CARBON MOLES OUT FROM CO, CO2 AND THC [KMOLES]
C  COAMB     - AVG AMBIENT ATMOSPHERE CO MOLE FRACTION
C             [KMOL CO/KMOL AIR]
C  COCST     - TO ADJUST CO [MOLE FRACTION/CONC.(ppm OR %)]
C  CORNG     - RANGE OF CO ANALYZER [ppm OR %]
C  COYLD     - CO YIELD [KG CO PRODUCED/KG FUEL BURNED]
C  CO2AMB    - AVG AMBIENT ATMOSPHERE CO2 MOLE FRACTION
C             [KMOL CO2/KMOL AIR]
C  CO2CST    - TO ADJUST CO2 [MOLE FRACTION/CONC.(ppm OR %)]
C  CO2RNG    - RANGE OF CO2 ANALYZER [ppm OR %]
C  CO2YLD    - CO2 YIELD [KG CO2 PRODUCED/KG FUEL BURNED]
C  DATE      - DATE OF EXPERIMENT [TEXT]
C  DELHC     - HEAT OF COMBUSTION OF FUEL [KJ/Kg]
C  DTIME     - INTERMEDIATE VALUE TO CALCULATE FUEL RATE [S]
C  DTIME2    - INTERMEDIATE VALUE TO CALCULATE FUEL RATE [S]
C  D2FUEL    - 2nd DERIVATIVE OF FUEL W.R.T. TIME [KG/S^2]
C  DENOM     - DENOMINATOR OF DRY TO WET CONC CONVERSION [UNITLESS]
C  DENSTY    - INLET DUCT AIR DENSITY [KG/M^3]
C  DRYCO(I)  - DRY CO CONCENTRATION [ppm OR %]
C  DRYCO2(I) - DRY CO2 CONCENTRATION [%]
C  DRYO2(I)  - DRY O2 CONCENTRATION [%]
C  DCTFLW    - EXHAUST DUCT VOLUME FLOW RATE [M^3/S]
C  EQUIV     - PLUME EQUIVALENCE RATIO [UNITLESS]
C  EXMOLS    - TOTAL NUMBER OF MOLES IN COMPARTMENT [KMOL EXHAUST/S]
C             ASSUMES EXHAUST HAS AVG MOLE WT OF AIR

```

C EXCOEF - EXTINCTION COEFFICIENT FROM BEER'S LAW [1/m]  
C EXTDAT - REDUCED DATA FILE EXTENSION [TEXT] (ie. '.DTA')  
C EXTRAW - RAW DATA FILE EXTENSION [TEXT] (ie. '.RAW')  
C FOWT - BEGINNING WEIGHT OF FUEL [Kg]  
C FID(I) - SIGNAL FROM FID [mV\*FIDRANGE]  
C FIDCAL - FID SPAN GAS READING [mV \* FIDRANGE]  
C FIDCST - TO ADJUST THC [MOLE FRACTION/ppm C2H4]  
C FIDRNG - FID RANGE [UNITLESS FACTOR]  
C FIDSPN - FID SPAN GAS CONCENTRATION [ppm C2H4]  
C FIDZER - FID ZERO (ATMOSPHEREIC SAMPLE) READING [mV \* FIDRANGE]  
C FNAME - DATA FILE NAME [7 CHAR'S, ie. HALL001]  
C FNAMEX - TOTAL NAME FOR OPENING ALL FILES [TEXT] (ie. 'HALL001 .RAW')  
C FTOA - MEASURED MASS FUEL TO MASS AIR RATIO [KG FUEL/KG AIR]  
C FUEL(I) - FUEL MASS [KG]  
C FUELRT - FUEL MASS BURN RATE [KG FUEL/S]  
C GF - FUEL VOLATILIZATION RATE [g FUEL/S]  
C HTOC - H TO C RATIO OF FUEL [# H/# C, UNITLESS]  
C I - TOTAL NUMBER OF RECORDEDD DATA POINTS [#]  
C ICORG - CO RANGE (1, 2, OR 3) [#]  
C ICO2RG - CO2 RANGE (1, 2, OR 3) [#]  
C IFIDRG - FID RANGE [POWER OF 100]  
C IGNI - IGNITION INDEX [UNITLESS]  
C IICALC - FLAG FOR IGNITION INDEX CALCULATION, 1 = CALCULATE [#]  
C IPROBE - PROBE LOCATION [#]  
C = 1 IF COMPARTMENT SAMPLED  
C = 2 IF EXHAUST DUCT SAMPLED  
C = 3 IF HALLWAY SAMPLED  
C IRUNNO - RUN NUMBER [#]  
C ISTEP - DATA POINT USED STEP SIZE [#] (1 = USE ALL)  
C IQUIT - DUMMY ABORT REDUCTION FLAG VARIABLE [NONE]  
C J,JJ - DUMMY COUNTER INTEGER [#]  
C K - DATA POINT COUNTER [#]  
C K1 - SPECIES ANALYZER LAG COMPENSATED TIME DATA POINT COUNTER  
C [#]  
C K2 - FID LAG COMPENSATED TIME DATA POINT COUNTER [#]  
C LASPTH - EXHAUST DUCT SMOKE LASER PATH LENGTH [m]  
C MASODL - MASS OPTICAL DENSITY OF SMOKE PER UNIT PATH LENGTH [m^2/g]  
C MOLWT - MOLECULAR WEIGHT OF FUEL [KG FUEL/KMOLE FUEL]  
C N - DUMMY INTEGER COUNTER [#]  
C NPCP - PRODUCT MOLES X PRODUCT SPECIFIC HEAT [KJ/K]  
C USED IN IGNITION INDEX CALCULATION  
C NST - TOTAL MOLES OF STOICHIOMETRIC MIXTURE [Kmoles]  
C USED IN IGNITION INDEX CALCULATION  
C ODL - OPTICAL DENSITY OF SMOKE PER UNIT PATH LENGTH (1/m)  
C O2AMB - AVG AMBIENT ATMOSPHERE O2 MASS FRACTION [Kg O2/Kg AIR]  
C O2CST - TO ADJUST O2 [MOLE FRACTION/CONC.(ppm OR %)]  
C O2RNG - MAXIMUM MEASURABLE O2 CONCENTRATION [%]  
C O2YLD - O2 YIELD [KG O2 USED/KG FUEL BURNED]  
C PA - AMBIENT PRESSURE [mm Hg] (TYP. 710 mmHg)  
C PBELOC - DESCRIPTION OF PROBE LOCATION IN HALLWAY [TEXT]  
C PRESS - EXHAUST DUCT ORIFACE PRESSURE DROP [mmHg=Torr] (TYP. 15.8)

C PROBE - PROBE LOCATED DESCRIPTION [TEXT]  
 C PNSIZE - FUEL PAN SIZE [inches]  
 C PNWT - WEIGHT OF FUEL PAN [Kg]  
 C PTSPST - # OF DATA POINTS PAST END OF FIRE [#]  
 C PTSTRT - LAG TIME AS # OF DATA POINTS [#] (FUNC. OF PROBE LOCATION)  
 C Q - HEAT RELEASE RATE [KW]  
 C RESTIM - RESIDENCE TIME OF GASSES IN COMPARTMENT [S]  
 C RUNTIM - TOTAL RUN TIME [S]  
 C SEC - SPECIFIC EXTINCTION COEFFICIENT FOR SMOKE [m<sup>2</sup>/g]  
 C SMK10 - SMOKE0 CALCULATED FROM 1ST 5 SMOKE1 DATA POINTS  
 C [RELATIVE LIGHT INTENSITY]  
 C SMKMAX - MAX SMOKE VOLUME (MOLE) FRACTION DURING FIRE [ppb]  
 C SMKYLD - SMOKE YIELD [KG SMOKE PRODUCED/KG FUEL BURNED]  
 C SMOKE0(I) - MEASURED I0 FOR BEER'S LAW (NOT WORKING/NOT USED)  
 C [RELATIVE LIGHT INTENSITY]  
 C SMOKE1(I) - I FOR BEER'S LAW [RELATIVE LIGHT INTENSITY]  
 C SMKVf - SMOKE VOLUME FRACTION IN DUCT [ppm]  
 C SOFF1 - HEIGHT OF SOFFIT FROM COMPARTMENT TO HALLWAY [inches]  
 C ALSO CEILING HEIGHT ABOVE TOP OF COMPARTMENT VENT  
 C SOFF2 - HEIGHT OF SOFFIT AT EXIT OF HALLWAY [inches]  
 C SSTIME - RATIO OF RESIDENCE TIME TO D2FUEL [UNITLESS]  
 C STOIC - STOICHIOMETRIC AIR TO FUEL RATIO BY MASS [KG AIR/KG FUEL]  
 C STO2 - STOICHIOMETRIC OXYGEN FOR MEASURED GASES [%]  
 C USED FOR IGNITION INDEX CALCULATION  
 C TAMBA - AMBIENT ATMOSPHERIC TEMPERATURE INPUT BY USER [K]  
 C TAMBC - AMBIENT COMPARTMENT TEMPERATURE INPUT BY USER [K]  
 C AVERAGE THE TOP 3 COMPARTMENT TC RAKE THERMOCOUPLES  
 C TCC(1) - COMPARTMENT THERMOCOUPLE TREE TEMPERATURES [K] (1 = TOP)  
 C - TCC(8)  
 C TCC3 - 3RD TC OF COMPARTMENT TC TREE TEMPERATURE [K]  
 C TCH(1) - HALLWAY THERMOCOUPLE TREE TEMPERATURES [K] (1 = TOP)  
 C - TCH(9)  
 C TCEV - EXHAUST VENT THERMOCOUPLE [K]  
 C TCED - EXHAUST DUCT THERMOCOUPLE [K]  
 C TCID - AIR INLET DUCT THERMOCOUPLE [K]  
 C TDMOLS - TOTAL NUMBER OF MOLES IN EXHAUST DUCT [KMOL EXHAUST/S]  
 C TEG - TEMPERATURE OF EXHAUST GASES [K]  
 C USED FOR IGNITION INDEX CALCULATION  
 C TFUEL - FUEL TYPE NAME [TEXT]  
 C THC - UNBURNED HYDROCARBONS [KMOLES UHC/KMOLES TOTAL]  
 C TIME - TIME FROM START OF FIRE [S]  
 C TMEPST - TIME PAST END OF FIRE THAT DATA WAS COLLECTED [S]  
 C T0R - INITIAL STOIC. MIXTURE TEMPERATURE [K]  
 C USED FOR IGNITION INDEX CALCULATION  
 C VENT - VENT SIZE [TEXT: inches]  
 C VOLC - AVG VOLUME OF UPPER LAYER [M<sup>3</sup>]  
 C WETCO - WET CO CONCENTRATION [ppm OR %]  
 C WETCO2 - WET CO2 CONCENTRATION [%]  
 C WETH2 - WET H2 CONCENTRATION [%]  
 C WETH2O - WET H2O CONCENTRATION [%]  
 C WETO2 - WET O2 CONCENTRATION [%]



```

C   XCO       - CO CONCENTRATION IN STOICHIOMETRIC MIXTURE [%]
C             USED FOR IGNITION INDEX CALCULATION
C   XH2       - H2 CONCENTRATION IN STOICHIOMETRIC MIXTURE [%]
C             USED FOR IGNITION INDEX CALCULATION
C   XTHC      - THC CONCENTRATION IN STOICHIOMETRIC MIXTURE [%]
C             USED FOR IGNITION INDEX CALCULATION
C
C   FILES ACCESSED:
C   (HALL####.*, WHERE #### IS THE RUN NUMBER, ie. HALL0001 )
C
C   READ:
C
C   HALL####.RAW - RAW EXPERIMENTAL SERIAL DATA FILE CREATED BY FIRES5.BAS
C
C   WRITTEN:
C
C   HALL####.DTI - EXPERIMENTAL INFORMATION DATA FILE (CONTAINS: FILE NAME
C                 TEST DATE, AMBIENT CONDITIONS, ANALYZER SETTINGS, ETC)
C   HALL####.DTA - EXPERIMENTAL CHRONOLOGICAL DATA FILE (CONTAINS: TIME,
C                 WET CONC'S, YIELDS)
C   HALL####.DTB - EXPERIMENTAL CHRONOLOGICAL DATA FILE (CONTAINS: TIME,
C                 FUEL & INLET AIR DATA, CARBON ERROR, EQUIVALENCE RATIO)
C   HALL####.DTC - EXPERIMENTAL CHRONOLOGICAL DATA FILE (CONTAINS: TIME,
C                 TIME SCALES, DRY CONC'S, THC, HEAT RELEASE, DILUTION)
C   HALL####.DTD - EXPERIMENTAL CHRONOLOGICAL DATA FILE (CONTAINS: TIME,
C                 SMOKE DATA, WET H2O & H2 CONC'S)
C   HALL####.DTE - EXPERIMENTAL CHRONOLOGICAL DATA FILE (CONTAINS: TIME,
C                 HALLWAY THERMOCOUPLE DATA)
C   HALL####.DTF - EXPERIMENTAL CHRONOLOGICAL DATA FILE (CONTAINS: TIME,
C                 COMPARTMENT THERMOCOUPLE DATA, INLET AIR & EXHAUST
C                 THERMOCOUPLE DATA)
C   HALL####.DTG - EXPERIMENTAL CHRONOLOGICAL DATA FILE (CONTAINS: TIME,
C                 IGNITION INDEX, ESTIMATED SPECIES CONCENTRATIONS
C
C * INITIALIZATION
C   IMPLICIT DOUBLE PRECISION (A-H,O-Z)
C   DIMENSION TIME(1300),DRYCO(1300),DRYCO2(1300),DRYO2(1300)
C   DIMENSION FUEL(1300),AIRVEL(1300),TCC(8),TCH(9),TCC3(1300)
C   DIMENSION FUELRT(1300),AIRRAT(1300),RESTIM(1300),Q(1300)
C   DIMENSION D2FUEL(1300),SMOKE1(1300),SMOKE0(1300),FID(1300)
C   DIMENSION FTOA(1300),TCEV(1300),TCED(1300),TCID(1300)
C   INTEGER PTSTRT,PTSPST,PNSIZE,SOFF1,SOFF2
C   DOUBLE PRECISION MASODL,MOLWT,NST,NPCP,IGNI
C   REAL LASPTH
C   CHARACTER*4 EXTDAT,EXTRAW
C   CHARACTER*8 FNAME
C   CHARACTER*9 DATE
C   CHARACTER*12 FNAMEX
C   CHARACTER*20 TFUEL
C   CHARACTER*30 VENT,PROBE
C   CHARACTER*60 NOTE1,NOTE2,NOTE3,NOTE4,PBELOC

```

```

C      7-----
C * INITIALIZE VARIABLES
      IQUIT = 1
      FIDRNG = 1.0E-11
      ISTEP = 1
      SMKVF = 0.0
      EXCOEF = 0.0
      SMK10 = 0.0
      DO 10 N = 1, 1300
          TCC3(N) = 0.0
          SMOKE0(N) = 0.0
          SMOKE1(N) = 0.0
          FID(N) = 0.0
          FUELRT(N) = 0.0
          RESTIM(N) = 0.0
10     CONTINUE
      WETH2O = 0.000
      WETH2 = 0.000
C * INITIALIZE CONSTANTS
      AREA = 0.0699573
      FIDSPN = 615.0
      PRESS = 14.3
      VOLC = 1.137
C ONLY FOR EXHAUST DUCT, HEAVILY DILUTED
      COAMB = 0.000000
      CO2AMB = 0.000400
      O2AMB = 0.232
C      7-----
C * INPUT RUN PARAMETERS
      WRITE(*,*)'ENTER FILE NAME W/O EXT, 8 CHARACTORS (i.e. HALL0001)'
      READ(*,21)FNAME
21     FORMAT(A8)
      WRITE(*,*) 'ENTER RUN #'
      READ(*,*) IRUNNO
      WRITE(*,*) 'ENTER DATE (ie. "12-23-93")'
      READ(*,21) DATE
41     TFUEL='HEXANE'
      ISTEP=1
      DELHC=44735.0
      HTOC=2.333
      STOIC=15.2010
      MOLWT=86.18
      CCT=6.0
45     WRITE(*,*)TFUEL
      WRITE(*,*) 'ENTER PAN SIZE (6, 8, 9, 11) [inches]'
      READ(*,22) PNSIZE
22     FORMAT(I2)
23     FORMAT(A13)
      WRITE(*,*) 'ENTER FUEL PAN WEIGHT [Kg]'
      READ(*,*) PNWT
      WRITE(*,*) 'ENTER BEGINNING WEIGHT OF FUEL ONLY [Kg]'

```

```

READ(*,*) F0WT
WRITE(*,*) ' ENTER EXHAUST VENT SIZE (ie. 20 X 6.25) [inches]'
READ(*,23) VENT
WRITE(*,*) ' ENTER COMPARTMENT/HALLWAY SOFFIT HEIGHT or'
WRITE(*,*) ' HALL CEILING HEIGHT FROM TOP OF COMPARTMENT EXH VENT'
WRITE(*,*) ' (0, 4, 8) [inches]'
READ(*,22) SOFF1
WRITE(*,*) ' ENTER HALLWAY EXIT SOFFIT HEIGHT (0, 4, 8) [inches]'
READ(*,22) SOFF2
WRITE(*,*) ' ENTER CO RANGE 1 (1000 ppm), 2 (1%) or 3 (10%)'
READ(*,*) ICORG
WRITE(*,*) ' ENTER CO2 RANGE 1 (2%), 2 (15%) or 3 (20%)'
READ(*,*) ICO2RG
30  WRITE(*,*) ' (1) COMPARTMENT, (2) EXHAUST DUCT, OR (3) HALLWAY'
    WRITE(*,*) ' ENTER 1, 2 or 3'
    READ(*,*) IPROBE
    GOTO(31,32,33)IPROBE
    GOTO 30
C COMPARTMENT SAMPLED
31  PROBE = 'COMPARTMENT'
    PTSTRT = 4
    GOTO 34
C EXHAUST DUCT SAMPLED
32  PROBE = 'EXHAUST'
    PTSTRT = 3
    GOTO 34
C HALLWAY SAMPLED
33  PROBE = 'HALLWAY'
    PTSTRT = 4
34  WRITE(*,*)PROBE
    WRITE(*,*) ' ENTER PROBE LOCATION (60 CHARACTORS)'
    WRITE(*,*) ' ( ie. EXH DUCT: L=132, H=2, W=0 IN., -OR-'
    WRITE(*,*) ' HALL: L=72, H=2(6), W=-1(1) IN. RAKE (SAMPLE) )'
    READ(*,24) PBELOC
24  FORMAT(A60)
    WRITE(*,*) ' ENTER AMBIENT ATMOSPHERIC TEMPERATURE [°C]'
    READ(*,*)TAMBA
    TAMBA = TAMBA + 273.15
    WRITE(*,*) ' ENTER AMBIENT COMPARTMENT TEMPERATURE [°C]'
    WRITE(*,*) ' AVERAGE THE TOP 3 COMPARTMENT TC RAKE THERMOCOUPLES'
    READ(*,*)TAMBC
    TAMBC = TAMBC + 273.15
    WRITE(*,*) ' ENTER AMBIENT PRESSURE [mm Hg]'
    WRITE(*,*) ' DEFAULT IS 713.0 mm Hg'
    READ(*,*)PA
    WRITE(*,*) ' ENTER THE FID SPAN GAS CONCENTRATION [ppm C2H4]'
    READ(*,*)FIDSPN
    FIDCST = 1000000.0
    WRITE(*,*) ' ENTER THE FID OPERATING RANGE (for 1E-10, enter 10)'
    READ(*,*)IFIDRG
    FIDRNG = 10.0**(-IFIDRG)

```

```

WRITE(*,*)' ENTER THE FID ZERO GAS READING AS [mV]'
READ(*,*)FIDZER
FIDZER = FIDZER*FIDRNG
WRITE(*,*)' ENTER THE FID SPAN GAS READING AS [mV]'
READ(*,*)FIDCAL
FIDCAL = FIDCAL*FIDRNG
WRITE(*,*)' USES A RUN TIME PAST END OF FIRE = 30 sec'
TMEPST=30.0D0
WRITE(*,*)' CALCULATE IGNITION INDEX ?, 1 = CALCULATE '
READ(*,*)IICALC
WRITE(*,*)' CONTINUE WITH REDUCTION ? ENTER "0" TO QUIT'
READ(*,*) IQUIT
IF (IQUIT.EQ.0)GOTO 9999
WRITE(*,*)' OK, HERE WE GO...'
C 7-----
C * CALCULATIONS BEGIN
C ** O2 ANALYZER
O2RNG = 22.0
O2CST = 100.0
C ** CO ANALYZER
GOTO(51,52,53)ICORG
51 CORNG = 1000.0
COCST = 1.000E+6
GOTO 54
52 CORNG = 1.
COCST = 100.
GOTO 54
53 CORNG = 10.
COCST = 100.
C ** CO2 ANALYZER
54 GOTO(55,56,57)ICO2RG
55 CO2RNG = 2.
CO2CST = 100.
GOTO 58
56 CO2RNG = 15.
CO2CST = 100.
GOTO 58
57 CO2RNG = 20.
CO2CST = 100.
C 7-----
C * READ DATA AND CREATE AN ARRAY FOR EACH CHANNEL
C OPEN *.RAW DATA FILE
58 EXTRAW = '.RAW'
FNAMEX = FNAME
FNAMEX(9:12) = EXTRAW(1:4)
OPEN(15,FILE = FNAMEX)
WRITE(*,*)' '
WRITE(*,*)' READING DATA FILE ',FNAMEX
C OPEN NEW *.DTE AND *.DTF DATA FILES
EXTDAT = '.DTE'
FNAMEX(9:12) = EXTDAT(1:4)

```

```

DO 59 JJ = 1, 2
  FNAMEX(12:12) = CHAR(68+JJ)
  OPEN(UNIT=24+JJ, FILE=FNAMEX, STATUS='NEW')
  WRITE(*,*)' AND WRITING DATA FILE 'FNAMEX
59  CONTINUE
  I=1
C BEGINNING OF READING DO LOOP
60  READ(15,*,END=65) TIME(I)
    RUNTIM = TIME(I)
    READ(15,*) DRYCO(I)
    READ(15,*) DRYCO2(I)
    READ(15,*) DRYO2(I)
    READ(15,*) FUEL(I)
    READ(15,*) AIRVEL(I)
    READ(15,*) FID(I)
    READ(15,*) SMOKE0(I)
    READ(15,*) SMOKE1(I)
    READ(15,*) TCH(1)
    READ(15,*) TCH(2)
    READ(15,*) TCH(3)
    READ(15,*) TCH(4)
    READ(15,*) TCH(5)
    READ(15,*) TCH(6)
    READ(15,*) TCH(7)
    READ(15,*) TCH(8)
    READ(15,*) TCH(9)
    READ(15,*) TCC(1)
    READ(15,*) TCC(2)
    READ(15,*) TCC(3)
    READ(15,*) TCC(4)
    READ(15,*) TCC(5)
    READ(15,*) TCC(6)
    READ(15,*) TCC(7)
    READ(15,*) TCC(8)
    READ(15,*) TCEV(I)
    READ(15,*) TCED(I)
    READ(15,*) TCID(I)
C TEMPERATURE REDUCTION - CONVERT TEMPERATURES TO KELVIN
DO 63 JJ = 1, 8
  TCH(JJ) = TCH(JJ)+273.15
  TCC(JJ) = TCC(JJ)+273.15
63  CONTINUE
  TCH(9) = TCH(9)+273.15
  TCEV(I) = TCEV(I)+273.15
  TCED(I) = TCED(I)+273.15
  TCID(I) = TCID(I)+273.15
  TCC3(I) = TCC(3)
C WRITE TEMPERATURE DATA TO FILES
  WRITE(25,2005)TIME(I),TCH(1),TCH(2),TCH(3),TCH(4),TCH(5),TCH(6),
$ TCH(7),TCH(8),TCH(9)
  WRITE(26,2006)TIME(I),TCC(1),TCC(2),TCC(3),TCC(4),TCC(5),TCC(6),

```

```

      $ TCC(7),TCC(8),TCEV(I),TCED(I),TCID(I)
2005 FORMAT(F7.1,9F6.0)
2006 FORMAT(F7.1,11F6.0)
      I = I+1
      GOTO 60
65    I = I-1
      CLOSE (15)
      CLOSE (25)
      CLOSE (26)
      WRITE(*,3001)FNAME,'RAW READ! '
3001 FORMAT(1X,A8,A14)
      WRITE(*,*)' '
      WRITE(*,3001)FNAME,'DTE WRITTEN!'
      WRITE(*,3001)FNAME,'DTF WRITTEN!'
      WRITE(*,*)' '
      WRITE(*,*)' TEMPERATURE DATA REDUCED!'
C      7-----
C * CREATE EXPERIMENT INFORMATION FILE
      EXTDAT = '.DTI'
      FNAMEX(9:12) = EXTDAT(1:4)
      OPEN(UNIT=20, FILE=FNAMEX, STATUS='NEW')
C * WRITE TO INFO FILE
      WRITE(20,1001)FNAME
      WRITE(20,1002)DATE,IRUNNO,ICORG,ICO2RG,IProbe,TMEPST
      WRITE(20,1003)PROBE
      WRITE(20,1004)PA,TAMBA,TAMBC
      WRITE(20,1005)TFUEL
      WRITE(20,1006)IFUEL,ISTEP,DELHC,HTOC,STOIC,MOLWT,CCT
      WRITE(20,1007)FIDSPN,FIDRNG,FIDZER,FIDCAL
      WRITE(20,1008)RUNTIM,F0WT,PNSIZE,VENT,SOFF1,SOFF2
      WRITE(20,1009)PBELOC
1001 FORMAT(1X,A8)
1002 FORMAT(1X,A8,I5,3I2,F9.3)
1003 FORMAT(1X,A30)
1004 FORMAT(1X,3F9.3)
1005 FORMAT(1X,A20)
1006 FORMAT(1X,2I3,F10.1,F8.3,F10.4,F10.3,F6.1)
1007 FORMAT(1X,F12.1,E11.1,2E15.4)
1008 FORMAT(1X,F7.1,F8.3,I3,A14,2I3)
1009 FORMAT(1X,A60)
      CLOSE(20)
      WRITE(*,3001)FNAME,'DTI WRITTEN!'
C      7-----
C * DATA MANIPULATION FOR EACH CHANNEL LOOP J=1 to I
      WRITE(*,*)' '
      WRITE(*,*)' PLEASE WAIT -- CALCULATING '
      PTSPST = NINT(TMEPST/1.97)
C BEGINING OF ANALYZER DATA CONVERSION DO LOOP
      DO 77 J = 1, I-PTSPST
      K1 = J+PTSTRT-1
C ** CONVERT INSTRUMENT MEASUREMENTS FROM VOLTS TO CONCENTRATIONS

```

```

C *** CO ANALYZER [%]
  IF(DRYCO(K1).LT.0.0)THEN
    DRYCO(K1) = 0.0
  ENDIF
  DRYCO(J) = (DRYCO(K1)/5.0)*CORNG/COCST
C *** CO2 ANALYZER [%]
  IF(DRYCO2(K1).LT.0.0)THEN
    DRYCO2(K1) = 0.0
  ENDIF
  DRYCO2(J) = (DRYCO2(K1)/5.0)*CO2RNG/CO2CST
C *** O2 ANALZER [%]
  IF(DRYO2(K1).LT.0.0)THEN
    DRYO2(K1) = 0.0
  ENDIF
  DRYO2(J) = (DRYO2(K1)/5.08)*O2RNG/O2CST
C *** THC [%]
  K2 = J + PTSTRT
74  FID(J) = FID(K2)
  IF (FID(J).LT.0.0)THEN
    FID(J) = 0.000
  ENDIF
  FID(J) = FID(J)*1000.0*FIDRNG
77  CONTINUE
  WRITE(*,*)' ANALYZER DATA CONVERTED AND COMPENSATED FOR LAG!'
  DO 80 J = 1, I
C *** FUEL WEIGHT [kg]
  FUEL(J) = (FUEL(J)-1.0)*10.0/4.0
C *** INLET AIR VELOCITY [m/s]
  AIRVEL(J) = (AIRVEL(J)*2.0D0/5.0D0)*(TCID(J)/298.D0)*(760.D0/PA)
80  CONTINUE
  WRITE(*,*)' FUEL AND AIR DATA CONVERTED AND COMPENSATED FOR LAG!'
C *** ELIMINATE INCORRECT FUEL DATA POINTS
  DO 85 J = 2, I-2
    IF(FUEL(J+1).GT.FUEL(J)) THEN
      FUEL(J+1) = FUEL(J)
    ENDIF
85  CONTINUE
C *** CALCULATE FUEL BURN RATE USING AVERAGING SMOOTHING [kg/sec]
  DO 90 J = 6, (I-5)
    FUELRT(J) = (FUEL(J-5)-FUEL(J+5))/(TIME(J+5)-TIME(J-5))
90  CONTINUE
C *** ESTIMATE INITIAL FUEL BURN RATES [kg/sec]
  DO 95 J = 1, 5
    FUELRT(J) = FUELRT(8)
95  CONTINUE
C *** ESTIMATE LAST FUEL BURN RATES [kg/sec]
  DO 97 J = (I-4), (I-2)
    FUELRT(J) = (FUEL(J-2)-FUEL(J+2))/(TIME(J+2)-TIME(J-2))
97  CONTINUE
  DTIME = TIME(I)-TIME(I-2)
  FUELRT(I-1) = (FUEL(I-2)-FUEL(I))/DTIME

```

```

        DTIME2 = TIME(I)-TIME(I-1)
        FUELRT(I) = (FUEL(I-1)-FUEL(I))/DTIME2
        DO 100 J = (I-PTSPST+1),I
            FUELRT(J) = 0.0
100    CONTINUE
        WRITE(*,*)' BURN RATE CALCULATIONS COMPLETE'
C *** CALCULATE SMK10 (SMOKE0) FROM 1ST 5 SMOKE1'S
        SMK10 = 0.000
        DO 110 J = 1, 5
            SMK10 = SMK10 + SMOKE1(J)/5.
110    CONTINUE
C   7-----
C * CREATE OUTPUT FILES
        EXTDAT = 'DTA'
        FNAMEX(9:12) = EXTDAT(1:4)
        DO 140 J = 1, 4
            FNAMEX(12:12) = CHAR(64+J)
            OPEN(UNIT=20+J, FILE=FNAMEX, STATUS='NEW')
140    CONTINUE
        IF (IICALC.EQ.1) THEN
            EXTDAT = 'DTG'
            FNAMEX(9:12) = EXTDAT(1:4)
            OPEN(UNIT=27,FILE=FNAMEX, STATUS='NEW')
        ENDIF
C   7-----
C 1 TIME INITIALIZATIONS BEFORE LOOP (150)
        SMKMAX = 0.0
        DO 150 K = 1, I-PTSPST, ISTEP
C   7-----
C * CALCULATE HEAT RELEASE RATE (kW)
        Q(K) = FUELRT(K)*DELHC
C   7-----
C * CALCULATE AIR FLOWRATE (kg/sec)
C   AND RESIDENCE TIME (sec)
        DENSTY = (PA/TCID(K)/0.287)*0.1333
        IF (AIRVEL(K).LE. 0.0) THEN
            WRITE(*,*)' AIR VELOCITY ERROR ! (AIRVEL < 0)'
            RESTIM(K) = 999.
        ELSE
            RESTIM(K) = VOLC/(AIRVEL(K)*AREA*TCC3(K)/TCID(K))
        ENDIF
        AIRRAT(K) = AIRVEL(K)*DENSTY*AREA
C   7-----
C * CALCULATE FUEL/AIR RATIO
        IF (AIRRAT(K).LE.0.0) THEN
            FTOA(K) = 0.0
        ELSE
            FTOA(K) = FUELRT(K)/AIRRAT(K)
        ENDIF
C *** CALCULATE WET CONCENTRATIONS, YIELDS AND STORE DATA IN FILES
C   7-----

```



```

C * VOLUMETRIC FLOWRATE (m^3/s) IN EXHAUST DUCT
  EXMOLS = (AIRRT(K)+FUELRT(K))/28.97
  DCTFLW = 1.2099*DSQRT(PRESS*TCED(K)/PA)
  TDMOLS = DCTFLW*PA*0.1333/(8.3144*TCED(K))
C   7-----
C * FOR EXHAUST DUCT SAMPLED FIRES
C ASSUMED SINCE DUCT IS VERY DILUTED, H2O HAS LITTLE EFFECT
  IF (IPROBE.EQ.2) THEN
    WETCO = DRYCO(K)
    WETCO2 = DRYCO2(K)
    WETO2 = DRYO2(K)
  ELSE
C * FOR (UNDILUTED) HALLWAY AND COMPARTMENT SAMPLED FIRES
    DENOM = 1.0+((HTOC/2.0)*DRYCO2(K))
    WETCO = DRYCO(K)/DENOM
    WETCO2 = DRYCO2(K)/DENOM
    WETO2 = DRYO2(K)/DENOM
  ENDIF
C   7-----
C SET YIELDS TO 0 IF FUELRT = 0
C OR IF HALLWAY SAMPLED
  IF (FUELRT(K).EQ.0.0.OR.IPROBE.EQ.3) THEN
    COYLD = 0.0
    CO2YLD = 0.0
    O2YLD = 0.0
  ELSE IF (IPROBE.EQ.2) THEN
C EXHAUST DUCT SAMPLED
    COYLD = (WETCO-COAMB)*TDMOLS*28.01/FUELRT(K)
    CO2YLD = (WETCO2-CO2AMB)*TDMOLS*44.01/FUELRT(K)
    O2YLD = 0.0
  ELSE
C COMPARTMENT SAMPLED
    COYLD = (WETCO-COAMB)*EXMOLS*28.01/FUELRT(K)
    CO2YLD = (WETCO2-CO2AMB)*EXMOLS*44.01/FUELRT(K)
    O2YLD = ((O2AMB*AIRRT(K))-(WETO2*EXMOLS*32.00))/FUELRT(K)
  ENDIF
C   7-----
C CHECK FOR YIELD ERRORS
  IF (CO2YLD.GT.100.0) THEN
    WRITE(*,*)' ERROR IN CO2 YIELD! > 100'
  ENDIF
  IF (COYLD.GT.100.0) THEN
    WRITE(*,*)' ERROR IN CO YIELD! > 100'
  ENDIF
  IF (O2YLD.GT.100.0) THEN
    WRITE(*,*)' ERROR IN O2 YIELD! > 100'
  END IF
  WRITE(*,*)' WET CONCENTRATIONS AND YIELDS COMPLETE'
C   7-----
C * CALCULATE SMOKE VOLUME FRACTION IN [ppb]
  IF (SMOKE1(K).EQ.0.)THEN

```

```

WRITE(*,*)' ERROR IN SMOKE VOLUME FRACTION CALCULATION !'
WRITE(*,*)' SMOKE1 SIGNAL = 0 !'
EXCOEF = 999.
SMKVF = 999.
ELSE
  LASPTH = 0.4572
  IF (SMOKE1(K).GE.SMK10) THEN
    EXCOEF = 0.000
  ELSE
    EXCOEF = DLOG(SMK10/SMOKE1(K))/LASPTH
  ENDIF
  SMKVF = 1.3697E-07*EXCOEF*1.0E+9
  IF (SMKVF.LT.0.0)THEN
    SMKVF = 0.0
  ENDIF
C 7-----
C * CALCULATE SMOKE YIELD
  IF (FUELRT(K).LE.0.0)THEN
    WRITE(*,*)' ERROR IN SMOKE YIELD CALCULATION !'
    WRITE(*,*)'FUELRATE = 0 =' ,FUELRT(K),'AT TIME = ',TIME(K)
    SMKYLD = 999.
  ELSE
    GF = FUELRT(K)*1000.
    ODL = EXCOEF/2.303
    MASODL = ODL * DCTFLW / GF
    SEC = 3.213/(0.67*1.1)
    SMKYLD = MASODL / SEC
  ENDIF
ENDIF
WRITE(*,*)' SMOKE CALCULATIONS COMPLETE'
C 7-----
C * EQUIVALENCE RATIO
  EQUIV = FTOA(K)*STOIC
  IF (EQUIV.LE.0.0)THEN
    EQUIV = 0.0
  ENDIF
C 7-----
C * CALCULATE DERIVATIVE OF FUEL BURN RATE
  IF (K.LE.5.OR.K.GE.I-PTSPST-4) THEN
    D2FUEL(K) = 0.0
  ELSE
    D2FUEL(K)=(FUELRT(K+5)-FUELRT(K-5))/(TIME(K+5)-TIME(K-5))
  ENDIF
C 7-----
C * STEADY STATE TIME RATIO
  IF (FUELRT(K) .EQ. 0.0) THEN
    FUELRT(K) = 0.00001
  ENDIF
  SSTIME = RESTIM(K)*D2FUEL(K)/FUELRT(K)
  IF (ABS(SSTIME).GT.10.0) THEN
    SSTIME = 10.0

```

```

        ENDIF
C      7-----
C * CALCULATE UNBURNED HYDROCARBON CONCENTRATIONS AND YIELDS
      IF (FID(K).LE.0.0) THEN
        THC = 0.0
        THCYLD = 0.0
      ELSE
        THC = (FIDSPN/FIDCST)*(FID(K)-FIDZER)/(FIDCAL-FIDZER)
        IF (IPROBE.EQ.1) THEN
          THCYLD = (THC*(EXMOLS)*28.05)/FUELRT(K)
        ELSE IF (IPROBE.EQ.2) THEN
          THCYLD = (THC*(TDMOLS)*28.05)/FUELRT(K)
        ELSE
          THCYLD = 0.0
        ENDIF
      ENDIF
      WRITE(*,*) 'THC CALCULATIONS COMPLETE'
C      7-----
C * CARBON BALANCE ERROR CHECK
      IF (IPROBE.EQ.3) THEN
        CERROR = 999.0
        GOTO 145
      ENDIF
      IF (FUELRT(K).LE.0.0) THEN
        WRITE(*,*) 'ERROR IN CARBON BALANCE CHECK!'
        WRITE(*,*) 'FUELRT = 0 AT TIME = ',TIME(K)
        CERROR = 999.0
        GOTO 145
      ENDIF
C      7-----
C * MOLES OF CARBON IN FROM FUEL
      CMOLIN = CCT*FUELRT(K)/MOLWT
      IF (CMOLIN.LE.0.0) THEN
        WRITE(*,*) 'ERROR IN CARBON BALANCE CHECK W/ CMOLIN!'
        CERROR = 999.0
        GOTO 145
      ENDIF
C      7-----
C * MOLES ACCOUNTED FOR BY MEASUREMENTS
C IF COMPARTMENT SAMPLED
      IF (IPROBE.EQ.1) THEN
        CMOLOT = (WETCO+WETCO2+2.0*THC)*EXMOLS
      ELSE
C IF EXHAUST DUCT SAMPLED
        CMOLOT = (WETCO-COAMB+WETCO2-CO2AMB+2.*THC)*TDMOLS
      ENDIF
      CERROR = (CMOLOT-CMOLIN)*100.0/CMOLIN
145  IF (ABS(CERROR).GT.999.1) THEN
        CERROR = 999.0
      ENDIF
      WRITE(*,*) 'CARBON ERROR CALCULATIONS COMPLETE'

```

```

C      7-----
C * IGNITION INDEX CALCULATION
      IF (IICALC.EQ.1) THEN
C MOLE FRACTION ASSUMPTIONS
      WETH2O=1.167D0*WETCO2
      WETH2=0.5D0*WETCO
      WETN2=1.0D0-(WETCO+WETCO2+WETO2+WETH2O+WETTHC+WETH2)
C STOICHIOMETRIC O2 CALCULATION (FOR CO, H2, THC OXIDATION)
      STO2=0.5D0*(WETCO+WETH2)+3.0D0*(WETTHC)-WETO2
      IF (STO2.LT.0.001) THEN
          STO2=0.0D0
      ENDIF
C TOTAL MOLES CALC FOR MIXTURE WITH STOIC. O2
      NST=1.0D0+(STO2*4.76D0)
C CALC NEW MOLE FRACTIONS WITH ADDITIONAL AIR
      XCO=WETCO/NST
      XH2=WETH2/NST
      XTHC=WETTHC/NST
C CALC MOLES PRODUCTS X Cp
      NPCP=(WETCO+WETCO2+2.0D0*WETTHC)*54.2D0/NST+
$         (2.0D0*WETTHC+WETH2O+WETH2)*41.4D0/NST+
$         (WETN2+STO2*3.76D0)*32.8D0/NST
C CALC INITIAL TEMP OF GASES MIXED W/ ROOM TEMP AIR
      TEG=TCC(1)+TCC(2)+TCC(3)
      TOR=(TEG+STO2*4.76D0*320.0D0)/NST
C CALCULATE IGNITION INDEX
      IGNI=XCO*283000.0D0/(NPCP*(1450.0D0-TOR))+
$         XTHC*1411000.0D0/(NPCP*(1700.0D0-TOR))+
$         XH2*242000.0D0/(NPCP*(1080.0D0-TOR))
C WRITE IGNITION INDEX AND TIME TO FILE
      WRITE(27,2700)TIME,IGNI,WETH2O,WETH2,WETN2,STO2,TOR
2700  FORMAT(F7.1,F8.3,4E10.3,F6.0)
      ENDIF
C      7-----
C * STORE DATA (80 CHARACTORS / LINE MAX)
      WRITE(21,2001)TIME(K),WETCO,WETCO2,WETO2,COYLD,CO2YLD,O2YLD,
$ SMKYLD,THCYLD
      WRITE(22,2002)TIME(K),FUEL(K),FUELRT(K),AIRVEL(K),AIRRAT(K),
$ D2FUEL(K),CERROR,EQUIV
      WRITE(23,2003)TIME(K),RESTIM(K),SSTIME,DRYCO(K),DRYCO2(K),
$ DRYO2(K),THC,Q(K),TDMOLS/EXMOLS
      WRITE(24,2004)TIME(K),SMKVF,SMOKE0(K),SMOKE1(K),EXCOEF,WETH2O,
$ WETH2
2001  FORMAT(F7.1,3E10.3,F7.4,2F10.4,F9.3,F7.4)
2002  FORMAT(F7.1,F10.3,F10.4,F10.2,F10.3,F9.5,F11.2,F8.3)
2003  FORMAT(F7.1,F6.1,F7.2,3E10.3,F10.6,F10.2,F6.1)
2004  FORMAT(F7.1,F8.2,5F10.3)
150  CONTINUE
      CLOSE (21)
      CLOSE (22)
      CLOSE (23)

```

```

CLOSE (24)
IF (IICALC.EQ.1) THEN
    CLOSE (27)
ENDIF
WRITE(*,*) ' DATA REDUCTION COMPLETED!'
WRITE(*,*) ' '
WRITE(*,*) ' '
WRITE(*,*) ' FILES WRITTEN:'
WRITE(*,*) ' '
WRITE(*,3000)FNAME,'.DTI'
WRITE(*,3000)FNAME,'.DTA'
WRITE(*,3000)FNAME,'.DTB'
WRITE(*,3000)FNAME,'.DTC'
WRITE(*,3000)FNAME,'.DTD'
WRITE(*,3000)FNAME,'.DTE'
WRITE(*,3000)FNAME,'.DTF'
IF (IICALC.EQ.1) THEN
    WRITE(*,3000)FNAME,'.DTG'
ENDIF
3000 FORMAT(1X,A8,A4)
9999 STOP
END

```

**APPENDIX B**  
**UNCERTAINTY ANALYSIS**

## INTRODUCTION

This analysis is divided into two sections. Section I presents the uncertainty analysis for the properties that were measured directly. These properties include dry gas concentrations, total hydrocarbon concentrations, fuel weight, inlet duct air mass flow rate, laser extinction signal, and temperature measurements. Section II presents the uncertainty analysis for the properties that were calculated from the measured properties. These properties include the global equivalence ratio, wet gas concentrations, species and soot yields, and the ignition index.

The absolute error of a given property,  $X$ , is given the symbol  $\epsilon(X)$ , and carries the same units as  $X$ . The percent relative uncertainty of a given property  $X$ , is given the symbol  $U(X)$ , and represents a fraction. The relation between absolute error and uncertainty is given by:

$$U(X) = \epsilon(X) / X. \quad (B.1)$$

Combining individual uncertainties of related properties to get an overall uncertainty for the property of interest is performed by the method of root mean squares. For a given property,  $X$ , a function of the properties  $x_1, x_2, \dots, x_n$ , written as:

$$X = f(x_1, x_2, \dots, x_n), \quad (B.2)$$

the propagation of uncertainties from the  $x$  properties to the  $X$  property can be determined by:

$$U(X) = [U(x_1)^2 + U(x_2)^2 + \dots + U(x_n)^2]^{1/2}, \quad (B.3)$$

which is the method of root mean squares. Thus, the true value of the property  $X$ ,  $X_{\text{true}}$ , exists somewhere between the limits of uncertainty, or:

$$X_{\text{true}} = X \cdot (1 \pm U(X)) \quad (B.4)$$

## I. MEASURED PROPERTY UNCERTAINTY

### A. GAS CONCENTRATIONS

The gas concentrations investigated included CO, CO<sub>2</sub>, and O<sub>2</sub> measured dry (water removed from the sample gases) and total unburned hydrocarbons (THC) measured wet. Three dominating uncertainty factors were identified for these measurements as the analyzer repeatability,  $U_{\text{analy}}$ , the calibration gas composition uncertainty,  $U_{\text{cg}}$ , and the calibration uncertainty,  $U_{\text{cal}}$ . The A/D conversion error was determined to be negligible compared to these dominating uncertainties.

The analyzer repeatability was reported by the manufacturer of each instrument to be 1%,  $U_{\text{analy}} = 0.010$ , for all analyzers. The calibration gas composition uncertainty of the gas chromatography analysis values was estimated as 2%,  $U_{\text{cg}} = 0.020$ . The calibration uncertainties for each analyzer is given in Table B1, separated by the different sampling locations. The concentration range with the largest uncertainty of all ranges used for the given sample location was chosen for a conservative analysis, although there was little difference between ranges. The total concentration uncertainties,  $U(\text{sp conc})$ , based on the three uncertainty sources are also given in Table B1.

**Table B1**  
Measured gas concentration\* uncertainties and calibration uncertainties,  
separated by gas sampling location

Analyzed gas	$U_{\text{cal}}$ , Exhaust duct-sampled	$U(X_{\text{SD}})^*$ , Exhaust duct-sampled	$U_{\text{cal}}$ , Hallway-sampled	$U(X_{\text{SD}})^*$ , Hallway-sampled
CO	0.0011	0.022	0.011	0.025
CO <sub>2</sub>	0.0052	0.023	0.0074	0.024
O <sub>2</sub>	N/A	N/A	0.0042	0.023
THC	0.0042	0.023	0.0063	0.023

\* CO, CO<sub>2</sub>, and O<sub>2</sub> were measured dry; THCs were measured wet.



## B. FUEL WEIGHT AND INLET AIR MASS FLOW RATE

The main source of uncertainty in the fuel weight measurement was the electronic drift of the load cell due to thermal effects from the burning compartment. The uncertainty of the drift was determined to be less than  $\pm 2\%$  by reviewing the fuel pan weight data recorded at the end of each experiment, and comparing it with the initial fuel pan weight manually recorded before each experiment. Both the instrument resolution uncertainty and the A/D conversion uncertainty were found to be negligible compared to the thermal drift. Therefore, the fuel weight uncertainty was also 2%, or  $U(M_{\text{fuel}}) = 0.020$ .

The installed velocity probe calibration was checked with a series of methane tracer gas tests. A known flow rate of high grade methane (99.99% pure) was injected into the inlet duct, while air was also drawn through the inlet duct by forcing flow out of the compartment with a fan. The diluted concentration of methane was measured at the opening of the inlet duct into the air distribution plenum. This allowed calculation of the dilution ratio, and air mass flow rate through the inlet duct. The uncertainty of the air mass flow rate calculated from the velocity probe signal was determined by comparison to the flow rate calculated from the methane tracer measurements. The total uncertainty of the air flow rate, calculated from the velocity probe measurement, was determined to be less than  $\pm 5\%$ , or  $U(M'_{\text{air}}) = 0.050$ .

## C. LASER EXTINCTION SIGNAL

The signal measured from the laser extinction system in the exhaust duct was an amplified voltage signal from a photo diode detector. This signal was compared to the reference signal determined during the initial 10 seconds of each experiment, before significant amounts of soot reached the laser extinction system. The measurement used to

calculate the soot yield was the ratio of the measured signal to the reference signal,  $I/I_0$ . The uncertainty of this ratio was estimated to be less than 0.2%, or  $U(I/I_0) = 0.002$ .

#### D. GAS TEMPERATURES

The uncertainty in the temperature measurements was determined from two main factors. First, the thermocouples used to obtain the temperature measurements had uncertainty limits of  $\pm 0.5\%$ , or  $U_{TC} = 0.0050$ . Second, the uncertainty introduced by storing temperature data to the nearest degree was no greater than  $1^\circ\text{K} / 300^\circ\text{K} = 0.33\%$ , or  $U_{Sto} = 0.0033$ . The uncertainty from the A/D board was negligible compared to these uncertainties.

For the bare thermocouple measurements in the inlet duct and the exhaust duct, with no exposure to a significant radiating source, the uncertainty resulting from these two factors alone was 0.6%, or  $U(TC_{nr}) = 0.006$ . However, the thermocouples in the hallway and compartment were exposed to the radiation of flames and very hot gases and surfaces, resulting in an additional source of uncertainty.

Three types of thermocouple configurations were used to perform gas temperature measurements in the hallway. The first type, classified type 1, was a single bare thermocouple (type K, 30 gage), which provided temperature measurements with full radiation effects. During sustained external burning, radiation from the flame caused the bare thermocouple to measure a temperature higher than the actual gas temperature. However, the distinct advantage of the bare thermocouple was a fast response time.

The other two types of configurations provided shielding from the radiation. Thermocouples (type K, 30 gage) were placed inside open stainless steel tubes of an aspirated rake. Gases were drawn into the tubes to allow a continuous flow of gases to pass over the thermocouple, and provide the gas temperature measurement. The

thermocouple was located at two different depths within the tube for the different configuration types.

In initial experiments, the thermocouples were recessed approximately 3 to 4 cm in the tube, providing a long entry length for gas flow before reaching the thermocouple. In this configuration type, classified type 2, the shielding tube provided near complete protection from radiation incident on the thermocouple. A negative effect of the type 2 configuration was a drastically slow response time. The thermal conductivity of the stainless steel tube shields and the steel pipe on which they were mounted acted as a large heat sink. The heat sink provided heat transfer to or from the gases entering the tube, dampening out any responses to quick changes in the gas temperature.

To provide a compromise between the first two thermocouple types, the shielded thermocouples were relocated to just inside the entrance to the radiation shield tube for the type 3 configuration. This configuration provided a much faster time response than with the recessed thermocouple, but at the price of some incident radiation. The type 3 thermocouple configuration was indicated as the most accurate of the three types, and was chosen as the preferred method of temperature measurement used for most of the experiments. The compromise still resulted in a fairly large uncertainty, due to the combined effects of radiation and a slow time response. The magnitudes of these effects varied during different stages of the fire, since sustained external burning began and ended suddenly during experiments, adding to the large uncertainty.

In an effort to quantify the uncertainty in the temperature measurements, the experimental data was reviewed and compared for all three thermocouple configurations. The uncertainty for the type 3 configuration was estimated from the difference between

the types 1 and 3. The poor time response of the type 2 thermocouple resulted in very large errors due to the large heat sink.

The uncertainty for the type 3 thermocouple was determined for two different periods. The largest uncertainty was determined to occur when sustained external burning first occurred, and was estimated from the data comparison to be approximately  $\pm 15\%$ , or  $U(TC_{\text{hall max}}) = 0.15$ . During the "quasi" steady state period the uncertainty decreased due to the fairly steady true gas temperatures, approximated from the data as  $\pm 10\%$ , or  $U(TC_{\text{hall steady}}) = 0.10$ . This is the uncertainty in the averaged temperatures shown in hallway profile plots.

The only thermocouple configuration available for the 0 / 0 soffit case experiments was the type 2. However, these temperatures were corrected approximately for the time response errors, based on comparisons between the type 2 and type 3 thermocouple configurations made in later experiments. The increased uncertainty of these hallway temperatures reported for the 0 / 0 soffit case experiments was estimated as approximately  $\pm 20\%$ , or  $U(TC_{\text{hall 0 / 0 soffits}}) = 0.20$ .

Temperatures inside the compartment were also measured using an aspirated thermocouple rake, with the type 2 thermocouple configuration. However, in the compartment this configuration did not lead to the same problems observed in the hallway. This was mainly due to the fact that temperatures in the compartment did not change nearly as fast as in the hallway, i.e. when sustained external burning initiates. The upper layer of hot exhaust gases in the compartment acted as a thermal buffer, so that the temperature of the gases in the upper layer changed slowly and heated the tubing of the thermocouple rake. The temperature of a bare thermocouple was also recorded in the compartment for comparison purposes. Comparing the bare thermocouple temperature to

the rake temperatures from experimental data allowed the uncertainty to be estimated as  $\pm 5\%$ , or  $U(TC_{comp}) = 0.05$ .

## II. CALCULATED PROPERTY UNCERTAINTY

### A. GLOBAL EQUIVALENCE RATIO

The equation for the GER was:

$$GER = (\dot{M}_{fuel} / \dot{M}_{air}) / \text{stoichiometric ratio} \quad (B.5)$$

Since the stoichiometric ratio was known exactly, the uncertainty in the GER was dependent on the fuel vaporization rate,  $\dot{M}_{fuel}$ , and the air mass flow rate,  $\dot{M}_{air}$ . The fuel vaporization rate at time  $t$  was calculated by numerically differentiating the fuel weight, calculated from:

$$\dot{M}_{fuel}(t) = [M_{fuel}(t+10\text{sec}) - M_{fuel}(t-10\text{sec})] / 20\text{sec}. \quad (B.6)$$

The error for the fuel vaporization rate due to numerical differentiation is given as:

$$\epsilon(\dot{M}_{fuel}) \leq (1/6) \cdot h^2 \cdot \ddot{M}_{fuel}(\xi), \quad (B.7)$$

where  $h$  was the time step of 10 seconds, and  $\ddot{M}_{fuel}(\xi)$  was taken as the largest third derivative of the fuel weight on the 20 second time interval.  $\ddot{M}_{fuel}(\xi)$  was estimated from the slope of the second derivative of the fuel weight, calculated similar to the first derivative. The largest value for  $\ddot{M}_{fuel}(\xi)$  was observed when sustained external burning began, and was determined to be approximately  $0.00002 \text{ Kg/s}^3$  from review of the data. This determined the maximum uncertainty in the fuel vaporization rate to less than 2.2%, or  $U(\dot{M}'_{fuel} \text{ max}) = 0.022$ . However, during the "quasi" steady period,  $\ddot{M}_{fuel}(\xi)$  was determined to be  $0.0000005 \text{ Kg/s}^3$ , significantly smaller than the maximum value. The uncertainty due to thermal drift of the load cell between consecutive data points, negligible

compared to the maximum uncertainty, became comparable. The thermal drift uncertainty over 20 seconds was estimated as 0.0008 Kg, from the total drift of 2% occurring over 500 seconds typically. This resulted in an uncertainty of 0.10%, or  $U(M'_{\text{fuel steady}}) = 0.0010$ .

The uncertainty in the air mass flow rate was determined in section I.B as 5%,  $U(M'_{\text{air}}) = 0.050$ . Combining these uncertainties produced  $U(\text{GER max}) = 0.055$ , and  $U(\text{GER steady}) = 0.050$ .

## B. WET CONCENTRATIONS

The wet concentrations, or mole fractions, of CO, CO<sub>2</sub>, and O<sub>2</sub> were calculated from the respective measured dry concentrations assuming the stoichiometric ratio of CO<sub>2</sub> to water holds for any equivalence ratio. The equation is given as:

$$x_{\text{sp wet}} = X_{\text{sp dry}} / (1 + 1.167 X_{\text{CO}_2 \text{ dry}}), \quad (\text{B.8})$$

where sp represents any of the three dry measured species. The uncertainty of the wet concentrations was dependent on the uncertainty of the assumed ratio of CO<sub>2</sub> to water (1.167), which was estimated to be less than 6% by Gottuk [11] based on data from the hood experiments of Beyler [22]. The wet concentration uncertainties also depended on the uncertainties of  $X_{\text{sp dry}}$  and  $X_{\text{CO}_2 \text{ dry}}$ . These uncertainty values are given in Table B1, separated by the gas sampling location. Table B2 shows the calculated uncertainties for the wet concentrations based on the other three uncertainties discussed. Since THCs were measured as wet concentrations, the values reported in Table B1 are repeated in Table B2 for convenience.

**Table B2**  
Calculated wet concentration uncertainties,  
separated by gas sample location.

Species	U(X <sub>sp</sub> wet), sampled in exhaust duct	U(X <sub>sp</sub> wet), sampled in hallway
CO	0.068	0.069
CO <sub>2</sub>	0.068	0.069
O <sub>2</sub>	N/A	0.069
THC	0.023	0.023

### C. GAS SPECIES YIELDS

Gas species yields were calculated from the equation:

$$Y_{sp} = \dot{M}_{sp} / \dot{M}_{fuel}, \quad (B.9)$$

where  $\dot{M}_{sp}$  was the species mass production rate and  $\dot{M}_{fuel}$  was the fuel vaporization rate. The uncertainty of the fuel vaporization rate during the "quasi" steady period was determined in section II.A to be 0.1%. The uncertainty of the species mass production rate was dependent on the uncertainties of the species measured wet concentration,  $X_{sp\text{ wet}}$ , and the molar flow rate through the exhaust duct,  $\dot{n}_{ed}$ . The uncertainty of the gas molecular weight was determined to be negligible.

The uncertainty of the wet species concentrations is given in Table B2. The molar flow rate through the exhaust duct was calculated from the volumetric exhaust duct flow rate, and corrected for the ambient pressure and measured air temperature. The exhaust duct volumetric flow rate depended on the pressure drop measured across the orifice plate, the exhaust duct gas temperature and the ambient pressure. The uncertainty in the constants of the equation was also a factor, and estimated to be about 10%. The measured pressure drop uncertainty was estimated from the accuracy of the water manometer used for the measurement as the resolution of 0.05 out of a measurement of

7.7, providing 0.65% uncertainty. The uncertainty of the ambient pressure was estimated to be approximately  $2 / 710$  Torr, or 0.3%. The uncertainty of the temperature measurement was determined in section I.D as 0.52%. Combining all of the appropriate uncertainties resulted in a 10% uncertainty in both the volumetric flow rate and molar flow rate. Table B3 shows the uncertainties calculated for the species mass production rates and species yields for CO, CO<sub>2</sub>, and THC.

**Table B3**  
Calculated uncertainties in the species yields and species mass production rates.

Species	$U(\dot{M}_{sp})$	$U(Y_{sp})$
CO	0.12	0.12
CO <sub>2</sub>	0.12	0.12
THC	0.10	0.10

#### D. SMOKE YIELD

The extinction coefficient was calculated based on the measured laser signal ratio and the path length. The uncertainties of these two measurements were 0.1%, from section I.C, and 0.35% respectively. These values correspond to an extinction coefficient uncertainty of 0.36%, or  $U(\text{ext coeff}) = 0.0036$ .

The smoke yield calculation had a relatively large uncertainty, dominated by the uncertainty in the specific extinction coefficient,  $\xi$ . The specific extinction coefficient has been characterized for well ventilated fires as a function of the incident light wavelength. However, the specific extinction coefficient has been reported to vary with the global equivalence ratio for underventilated fires, although no detailed characterization has been conducted.

The correlation developed for well ventilated fires was used for lack of a more accurate method. The maximum uncertainty involved could be as large as 50%



determined from values reported in the referenced literature [19,20], and most likely varies during different stages of the fire. Due to this large uncertainty, reported results were used for relative comparison between experiments of this study, and to the results of Gottuk et al. [7,11,12] where the same method was utilized to calculate smoke yields.

#### **E. IGNITION INDEX**

The uncertainty of the ignition index calculated was relatively large due to a few dominating factors. Most significantly, the concentration of hydrogen, used directly in the calculation, was estimated from the concentration of CO. The error involved with this assumption was estimated as 10% by Gottuk [11].

The next significant uncertainty resulted from the assumption used to calculate wet concentrations, especially for CO used to calculate the hydrogen concentration and also used directly in the calculation. The error associated with the wet CO concentration was determined in section II.B to be less than 7%. Another uncertainty of significant, but unknown magnitude, was due to sampling in the hallway, approximately 45 cm from where ignition actually occurred. The uncertainty before and slightly after the occurrence of sustained external burning was most likely reasonable, although the uncertainty due to the changing gas composition with oxidation during sustained external burning was considered unacceptable. The uncertainty of the ignition index based on the uncertainties presented were estimated to be less than 20%.

## VITA

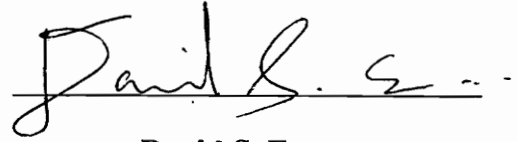
David S. Ewens was born on December 23, 1969 at the Bethesda Naval Hospital in Bethesda, Maryland to Patricia and Peter Ewens. His brother Andrew was born on March 16, 1974 at Sibley Memorial Hospital in Washington D.C.

During his attendance at Fairfax High School in Fairfax, Virginia, David participated in an introduction to engineering pilot class in his junior and senior years. This class initiated his interest and enthusiasm in engineering, and encouraged him to continue his education in the field of engineering. David graduated from Fairfax High School in June of 1987.

David entered Virginia Polytechnic Institute and State University in the College of Engineering in August of 1987. David's studies in Mechanical Engineering were supplemented by employment at the Center for Spacecraft Development at the Naval Research Laboratory in Washington D.C., through the Cooperative Education Program at Virginia Tech. David received his Bachelors of Science degree in Mechanical Engineering in May of 1992, graduating Magna Cum Laude. One week after graduation, David married Sharon Michelle "Micki" Littlely.

David's interest in the field of combustion was developed during his undergraduate studies on the aldehyde emissions from an alcohol fueled engine. The author decided to continue his graduate studies in the field of combustion at Virginia Polytechnic Institute and State University in the Department of Mechanical Engineering. David completed the graduation requirements for his Master's of Science degree in Mechanical Engineering in February of 1994.

David hopes to apply his experiences and knowledge gained during his education toward a career in the area of research and development of internal combustion engines, specifically in emissions control and alternative fuels.

A handwritten signature in black ink, reading "David S. Ewens", written over a horizontal line.

**David S. Ewens**